Gallagher, Carol

Subject: FW: Comment Seabrook NUREG-1437, Supplement 46, Section 5.0 - October 26, 2011
Attachments: COMMENT SEABROOK NUREG- 1437, SUPPLEMENT 46, SECTION 5.0 -Oct26,2011.pdf

---

From: Mary Lampert [mailto:mary.lampert@comcast.net]
Sent: Wednesday, October 26, 2011 2:44 PM
To: Wentzel, Michael
Cc: Ray Shadis; David Agnew
Subject: Comment Seabrook NUREG-1437, Supplement 46, Section 5.0 - October 26, 2011

8/5/2011
76 FR 47612
(16)

Hello:

Attached please find *Comment Seabrook NUREG-1437, Supplement 46, Section 5.0* submitted by Mary lampert, Raymond Shadis, and David Agnew.

We would appreciate your replying by return email to indicate receipt and that the comments will be docketed.

Thank you and have a pleasant afternoon,

Mary

SUNSI Review Complete
Template = ADM-013

E-RIDS = ADM-03
Add = M. Wentzel (MJW2)

COMMENT SEABROOK NUREG- 1437, SUPPLEMENT 46, SECTION 5.0

Oct 26, 2011

The following comments are focused on Section 5.0 Environmental Impacts of Postulated Accidents. They are submitted by the following parties. Mary Lampert is a stakeholder owning two residential properties in Boston on Beacon Hill that are located within 50-miles of Seabrook Station. Friends of the Coast – Opposing Nuclear Pollution (Friends of the Coast) and New England Coalition, Inc. (NEC) are co-signing the comments. They have standing and are a party to the LRA proceedings. Friends of the Coast/NEC has numerous members that reside in the immediate vicinity Seabrook Station and throughout New England; said members' concrete and particularized interests will be directly affected by this proceeding. Capedownwinders, although approximately 70 miles distant from Seabrook, are nevertheless at risk as evidenced by the spread of direct and indirect actual impacts in Japan.

We contend that NRC Staff incorrectly found the SAMA analysis adequate. NextEra's SAMA analysis improperly minimized offsite consequences and costs when filed in 2010 and those inadequacies were underscored, and others made apparent, by the new and significant issues raised by Fukushima regarding the probability of both a severe accident and containment failure, and subsequent larger off-site consequences and costs. If properly accounted for, mitigations that the public deserves to reduce risk would be found cost justified. The SAMA must be redone. NRC Staff are wrong.

ENVIRONMENTAL IMPACTS OF POSTULATED ACCIDENTS-POST FUKUSHIMA

I. INTRODUCTION

In the license renewal process, the Applicant is required under 10 CFR

§51(c)(ii)(L) to perform a severe mitigation analysis if they had not previously done so. The purpose of a SAMA review is to ensure that any plant changes that have a potential for significantly improving severe accident safety performance are identified and addressed.

Post Fukushima Daiichi, it plainly is necessary to redo NextEra's SAMA analysis to take into account new and significant information learned from Fukushima regarding the probability of a severe accident, including containment failure, in the event of an accident and the concomitant probability of a significantly larger volume of off-site radiological releases and costs.

NRC Staff's pre-Fukushima statement that, "The generic analysis (GEIS) applies to all plants... and that the probability- weighted consequences of atmospheric releases fallout onto open bodies of water, releases to ground water, and societal and economic impacts of severe accidents are of small significance for all plants" (SEIS 5-2, 5-3) requires a fresh look.

Further the Staff says that they "identified no new and significant information related to the postulated accidents of other available information. Therefore there are no impacts related to postulated accidents beyond those discussed in the GEIS." (Ibid, 5-3) Prior to Fukushima the analysis was wrong; Post -Fukushima it is ludicrous and NEPA requires NRC to perform a new analysis before license renewal.

II. NATIONAL ENVIRONMENTAL POLICY ACT

National Environmental Policy Act, NEPA, 42 USC § 4332, requires that the Staff look at new and significant information in order to "help public officials make decisions that are based on understanding of environmental consequences, and take decisions that protect, restore and enhance the environment." 40 CFR § 1500.1(c) (Emphasis added)

NRC "ha[s] a duty to take a hard look at the proferred evidence" *Marsh v Oregon Natural Resources Council, 490 U.S. 360, 385 (1989)* before relicensing Seabrook and before finalizing the SEIS. NEPA requires an agency to consider the environmental effects before decisions are made; the NRC must ensure that "important effects will not be overlooked or underestimated only to be discovered after resources have been committed or the die otherwise cast." *Robertson v Methow Valley Citizens Council, 490 U.S. 332,349 (1989)* NRC cannot rely on NextEra's June 1, 2010 SAMA analysis and minor updates.

The fundamental purpose of the National Environmental Policy Act, NEPA, 42 USC § 4332, is to "help public officials make decisions that are based on understanding of environmental consequences, and take decisions that protect, restore and enhance the environment." 40 CFR § 1500.1(c)

In its application for license renewal of Seabrook, NextEra was required under 10 CFR § 51 to provide an analysis of the impacts on the environment that could result if it is allowed to continue beyond its initial license. The environmental impacts that must be considered in NextEra's EIS include those which are "reasonably foreseeable" and have "catastrophic consequences, even if their probability of occurrence is low." 40 CFR §1502.22(b)(1). Therefore the Staff's position that the probability of a severe accident is remote is not simply wrong after Fukushima but immaterial to satisfying NEPA's obligations.

The NRC must assure Seabrook's SEIS and adjudication process considers issues raised by Fukushima prior to relicensing Seabrook; the Fukushima events plainly show that, even if they are not yet all conclusively understood, the environmental impacts of the NRC relicensing

Seabrook may "affect the quality of the human environment in a significant manner or to a significant extent not already considered." *Marsh* at 374; see also *Marsh* at 372-373

Unless the NRC Staff take the "hard look" required by NEPA and adjust the cost/benefit analysis based on lessons now learned, NextEra's 20106 SAMA analysis will stand as is, based on pre-Fukushima assumptions that seek to show that mitigation is not justified, that the risks to society are really too low, and that there is no need to spend that money for safety enhancements we now know the public needs and deserves. The degree to which a project may affect public health or safety is a major consideration under NEPA. See 40 C.F.R. 1508.27.

The public is not obligated to perform a complete and new SAMA analysis or conduct a comprehensive review of potential mitigation measures before the NRC that is obligated to take a hard look at the lessons learned from Fukushima: "[it]is the agency, not an environmental plaintiff, that has a 'continuing duty to gather and evaluate new information relevant to the environmental impacts of its actions." *Friends of the Clearwater v. Dombeck*, 222 F.3d 552, 559 (9th Cir. 2000) (*quoting Warm Springs Dam Task Force v. Gribble*, 621 F.2d 1017, 1023 (9th Cir. 1980)); *see also Te-Moak Tribe v. U.S. Dept of the Interior*, 608 F.3d 592, 605-06 (9th Cir. 2010); *Davis v. Coleman*, 521 F.2d 661, 671 (9th Cir. 1975) ("compliance with NEPA is a primary duty of every federal agency; fulfillment of this vital responsibility should not depend on the vigilance and limited resources of environmental plaintiffs."). NRC Staff has an obligation to go back to the drawing board and take the required "hard look" at issues raised herein and any other new, significant and material issues that arise from Fukushima.

As the First Circuit remarked in *Dubois v. U.S. Dept. of Agric.*, 102 F.3d 1273, 1291 (1st Cir. 1996), discussing the public's role under NEPA:

> 'Specifics' are not required... [T]he purpose of public participation regulations is simply to 'provide notice' to the agency, not to 'present technical or precise scientific or legal challenges to specific provisions' of the document in question...Moreover, NEPA requires the agency to try on its own to develop alternatives that will "mitigate the adverse environmental consequences" of a proposed project. *Robertson v. Methow Valley Citizens Council*, 490 U.S. 332, 351 (1989)

III. LESSONS LEARNED FROM FUKUSHIMA - INADEQUACIES SEIS 5.0

Based on new and significant information from Fukushima, the Environmental Report is inadequate post Fukushima Daiichi. NextEra's SAMA analysis ignores new and significant issues raised by Fukushima regarding the probability of both containment failure, and subsequent larger off-site consequences.

A. New and Significant Information Regarding The Probability of a Severe Accident

1. Probability of Reactor Core Damage and Radioactive Release - Cumulative Direct Experience

The probability of severe core damage and radioactive release can be estimated either from a PRA study or from direct experience. Fukushima has expanded our knowledge and provides a reality check for PRA estimates.

Estimating core-damage probability using PRA

The accident at Fukushima showed that Seabrook's SAMA analysis underestimates the extent of core damage (CDF) by an order of magnitude. Core damage probability, post Fukushima shows that of the 12 core-damage accidents at NPPs, five have occurred at Generation II plants and involved sunsbtantial core melting. These were at Three Mile Island, Unit 2(PWR), Chernobyl Unit 4 (RBMK plant) and Fukushima Units 1 through 3. (BWRs). These 5 occurred in a worldwide fleet of of commercial NPPS of which 440 are currently in

operation. The data provides a reality check on PRA estimates of CDF. Confidence is enhanced because the 5 occurred in different countries, at three different types of reactor designs, and over a period of 32 years. The 5 core damage accidents over a world wide experience of 14, 500 RY can be trnslated to a CDF of 3.4E-04 per RY (1 event per 2,900 reactor years). This is significantly different than NextEra's SAMA's baseline 1.5 X 10^{-5} RY (1.5 events per 100,000 RY). Therefore the SAMA analysis done by NextEra pre Fukushima must be redone with a baseline CDF orders of magnitude higher.

2. **Flooding and Seismic Hazards:** The probability of flooding and seismic hazards is higher than previously estimated post Fukushima. The October 11, 2011 SECY attests to its significance. Seabrook's location places it at a significant risk for flooding, a risk that will increase in subsequent years as a consequence of global warming.

3. Station Blackout: The probability of SBO is higher than previously estimated post Fukushima and increases the probability of a severe accident at Seabrook. The October 11, 2011 SECY attests to its significance. Lack of reliability of electric power is not properly accounted for in the PRA due to: (a) Seabrook's submerged Non- EQ (environmentally qualified) electric cables that carry offsite electricity needed to power safety systems; and (b) backup systems are insufficient and susceptible to damage from manmade and natural events.

4. **Spent Fuel:** Higher reelases than initally reproted by the Japanese and releases from the spent fuel pool cannot be discounted post-Fulushima.

Nature Magazine's October 25 report, Fallout forensics hike radiation toll: Global data on Fukushima challenge Japanese estimates[1], Geoff Brumfeil, Nature 478, 435-436 , October 25,

[1] Available on line at http://www.nature.com/news/2011/111025/full/478435a.html

2011 said:

> The disaster at the Fukushima Daiichi nuclear plant in March released far more radiation than the Japanese government has claimed. So concludes a study_1 that combines radioactivity data from across the globe to estimate the scale and fate of emissions from the shattered plant.
>
> The study also suggests that, contrary to government claims, pools used to store spent nuclear fuel played a significant part in the release of the long-lived environmental contaminant caesium-137, which could have been prevented by prompt action. The analysis has been posted online for open peer review by the journal Atmospheric Chemistry and Physics[2].
>
> Stohl believes that the discrepancy between the team's results and those of the Japanese government can be partly explained by the larger data set used. Japanese estimates rely primarily on data from monitoring posts inside Japan_3, which never recorded the large quantities of radioactivity that blew out over the Pacific Ocean, and eventually reached North America and Europe. "Taking account of the radiation that has drifted out to the Pacific is essential for getting a real picture of the size and character of the accident," says Tomoya Yamauchi, a radiation physicist at Kobe University who has been measuring radioisotope contamination in soil around Fukushima.
>
> The new analysis also claims that the spent fuel being stored in the unit 4 pool emitted copious quantities of caesium-137. Japanese officials have maintained that virtually no radioactivity leaked from the pool. Yet Stohl's model clearly shows that dousing the pool with water caused the plant's caesium-137 emissions to drop markedly.

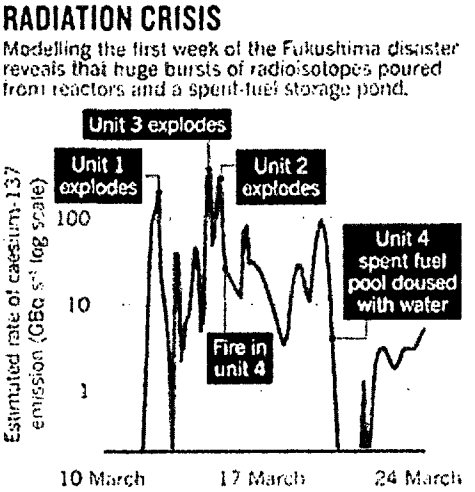

5. Concrete Degradation: Concrete is degrading presently at Seabrook Station; there is no evidence that it shall not continue. The environmental consequences are not analyzed in the SEIS

[2] Atmos. Chem. Phys. Discuss, 11, 28319-28394, 2011, www.atmos-chem-discuss.net/11/28319/2011/doi:10.5194/acpd-11-28319-2011

such as the environmental and economic consequences from lime leached from the concrete into the environment.

B. New and Significant Information Regarding the Magnitude of Release and Increased Offsite Costs

1. **Duration of Release:** The MACCS2 computer code used by NextEra limits the total duration of a radioactive release to no more than four (4) days, if the Applicant chooses to use four plumes occurring sequentially over a four day period.[3] NextEra chose not to take that option and limited its analysis to a single plume having a total duration of the maximum-allowed 24 hours[4]. The Analysis and SEIS fail to say how many hours were actually modeled by NextEra and we request that information. In any case either a 24-hour plume or a four-day plume is insufficient duration in light of lessons learned from Fukushima. The Fukushima crisis now stretches into its seventh month and shows that releases can extend into many days, weeks, and months; a longer release will cause more significant offsite consequences that, in turn, will affect cost-benefit analyses. Any attempt to deny this would be counterintuitive and absurd.

2. **Computer Codes In Use Are Totally Incapable Of Modeling A Chain Reaction That Continues After A Scram.** MACCS2 is no exception. Like all the computer codes, it is incapable of modeling a "severe accident" release that lasts weeks and months. The MACCS2 code used by NextEra, and all other codes, assumes that the reactor is scrammed when the accident begins, and that the production of all fission products ceases at that time. We know that criticality was continuing at Fukushima Unit 2 through and past April 27, 2011, and to shorter duration at Unit 1, because of their continued post-scram high findings of I-131 reported by

[3] NUREG/CR-6613 Code Manual for MACCS2: Volume 1, User's Guide, 2-2

4 The MACCS2 uses a Gaussian plume model with Pasquill-Gifford dispersion parameters (Users code 5-1). Its equation is limited to plumes of 10 hour duration.

TEPCO. The reactors were shut down, scrammed, on March 11.th I-131 has an 8-day half-life. If criticality had stopped after the reactors scrammed, the I-131 would have largely decayed. It would not, be at the levels TEPCO reported, that exceeded the Cesium readings. Conventional accident analysis of reactor accidents begin at reactor scram, t=0, and assume that the fission chain reaction ceases completely at that time, and that thereafter there is only "spontaneous" nuclear decay, with it being common practice to ignore the very tiny amount of "spontaneous fission" triggered by random neutrons from cosmic radiation hitting a fissile atom and creating infinitesimal amounts of I-131. A large problem created by the ongoing chain reaction is the calculation of food doses. The code has no way of modeling the continual production of I-131 and I-134 which can get to people both by milk and from fresh leafy-vegetable consumption.

The NRC Staff has an obvious duty to re-evaluate the Applicant's SAMA analysis on the basis of this new and significant information and its public health and safety consequences.

3. Probability of Higher Releases - Post Fukushima Analyses Deficiencies in Mitigation Measures-EDMGs/SAMGs

The NRC Task Force and October 3 SECY to the Commissioners, *Prioritization of Recommended Actions to Be Taken in Response to Fukushima Lessons Learned Task Force,* substantiate that NextEra's assumptions regarding probability and consequences pre-Fukushima were incorrect and overly "optimistic" regarding the effectiveness of mitigation measures. One fundamental problem is that both the SAMGs and EDMGs are voluntary and not evaluated or enforced by NRC. Therefore the weight given them in assuming a lower probability of an accident is not justified.

The capability of operators to mitigate an accident at Seabrook would affect the

probability of a radioactive release from the accident, including from a spent fuel pool fire. Fukushima showed that events can result in high radiation fields and explosions, and long periods without fresh water and electricity.

Examples- strategies to provide make-up water

Spent Fuel Pools: Review of NEI's newly-disclosed EDMGs (NEI, B.5.b Phase 2 &3 Submittal Guideline, NEI 06-12, Revision 2, December 2006) show that they are inadequate to respond to the type of accident we now can expect post-Fukushima. For example: various strategies are discussed to provide makeup water. However important considerations are ignored such as:

- Events that initiate the accident such as: hurricanes, ice storms, and blizzards could render the water supply unavailable.
- A radioactive release from the reactor or spent fuel pool could produce radiation fields that render the water supply truck unavailable or preclude its use.
- There is no recognition that spraying water on exposed fuel could exacerbate the accident and cause a steam explosion or in the pool feed a zirconium-steam fire.

Containment: There is recognition in the Severe Accident Mitigation Guidelines (SAMGs) of the need for huge amounts of water during a severe accident but in a narrow way. The weight of the water along with how much space it would occupy was considered. The SAMGs have a provision for using water from the lake, river, or ocean to fill the containment until the level is higher than the top of the active fuel in the reactor core. This option seeks to cool the reactor core, assuming all other means failed, by immersion in water. The plant-specific calculations performed to support this SAMG step consider how high the containment must be flooded to achieve this condition. The SAMGs direct the operators to position motor-operated valves and such to their desired positions before submerging them in water and disabling them. The SAMGs

also look at how much water much be added to achieve the desired level and the weight (water weighs about 8 pounds per gallon) this level has on the structural integrity of the containment.

However the SAMGs do not consider the need, as seen in Japan, to continuously fill because of evaporation and leakage; nor does it consider the added weight from the water in the containment in its seismic calculations. Probabilities are improperly assumed lower.

Feed & Bleed

Last the SAMGs do not consider the effect on contaminating the waters from the reactor bleeding large volumes of highly contaminated water into the ocean and significantly increasing offsite consequences/costs.

Prior to Fukushima NRC Staff in reviewing Seabrook's SAMA apparently did not consider the probability that a huge volume of water required to be poured into the reactor in a severe accident after the type of events that we see are now credible and the consequent huge amount of highly contaminated water flowing out directly into the ocean.

The Areva method to decontaminate the water failed.[5] The Scientific American reported that " a trial run of the new filtration system was halted on June 18 in less than five hours when it captured as much radioactive cesium 137 in that span as was expected to be filtered in a month." The inability to store large volumes of decontaminated water was not modeled.

An additional problem in Japan was that the currents are such that the contaminants keep coming back to shore and are predicted to bring the contaminants back for 20-30 years. There is

[5] http://www.scientificamerican.com/article.cfm?id=fukushima-meltdown-radioactive-flood&print=true Scientific American, Three months after its meltdown, the stricken nuclear power plant continues to struggle to cool its nuclear fuel--and cope with growing amounts of radioactive cooling water, David Biello | Friday, June 24, 2011

no indication that so-called "feed and bleed" and the effects of currents were modeled in Next Era's SAMA; thereby consequences/costs were minimized.

There are numerous press reports describing the impact on the environment from feed and bleed, ignored by NextEra's SAMA. For example: *Fukushima's radioactive sea contamination lingers*, Andy Coghlan, New Scientist, September 30, 2011

> Peak leaks: Official estimates from the Japanese government and TEPCO, the company that owns Fukushima-Daiichi, suggest that 3500 terabecquerels of caesium-137 from the plant entered the ocean between 11 March and late May. The pollution was exacerbated in April by problems locating a persistent leak of contaminated water and a decision by TEPCO to dump contaminated water at sea. A further 10,000 terabecquerels of caesium-137 is thought to have found its way into the ocean after escaping as steam from the facility. And TEPCO said last week that Fukushima-Daiichi may still be leaking as much as 500 tonnes of contaminated water into the sea every day. (Emphasis added)

Radioactive cesium may be brought back by Ocean in 20-30 years, Tokyo Times, 09.16.11

> Radioactive substances from the Fukushima nuclear facility which spilled into the ocean in the aftermath of the March quake and tsunami may reach the Japanese coasts again in 20-30 years, according to a new research.
>
> The Meteorological Research Institute and the Central Research Institute of Electric Power Industry compiled a study indicating that the leaked radioactive cesium may travel clockwise through the northern Pacific Ocean and return to the Japanese coast in two or three decades.

Radioactive plankton found near Fukushima plan, Mark Willacy, Reuters Kodo, October 15, 2011

> Researchers say high concentrations of radioactive caesium have been detected in plankton in the Pacific Ocean off the shattered Fukushima nuclear plant.
>
> The Fukushima nuclear plant was badly damaged in the March earthquake and tsunami that struck Japan, and has been leaking radiation ever since.
>
> It is feared more radiation could now enter the food chain.
>
> Researchers from Tokyo University collected plankton from the sea south of the Fukushima nuclear plant, discovering nearly 700 becquerels per kilogram of caesium in plankton close to the shore.
>
> Research leader professor Takashi Ishimaru told Japan's NHK network sea currents had carried contaminated water south from the nuclear plant, heavily contaminating the plankton.
>
> A wide range of fish and other marine species feed on the plankton, leading to fears it could have a serious impact on the food chain.

The GEIS, like the SEIS, modeled atmospheric releases fallout on open bodies of water but apparently not leaks of large quantities of water from the necessity to dump tons of water on

the top of the reactor followed by tons of water leaking out from the bottom through cracks into adjacent waters.

> The generic analysis (GEIS) applies to all plants... and that the probability- weighted consequences of atmospheric releases fallout onto open bodies of water, releases to ground water, and societal and economic impacts of severe accidents are of small significance for all plants." (SEIS 5-2, 5-3, emphasis added)

4. Cleanup Challenges and Offsite Costs Not Considered

New and significant information from Fukushima underscore what was already known and add new and significant information to show that the SAMA analysis for Seabrook significantly minimized offsite cleanup costs so that mitigation measures that properly should have been found cost effective to implement were not.

a. Size Area Contaminated- Underestimated (Duration Release, Meteorology & Averaging)

Estimated 13,000 square km eligible for decontamination Asahi.com (Asahi Shimbun), Oct 12, 2011 reported that 8077 miles will be decontaminated:

> The central government will be responsible for decontaminating about 13,000 square kilometers across eight prefecture, or about 3 percent of Japan's total landmass

Lessons learned from Fukushima confirmed that costs of offsite cleanup will reflect the size of the area contaminated. As discussed above (at 5) the MACCS2 code used by NextEra limits the total duration of a radioactive release to a single plume having a total duration of the maximum-allowed 24 hours[6] that is insufficient duration in light of lessons learned from

6 The MACCS2 uses a Gaussian plume model with Pasquill-Gifford dispersion parameters (Users code 5-1). Its equation is limited to plumes of 10 hour duration.

Fukushima. A longer release will cause offsite consequences that will increase contamination, and result in required re-decontamination, and significantly increase cleanup costs and the overall cost-benefit analyses. Assumptions need to be changed post-Fukushima.

Plume, Straight-line Variable: Fukushima showed that the plume did not travel simply in a straight-line.[7] Fukushima Daiichi, like Seabrook, is on the coast and the area around it topographically varied. The wind in Japan was variable, as it is and would be in a severe accident at Seabrook.

Further it is obvious that releases extending over a longer duration than a day will travel in varied directions over that extended time period. However, the MACCS2 code's ATMOS module, used by NextEra, assumes a straight-line Gaussian plume. Consequently it fails to predict the area impacted and significantly minimizes it. NEPA requires the SAMA analysis to be redone using a variable plume model.

Fallout forensics hike radiation toll, Global data on Fukushima challenge Japanese estimates, Nature 478, Geoff Brumfel, 435-436, October 25, 2011[8]

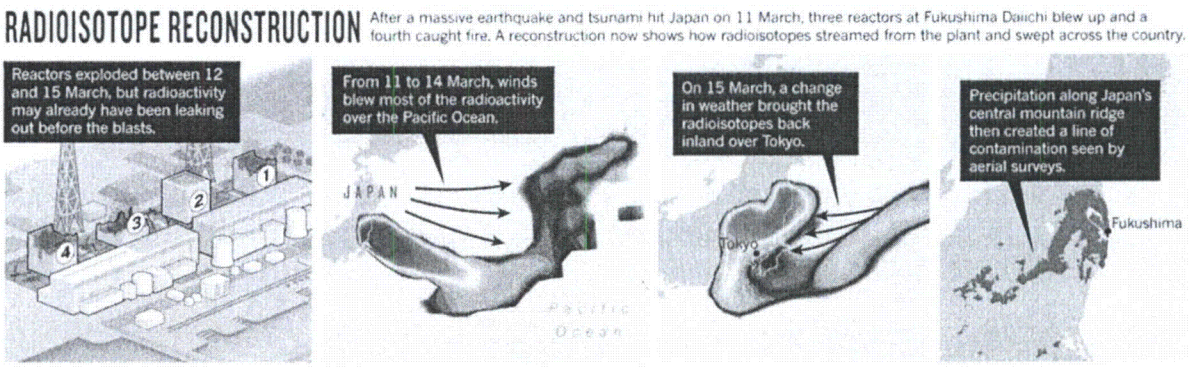

Radiation levels in Japan vary greatly by location. The Japanese Ministry of Education, Culture, Sports, Science and Technology has been posting radiation levels by prefecture on its

[7] Gov't radiation info in English http://radioactivity.mext.go.jp/en/

[8] Available on line at http://www.nature.com/news/2011/111025/full/478435a.html

English-language web site, with data going back to two days after the accident. For example the Mainichi Daily, October 7, reported that: *Gov't releases new radiation map for Tohoku, Kanto districts*[9]

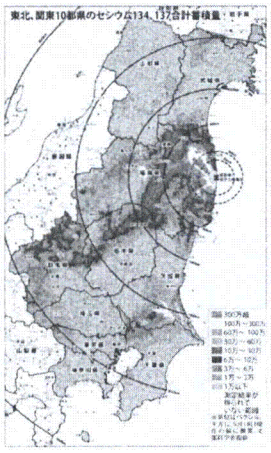

Mainichi Daily News reported that:

> The Japanese Ministry of Education, Culture, Sports, Science and Technology (MEXT) has released a new map showing the spread of radiation from the crippled Fukushima No. 1 Nuclear Power Plant across 10 prefectures, including Tokyo and Kanagawa.
>
> The map released on Oct. 6 shows levels of radioactive cesium (cesium-137 and cesium-134) that have accumulated in soil in the prefectures of Yamagata, Miyagi, Fukushima, Tochigi, Gunma, Ibaraki, Saitama, Chiba, Kanagawa and Tokyo.
>
> The map shows 30,000 to 60,000 becquerels of radioactive cesium per square meter of soil in the areas of Higashikanamachi, Mizumotokoen and Shibamata in Tokyo's Katsushika Ward, as well as some parts of Kitakoiwa in Tokyo's Edogawa Ward.
>
> Radioactive amounts ranging between 30,000 and 100,000 becquerels per square meter were detected in the mountain areas in northwestern Okutama, in western Tokyo.

Further, the press has numerous recent reports on the spread of contamination. For example: *Citizens' Testing Finds 20 Hot Spots Around Tokyo,* Hiroko Tabuchi, New York Times, Oct 14, 2011; *Residents' feelings mixed over discovery of radioactive strontium in Yokohama,* Mainichi Daily News, October 17, 2011 reported that: "YOKOHAMA -- Residents have expressed mixed

[9] Mainichi News, http://mdn.mainichi.jp/mdnnews/news/20111007p2a00m0na009000c.html

feelings over the discovery of radioactive strontium in Yokohama's Kohoku Ward, some 250 kilometers away from the crisis-hit Fukushima No. 1 Nuclear Power Plant."

Averaging Meteorological Data: Fukushima also makes plain the effect the Applicant's choice of averaging has on estimating consequences. The User can choose the averaging method in the code's OUTPUT file[10]. If the mean is chosen, as was the case in Seabrook's SAMA, then the site's meteorological variability is washed out - made meaningless. For example sea breeze occurs only in warmer months; therefore at the 95th percentile its impact is accounted for but not if the mean is used. Averaging is a choice; no NRC rule requires the Applicant to use the MACCS2 code or a particular statistical method. Whether NRC determines that the Applicant made the correct choice depends if: NRC Staff is on the side of NextEra and wishes to assure that they will not be required to spend monies for mitigation in the post- Fukushima world; or whether NRC is on the side of assuring public safety.

[10]**Explanation MACCS2 code's averaging**: For each plant damage state, the code is run over a meteorological data set to produce a set of consequence results. For each consequence endpoint, the values corresponding to various statistical parameters of the resulting data set (mean, median (50th percentile), 95th percentile, 99th percentile, and the maximum value over all weather trials considered) are provided in the MACCS2 code's OUTPUT file. Then, it is necessary for the SAMA analysis to determine which statistical parameter should be used as input into the SAMA analysis: e.g., the mean, the median or the 95th percentile. Once this input parameter is chosen, then the population dose-risks and off-site economic dose risks can be calculated, summed and compared to the costs of mitigative measures. The choice of statistical input parameter determines the level of protection which mitigative measures would be expected to provide. A choice of 95th percentile, for example, means that mitigative measures would be considered cost-beneficial if they were no more expensive than the value of the averted risk to the public from a severe accident for 95 percent of the meteorological conditions expected to occur over the course of a year. In contrast, use of the mean consequences would imply that measures would be cost-beneficial if they were no more expensive than the (significantly lower) value of the averted risk to the public for an accident occurring under average meteorological conditions. This is analogous to the situation of a homeowner who is considering whether to spend the money to install windows to protect against a 20-year storm or just an average storm. Thus the outcome of the SAMA analysis is functionally dependent on the choice of statistical input.

Comparative Studies Missing: We note also that the NRC Staff did not provide reference to, or ask the Applicant for, a single study that compared the results from: using a variable plume model versus a Gaussian plume model; or statistically treating the data with the 95th percentile versus the mean. Consequently, we question the basis for the Staff's assurance that they "identified no new and significant information related to the postulated accidents of other available information. Therefore there are no impacts related to postulated accidents beyond those discussed in the GEIS." (Ibid, 5-3)

Further, we also understand that the NRC does not have the capability or knowledge to run the MACCS2 code. If this is so, and we deserve to know, on what basis did the staff approve NextEra's analysis?

b. **Cleanup Standard**

Estimated 13,000 square km eligible for decontamination Asahi.com (Asahi Shimbun), Oct 12, 2011 reported that a change in cleanup standard dramatically affected the area required to be cleaned up and costs 7-fold.

> The central government will be responsible for decontaminating about 13,000 square kilometers (8077 miles) across eight prefecture, or about 3 percent of Japan's total landmass, under new standards for cleaning up radiation from the Fukushima No. 1 nuclear power plant, according to Asahi Shimbun estimates.
>
> The Environment Ministry on Oct. 10 endorsed a basic policy to make the government responsible for decontaminating all areas with radiation levels exceeding 1 millisievert per year. (100 mlrem)
>
> Based on an earlier annual threshold of 5 millisieverts, the ministry initially said about 1,800 square km of land in Fukushima Prefecture would be subject to decontamination. But under the new standard, the size of the area will grow sevenfold.

The cleanup standards that will determine what clean-up is required (and hence its cost) have not been defined in the U.S. and without defining how "clean is clean" there was no way for NextEra to make any reasonable estimate of offsite costs or for NRC Staff to make its evaluation in the SEIS.

Further lessons learned at Fukushima have shown that absent a cleanup standard set before the accident, there is added delay in getting started. Time is important in cleanup. The longer it takes to start the process of decontamination will result in an increase in damage to the environment, public health, and economy via resuspension and contamination of agricultural products – again increasing overall offsite costs.

Additionally, Fukushima has shown that the public will demand a lower standard and more inclusive area to be compensated because of known health effects from radiation and the discovery of hot spots resulting in variation from property to property and resuspension.

In One Japanese City, Hot Spots to Avoid, Wall Street Journal, Phred Dvorak, Sept 3, 2011

> The new hot spots are devilishly small and scattered: one out of five houses in the neighborhood of Kaki-no-uchi; six households of 10 in Aiyoshi. In some cases, next-door neighbors have received differing recommendations.
>
> In radiation-contaminated Date, Japan, Morio Onami was told his house doesn't qualify for evacuation, even though his son's home, just a few steps away, does. Date residents complain the measurements aren't reliable, and that the line between who stays and who goes is fuzzy. Families who qualify for evacuation get breaks on property taxes, insurance premiums and medical fees—assistance potentially worth thousands of dollars—fanning jealousy among neighbors who get nothing. And many residents aren't convinced it is safe to stay behind, particularly when others nearby are moving.

Background: As background to supplement lessons learned from Fukushima, the US Department of Homeland Security has commissioned studies for the economic consequences of a Rad/Nuc attack and although much more deposition would occur in reactor accident, magnifying consequences and costs, there are important lessons to be learned from these studies.

Barbara Reichmuth's study, Economic Consequences of a Rad/Nuc attack: Cleanup Standards Significantly Affect Cost, 2005,[1] Table 1 Summary Unit Costs for D & D (Decontamination and Decommissioning) Building Replacement and Evacuation Costs provides

[1] Economic Consequences of a Rad/Nuc attack: Cleanup Standards Significantly Affect Cost Barbara Reichmuth, Steve Short, Tom Wood, Fred Rutz, Debbie Swartz, Pacific Northwest National laboratory, 2005

estimates for different types of areas from farm or range land to high density urban areas. Reichmuth's study also points out that the economic consequences of a Rad/Nuc event are highly dependent on cleanup standards. "Cleanup costs generally increase dramatically for standards more stringent than 500 mrem/yr;" however currently a cleanup standard is not agreed upon by NRC and EPA and appears to range from 15 mrem/yr to 5 rem/yr.

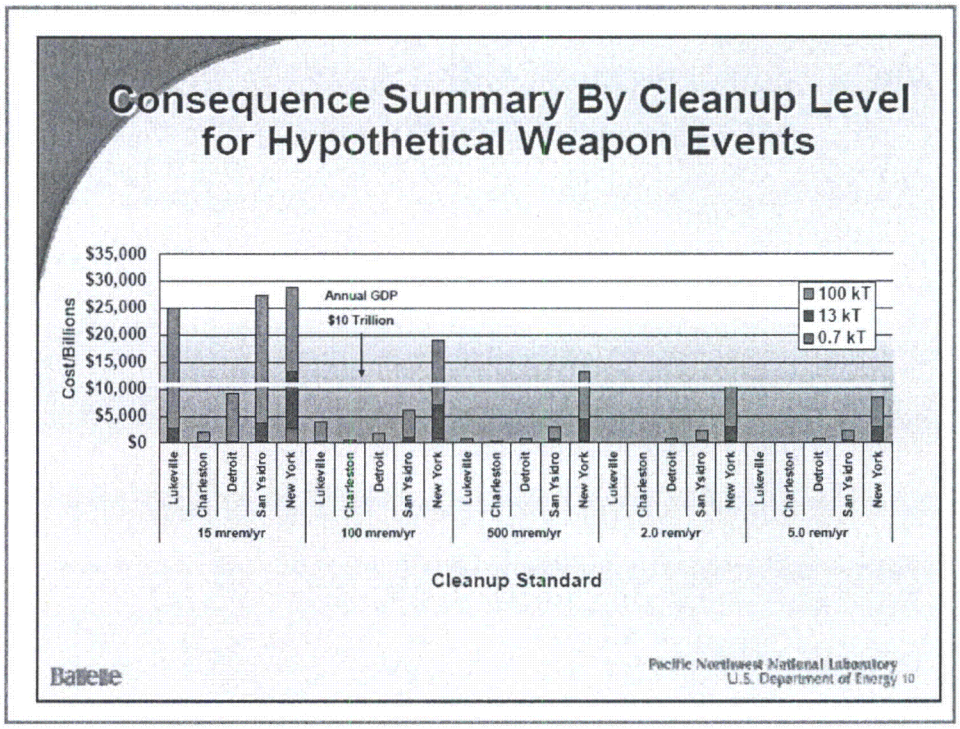

Source: Battelle Study-locations range from a small rural community to densely populated NYC)

The General Accounting Office (GAO) reports that the current EPA and NRC cleanup standards differ and these differences have implications for both the pace and ultimate cost of cleanup.[2] NextEra's SAMA does not account for this issue.

[2] GAO, "radiation Standards Scientific Basis Inconclusive, and EPA and NRC Disagreement Continues," June 2004

A similar study was done by Robert Luna, *Survey of Costs Arising from Potential Radionuclide Scattering Events.*[3] Luna concluded that,

> ...the expenditures needed to recover from a successful attack using an RDD type device ...are likely to be significant from the standpoint of resources available to local or state governments. Even a device that contaminates an area of a few hundred acres (a square kilometer) to a level that requires modest remediation is likely to produce costs ranging from $10M to $300M or more depending on the intensity of commercialization, population density, and details of land use in the area." (Luna, Pg., 6)

Therefore a severe accident at Seabrook from lessons learned at Fukushima is likely to result in huge costs; costs not accounted for by NextEra, because of the type and magnitude of radionuclides released in comparison with a RDD type device.

In place of the outdated decontamination cost figure in the MACCS2 code, the SAMA analysis for Seabrook must be redone to incorporate the lessons learned from ongoing actual experience in Japan.

Again, there is no basis for the Staff's assurance that they "identified no new and significant information related to the postulated accidents of other available information. Therefore there are no impacts related to postulated accidents beyond those discussed in the GEIS." (Ibid, 5-3)

c. <u>Waste Disposal - ignored</u>

It is evident from Japan's efforts today to deal with contaminated waste that NextEra and the MACCS2 code ignored the real costs and issues associated with radioactive waste disposal.

Radioactive soil can fill 23 Tokyo Domes, Five prefectures' nuclear burden a hot potato no one wants to catch, Setsuko Kamiya, Japan Times, September 29, 2011

[3] Survey of Costs Arising From Potential Radionuclide Scattering Events, Robert Luna, Sandia National laboratories, WM2008 Conference, February 24-28, 2008, Phoenix AZ

Radioactive soil and vegetation that must be removed in Fukushima and four adjacent prefectures could reach up to 28.79 million cu. meters, equal to filling the Tokyo Dome 23 times, according to a recent Environment Ministry estimate.

But finding a disposal or temporary storage site will be a tall order.

The estimate covers soil and dead leaves mainly from areas with radiation levels of more than 5 millisieverts per year in the prefectures of Fukushima, Miyagi, Yamagata, Tochigi and Ibaraki, whose data were used to mete out the rough figures.

In Fukushima, home of the nuclear plant leaking all the radiation, about 17.5 percent of the prefecture is contaminated to that level.

The estimate was submitted Tuesday to a 12-member expert panel working out decontamination plans. The panel assumed that 5 cm of topsoil should be removed from contaminated areas, including pinpoint decontamination efforts in certain locations with radiation of 1 to 5 millisieverts per year.

The government is hammering out details on plans to remove and store the soil and leaves. But finding a location to temporarily store such a huge amount of radioactive materials will be an extremely sensitive and politically difficult task for the central government.

Breaking down the total, contaminated soil from residential areas was estimated at 1.02 million cu. meters, farm land at 17.43 million cu. meters and forests at 8.76 million cu. meters, the Environment Ministry said.

A single facility capable of housing the entire 28.79 million cu. meters of soil would have to be 1 sq. km in area and 30 meters deep. But if the central government decides on multiple facilities, negotiations would have to be completed with numerous local governments.

The location for a temporary facility is still undecided, but the government is reportedly considering Fukushima Prefecture.

Contaminated soil can amount to 29 million cubic meters, Denki Shimbun, Sep. 30, 2011 estimated that the amount of soil contaminated from Fukushima could be as much as 29 million cubic meters (38 million cubic yards). For context, the waste if placed on a football field, including the end zones, would make a pile 6,000 feet high or over a mile.

Reuters in May estimated that the cleanup would take 10-20 years, cost $100 Billion dollars, require 10,000 nuclear cleanup workers, decontamination of a 100,000 square mile area, and produce 100,000 gallons of waste. They made note of the facts that: "Japan doesn't have robust shipping plans for nuclear waste and will have to develop them as the need comes to

transport and figure out how and where to bury, burn or ship the waste; Japan has no storage capability currently to contain the highly radioactive core and SFP debris.[11]"

The types of isotopes found offsite in Japan show what can be expected to be found in a severe accident here and represent unique waste disposal challenges. Japan Discovers Plutonium Far From Crippled Reactor, Wall Street Journal, Toko Sekiguchi, Oct 1, 2011 reported that, "TOKYO—Trace amounts of plutonium were found as far as 28 miles from the damaged Fukushima Daiichi nuclear-power plant, the first time that the dangerous element released from the accident was found outside of the immediate area of the plant."

In the meantime absent an acceptable storage facility for the waste, public health and the environment are impacted that will result in increased offsite costs. The same would happen here. Today, neither New Hampshire nor Massachusetts has access to a low-level radioactive waste disposal facility.

Japan faces costly, unprecedented radiation cleanup,[12] Yoko Kubota,TOKYO, Thu Aug 25, 2011 8:25am EDT

> Another major headache is where to store the radioactive waste like dirt and water generated from cleanup work.
>
> Currently, as with Takita's efforts, the waste is stored within the property where the cleanup took place. Some schools have a heap of radioactive dirt in the corner of their playgrounds, covered with plastic sheets, and residents bury sacks of contaminated waste in their yards.

---

[11] The Enormity Of Decontaminating Japan And Decommissioning Fukushima, Fukushima Project, Reuters, May 17, 2011 (Hyperlink)

[12] Japan faces costly, unprecedented radiation cleanup[12], http://www.reuters.com/article/2011/08/25/us-japan-nuclear-decontamination-idUSTRE77O3LI20110825, Yoko Kubota,TOKYO | Thu Aug 25, 2011 8:25am EDT

"The issue of disposal zones is the most important for decontamination and unless plans are made, it won't move forward," said Kunihiro Yamada, a professor at Kyoto Seika University who does cleanup work in Fukushima city.

The amount of radioactive waste from decontamination is likely to be tens of millions of tonnes and the government in the long run plans to build an underground disposal facility to store this, though when and where is unclear. (Emphasis added)

NextEra's SAMA application does not specifically mention a waste disposal plan and estimated costs. Section F.3.4.2 says simply: Cost of farm decontamination for the various levels of decontamination ($/hectare) = $1,084 & $3,408; Cost of non- farm decontamination for the various levels of decontamination ($/person)=$5,779 & $15,412; Average cost of decontamination labor ($/person-year) =$ 67,427. And at F.4.2 Offsite Economic Costs, it says that the process for cleanup and refurbishment or decontamination; but the total estimated cost for each process is not provided. Also, the SEIS fails to provide any information.

Background: For context, it is important to understand that the MACCS2 code assumptions were based upon a weapons event. In a weapon's event the waste could be shipped to Utah or to the Nevada Test Site. The Greater- than- Class C waste expected in a reactor accident would not have a repository likely available to receive such a large quantity of material in the foreseeable future. Like in Japan, it would be orphaned.

Also, the costs incurred for safeguarding the wastes and preventing their being re-suspended or seeping through to the groundwater is not accounted for in the model. Even optimistically assuming a repository becoming available, (Utah' site is approximately one-square mile and the volume of waste from a severe accident at NextEra, as we have seen from Fukushima would likely require an unimaginably larger facility) it seems unlikely that there would be a sufficient quantity of transport containers and communities not objecting to the hazardous materials going over their roads and through their communities. Fukushima is now

showing that leaving it in piles covered by tarps does not isolate it from the environment-groundwater or air.

Radioactive waste disposal conundrum slowing recovery efforts, Mainichi, Sept 5, 2011

> FUKUSHIMA -- The law had not anticipated the radioactive contamination beyond the gates of nuclear power plants, and has left not only Fukushima Prefecture but also municipalities in the Tokyo metropolitan area with radiation-tainted waste that has no place to go.
>
> In Fukushima Prefecture, the need to decontaminate residences and roads has become increasingly urgent, while little headway has been made in securing temporary storage for radiation-tainted mud. And while the central government is hoping to set up interim storage facilities in the prefecture, no concrete timeline has been established. In addition, rubble still litters Japan's northeastern coast.
>
> The Date Municipal Government has plans to decontaminate the entire city, which will involve the removal of mud and grass from gutters and gardens, where radioactive materials tend to accumulate. And while it is searching for waste storage locations in the five towns that existed before they were incorporated into the city, for the time being residents will be asked to keep the tainted materials on their property.
>
> Residents have been instructed by the city to store the waste in thick plastic bags, preventing the contents from seeping into groundwater. But those who use well water in their daily lives are not convinced of the measure's effectiveness.
>
> "We want the decontamination process to take place as soon as possible, and for the young people who have evacuated elsewhere to come back," Kanno said.
>
> Fukushima is the third largest prefecture in the country, with a large area of mountainous terrain. As a result, use of water mains stands at 92.4 percent of the population -- lower than the national average of 97.5 percent -- leaving many residents, like those in Kamioguni, worried about the effects of radioactive waste on their groundwater.
>
> The central government announced on Aug. 26 that "for the time being, it is realistic for cities, towns, villages and communities to set up temporary storage space for tainted waste that is left over from decontamination measures." While the government's nuclear disaster headquarters is aware that local governments are having difficulty securing temporary storage sites, it says, "We have no choice but to ask each municipality to make those decisions."
>
> "The government will likely force interim storage facilities onto the communities close to the nuclear power plant, where the chances of residents being able to return home are slim," one said.
>
> "It will take quite some time before (the government) earns the understanding and cooperation of residents. (Emphasis added)

Slow cleanup efforts and the absence of available interim secured waste disposal will result in recontamination of cleaned-up areas, increasing offsite costs.

Mainichi Japan reported, October 11, 2011, *Residents near Fukushima mountains face nuclear recontamination every rainfall* reported that:

> ...worries are growing particularly among Fukushima Prefecture residents over drawn-out and in some cases apparently futile nuclear decontamination operations.
>
> The unease is especially strong in areas in and around mountains that must be repeatedly decontaminated, as every rainfall brings a new batch of radioactive substance-contaminated leaves and soil washing down from the hills. **(Seabrook's LRA, 2.10 "The terrain varies from hilly to mountainous except along the coast.")**
>
> "There's no point in doing just one round of official decontamination," he told the Mainichi. "We residents will get nowhere near anything like peace of mind if decontamination operations can't be done regularly."
>
> According to guidelines in a Ministry of Agriculture, Forestry and Fisheries study released on Sept. 30, removing fallen leaves and other natural forest debris from the area within about 20 meters of residential properties is effective in keeping contamination at bay. However, the guidelines also warn that "conifer needles also accumulate radioactive cesium over time, and can normally be expected to fall after three to four years," signaling a constant and long-term need to keep clearing properties of fallen needles. **(SAMA does not consider)**
>
> Furthermore, the problem of where to put all the contaminated material collected in the cleanups remains a serious headache.
>
> On top of concerns about the sheer volume of contaminated material and manpower, there is also the issue of the important natural roles played by forests, such as collecting water that eventually ends up as well water.
>
> The village plans to decontaminate all the forest under its jurisdiction over the next 20 years, but "the village needs the forests to guarantee its source of fresh water," the decontamination project official said. "Is there no way to do decontamination while at the same time preserving the functions of the forest, without cutting down the trees?" **(Seabrook's LRA, F.4.2 implies 10 years for remediation/cleanup)**

Burning the contaminated materials, as we have seen in Japan, simply results in contaminating other areas and does not solve the waste problem due to the huge amount of "orphaned" radioactive ash.

Japan cities face growing radioactive ash, troubles ahead, Kiyoshi Takenaka, Reuters UK, October 17, 2011 reported that:

> Although the government aims to bring the Fukushima crisis under control by December, researchers say that problems arising from the radiation, scattered over mountains, rivers and residential areas, are set to persist for years.

"Residents say they are worried about their children's health and grandchildren's health. Faced with such pleas, we just cannot make a move," an Ohtawara city official said, explaining why the ash has not been taken to a nearby city dump.

Ohtawara has already cut the frequency of garbage collection by half to hold down the generation of radioactive ash, by-product of burning contaminated leaves and branches.Nonetheless, fresh bags of radioactive ash will have to be left in empty outdoor space at the incineration facility with no proper shelter around them, the official said.

A draft plan by the Environment Ministry calls for the government to take responsibility for disposing of ash and sludge with radiation levels above 8,000 becquerels/kg, but a ministry official said nothing concrete has been decided.
Following hydrogen explosions at the Fukushima plant in March, rainfall has brought radiation down to the earth's surface.

In northern Japan, stored-up radioactive ash and dehydrated sludge from the sewage treatment process alone totalled 52,000 tonnes in mid-September, up 63 percent from levels at the end of July, data from the Transport Ministry showed.

The volume is still growing by about 360 tonnes a day.

The growing piles of radioactive ash are also causing financial headaches for local governments. "I doubt the problem will go away in a year or two. It takes 30 years for caesium 137 to decay by half. Each time it rains, caesium deposited in mountains will be washed down to where people live," Kobe University professor Tomoya Yamauchi said.

In the meantime absent an acceptable storage facility for the waste, public health and the environment are impacted that will result in increased offsite costs. The same would happen here.

Once again, there is no basis for the Staff's assurance that they "identified no new and significant information related to the postulated accidents of other available information. Therefore there are no impacts related to postulated accidents beyond those discussed in the GEIS." (Ibid, 5-3)

d. Decontamination Methods Assumed in Model Ineffective – Costs Will Increase

The MACCS2 Decontamination Plan is described in part in the Code's Manual for MACCS2: Volume I, User's Guide (NUREG/CR-6613, Vol. 1) Prepared by D. Chanin and M.I.

Young, May 1998. Section 7.5 Decontamination Plan describes some of its cleanup assumptions. It says at 7-10 that,

> Many decontamination processes (e.g., plowing, fire hosing) reduce groundshine and resuspension doses by washing surface contamination down into the ground. Since these processes may not move contamination out of the root zone, the WASH-1400 based economic cost model of MACCS2 assumes that farmland decontamination reduces direct exposure doses to farmers without reducing uptake of radioactivity by root systems. Thus decontamination of farmland does not reduce the ingestion doses produced by the consumption of crops that are contaminated by root uptake. (Emphasis added)

The Japanese are using **hosing and plowing under fields** and demonstrate that this assumed method of cleanup, there and here, is not effective. Hosing and plowing do not remove the contamination; instead, it simply moves it to another place, such as the groundwater, to reappear at a later date and require more monies to either start again or bare the cost of writing off the area permanently.

True radiation decontamination still a long way away, Mainichi October 7, 2011

> The three main decontamination methods that have been highly publicized through media reports are: the stripping away of surface soil from school playgrounds and athletic fields, the removal of mud accumulated in gutters, and the washing of roofs using high-pressure water cleaners. While the first method is considered effective, the remaining two have been found to be effective only to a certain point, and some especially warn against overestimating the effects of high-pressure water cleaners.
>
> "It might make you feel like you're decontaminating, but there's a limit to the amount of radioactive cesium that's caked onto roofs that can be eliminated with high-pressure water cleaners," says Kunihiro Yamada, a professor of environmental science at Kyoto Seika University. "The water cleaners wash surface dirt off, but then that tainted water goes into sewers and can contaminate rivers, thereby affecting farm goods and seafood. If people in highly populated areas were to begin using water cleaners, we may end up finding people forcing tainted water onto each other."
>
> According to Yamada, ("Radiation Contamination and Recovery Project" with colleagues from Fukushima University and Osaka University) radioactive cesium is believed to exist in three states: dissolved in water, loosely bonded to organic materials such as moss and leaves, or tightly bonded to rock such as silicate salt. In other words, if soil is removed and washed away with high-pressure water cleaners, radioactive cesium found in surface soil and gutters can be eliminated. The cesium that has become affixed to roofs remains, however.
>
> "Apparently the roof had been cleaned using high-pressure water cleaners, but that was as low as the radiation levels got," says Yamauchi. "To bring the roof's radiation levels down, there's probably no other way but to replace the roof. First and foremost, we must aim to bring indoor radiation levels to 0.05 microsieverts, which they were before the disaster unfolded, and thereby creating safety zones."

According to Yamauchi, just like what has happened with roofs, radioactive cesium has become stuck to asphalt on the road, concrete utters and cobblestones, and high-pressure water cleaners can only do so much.

At a lecture held at the Japan National Press Club in Tokyo on Sept. 30, Kodama explained that radiation decontamination referred to isolation of radioactive materials in the environment to await its radioactive decay, and that the "radiation decontamination" that he had thus far conducted at kindergartens and other facilities in the Fukushima Prefecture city of Minamisoma were not enough. "The decontamination I've done is a type of emergency measure to protect children and pregnant women, and not true decontamination." He continued: "Permanent decontamination requires the knowledge and technology of experts and corporations, and a massive amount of funds. It must not become an interest-driven public project."

"What residents want is not half the exposure to radiation," says Yamada. "What they want is for a return to levels that allow them to live with peace of mind. Massive amounts of radioactive materials have been spread across wide areas in the ongoing disaster, so we can't count on the weathering effect. There's also the possibility that radiation will not only spread, but will start to accumulate in large concentrations in certain places. The half life of cesium 137 is approximately 30 years, but that of cesium 134 is 2 years. What the government has said is the equivalent of saying that they won't engage in full-fledged decontamination activities."

With challenges such as the designation of temporary radioactive waste dumps and interim storage facilities yet unsolved, the road to true decontamination remains a long one gage in full-fledged decontamination activities."

Why did the MACCS2 code, NRC Staff, NextEra and Japanese authorities assume hosing and plowing under fields was cleanup? Again, there is no basis for the Staff's assurance that they "identified no new and significant information related to the postulated accidents of other available information. Therefore there are no impacts related to postulated accidents beyond those discussed in the GEIS." (Ibid, 5-3)

The MACCS2 economic cost model, is based on WASH-1400; WASH-1400, in turn, was based on clean up after a nuclear explosion. However, cleanup after a nuclear bomb explosion is not comparable to clean up after a nuclear reactor accident and assuming so will underestimate cost. Nuclear explosions result in larger-sized radionuclide particles; reactor accidents release small sized particles. Decontamination is far less effective, or even possible, for small particle sizes. Nuclear reactor releases range in size from a fraction of a micron to a couple of microns; whereas nuclear bomb explosions fallout is much larger- particles that are ten to

hundreds of microns. These small nuclear reactor releases get wedged into small cracks and crevices of buildings making clean up extremely difficult or impossible.

WASH-1400's referenced nuclear weapon clean up experiments involved cleaning up fallout involving large mass loading where the there was a small amount of radioactive material in a large mass of dirt and demolished material. Only the bottom layer will be in contact with the soil and the massive amount of debris can be swept up with brooms or vacuums resulting in a relatively effective, quick and cheap cleanup that would not be the case with a nuclear reactors fine particulate. The Japanese have learned the hard way that it is not possible to get the contaminants out of crevices and off roofs and roads, as those in Chernobyl before had discovered.

Third a weapon explosion results in non-penetrating radiation so that workers only require basic respiration and skin protection. This allows for cleaning up soon after the event. In contrast a reactor release involves gamma radiation and there is no gear to protect workers from gamma radiation. Therefore cleanup cannot be expedited, unless workers health shamefully and unethically is ignored. Decontamination is less effective with the passage of time.

e. <u>Topography- Areas Unlikely to be Decontaminated- Ignored</u>

Lessons learned from Fukushima show that forests and shorelines, for example, cannot realistically be cleaned up and decontaminated. The area within 50-miles of Seabrook Station is mountainous, hilly, and encompasses large and small waterways, miles of beaches, wetlands, forests and park land. If properly considered offsite costs will escalate. **Again, there is no basis for the Staff's assurance** that they "identified no new and significant information

related to the postulated accidents of other available information. Therefore there are no impacts related to postulated accidents beyond those discussed in the GEIS." (Ibid, 5-3)

Forests: Institute probing radioactive contamination of Fukushima forests, Japan Times, Sep. 17, 2011

> In August, the government acknowledged difficulties in removing soil and ground cover from the forests, due mostly to the volume of radioactive waste that would be generated by the effort.
>
> "Huge volumes of soil and other (contaminated) items would be involved because the forests occupy a huge area."
>
> The government effectively shelved any approach to decontaminating forests when it said that removing both the contaminated soil and compost materials would strip the forests of important ecological functions, including water retention.

Ocean: Lessons learned from Fukushima shows that it is necessary to understand the ocean currents to determine whether or not the contamination will linger for years contaminating and re-contaminating beaches and marine life increasing costs from a continuous need to cleanup and pay for damages to the environment.[13] (Discussed above, page 9)

Urban areas: Fukushima also shows that urban areas will be considerably more expensive and time consuming to decontaminate and clean than rural areas. The LRA clearly shows urban areas within 50-miles likely to be contaminated in a release of long duration.

[13] Fukushima's radioactive sea contamination lingers, Andy Coghlan, New Scientist, Sept 30, 2011; Radioactive cesium may be brought back by Ocean in 20-30 years, Tokyo Times, 09.16.11; *Radioactive plankton found near Fukushima plant*, Mark Willacy, ABC News, October 15, 2011

5. Costs Severe Accident Will Be Huge- What Federal Agency will be in Charge and Will Pay?

No third party (NRC, EPA, or FEMA) has clear authority to cleanup offsite after a severe accident at Seabrook; Cleanup Standards are not determined; and no funding source for cleanup is identified.

On November 10, 2010, Inside EPA released a report (published by Inside Washington, Inside EPA/s Superfund Report), *Agencies Struggle to Craft Offsite Cleanup Plan for Nuclear Power Accidents*, by Douglas Guarino, Associate Editor. The report, along with its supporting FOIAs, is available on line.[14] If there is no federal authority in charge cleanup will take longer and the longer it takes the more expensive the process will be and the less likely cleanup will occur. Also if EPA is in charge state and local governments and the public are required to be allowed to participate in decision-making. This will increase costs. The impact of no agreed upon cleanup standard is discussed above. No funding source for cleanup has obvious implications for the nation's economy as a whole. None of these issues are addressed by Staff.

Fukushima has the exact same issues and underscores that until these issues are resolved – who is in charge, who pays, and what are the cleanup standards- cleanup will be delayed and result in higher consequences and costs. Consequences and offsite costs are related to time. The following articles make this plain.

---

[14] http://environmentalnewsstand.com/Environmental-NewsStand-General/Public-Content/agencies-struggle-to-craft-offsite-cleanup-plan-for-nuclear-power-accidents/menu-id-608.html

Tokyo Times - TEPCO will need 1 trillion yen from the govt for compensation of disaster victims Oct 23, 2011 explained the current estimate- 4.5 trillion yen.

> Tokyo Electric Power Co. intends to ask the government a sum of 1 trillion yen (US Dollars $13,027,611,657) to help in the immediate compensation of victims of the nuclear disaster in the Fukushima Daiichi power plant.
>
> The amount will cover compensation for mental sufferings of victims as a result of evacuation and to pay for the losses incurred by small businesses following the nuclear disaster.
>
> It is estimated that compensation for victims would cost TEPCO around 4.5 trillion yen in a two-year period. The 1 trillion yen sought from the government would cover the amount of compensation for victims for this fiscal year.

In the article, U.S. ill-equipped to deal with Japan-like nuclear meltdown, Eliot Caroom, Star-Ledger, September 201, 2011 quoting Howard Kunreuther, a Univ Pennsylvania Wharton School Professor, said:

> The disaster in Fukushima has laid bare one truth on which experts and officials from the Nuclear Regulatory Commission agree: A disaster here would result in losses requiring the government to make payouts of epic proportions.
>
> That's because ... the U.S. nuclear insurance fund, established by a 1957 law called the Price-Anderson Act, only has around $12.6 billion in reserve.
>
> "If you have an accident or something like Fukushima, then Price-Anderson can't handle those kinds of losses," said Wharton School professor Howard Kunreuther, who specializes in public policy.
>
> Even though U.S. plants aren't threatened by tsunamis like Japan's, they can still be damaged by hurricanes, terrorist attacks or earthquakes.
>
> The Associated Press reported this month that although the risk of an earthquake causing an accident at a U.S. nuclear plant is small, it's far greater than previously thought — 24 times as high in one case. Last week, staff at the NRC recommended nuclear power plant owners immediately re-evaluate earthquake and flooding hazards at their plants, following the advice of a task force created after Fukushima.
>
> If a catastrophe did strike and a nuclear accident rose to the level of Fukushima, who would pay the tab?The insurance mandated by the Price-Anderson act has more than $12 billion in it, an amount that has been raised over the years since the law was implemented in 1957.
>
> "If you broke down what the damage was, the cost of Fukushima, business interruption, supply chain problems, my guess is the (United States) government would not step in on any of that," said Kunreuther. "At the end of the day, there may very well be lawsuits or some kind of settlements with respect to what the government would have to do or the utilities would have to do."

Inside EPA's, referenced above, FOIA document NRC-FEMA-EPA White paper: Potential Authorities and/or Funding Sources for Off-site Cleanup Following a Nuclear Power Plant Accident, July 27, 2010, Pg., 6

> **Findings:**
>
> Potential Authorities and/or Funding Sources for Off-Site Cleanup Following a Nuclear Power Plant Incident
>
> - *Price-Anderson Act:*
>   - ANI does not cover environmental cleanup costs under their primary insurance policy. It is anticipated that the secondary insurance policy will behave in a similar manner.

Again, there is no basis for the Staff's assurance that they "identified no new and significant information related to the postulated accidents of other available information. Therefore there are no impacts related to postulated accidents beyond those discussed in the GEIS." (Ibid, 5-3)

IV. ADDITIONAL DEFICIENCIES IGNORED BY NRC STAFF THAT MINIMIZED OFFSITE COSTS

The SAMA analysis for Seabrook minimized the potential amount of radioactive releases in a potential severe accident at Seabrook Station in additional ways, many underscored by Fukushima. They include the following and were not properly considered in the draft SEIS. Before finalizing the SEIS we respectfully request that Staff consider the following; if the Staff disputes the points raised we ask that a written response is provided that includes the bases for the dispute inclusive of all references and studies for independent verification.

A. Source Term

The source terms used by NextEra to estimate the consequences of severe accidents (radionuclide release fractions generated by the Modular Accident Analysis Progression, MAAP[15]) code, has not been validated by NRC. They are consistently smaller for key radionuclides than the release fractions specified in NUREG-1465 and its recent revision for high-burnup fuel. The source term used results in lower consequences than would be obtained from NUREG-1465 release fractions and release durations.

It has been previously observed that MAAP generates lower release fractions than those derived and used by NRC in studies such as NUREG-1150. A Brookhaven National Laboratory study that independently analyzed the costs and benefits of one SAMA in the license renewal application for the Catawba and McGuire plants noted that the collective dose results reported by the applicant for early failures.

> ...seemed less by a factor between 3 and 4 than those found for NUREG-1150 early failures for comparable scenarios. The difference in health risk was then traced to differences between [the applicant's definitions of the early failure release classes] and the release classes from NUREG-1150 for comparable scenarios ... the NUREG-1150 release fractions for the important radionuclides are about a factor of 4 higher than the ones used in the Duke PRA. The Duke results were obtained using the Modular Accident Analysis Package (MAAP) code, while the NUREG-1150 results were obtained with the Source Term Code Package [NRC's state-of-the-art methodology for source term analysis at the time of NUREG-1150] and MELCOR. Apparently the differences in the release fractions ... are primarily attributable to the use of the different codes in the two analyses. [16]

Thus the use of source terms generated by MAAP, a proprietary industry code that has not been independently validated by NRC, appears to lead to anomalously low consequences when compared to source terms generated by NRC staff. In fact, NRC has been aware of this

[15] See, for example, ER. E. F-32, F-45-48

[16] J. Lehner et al., "Benefit Cost Analysis of Enhancing Combustible Gas Control Availability at Ice Condenser and Mark III Containment Plants," Final Letter Report, Brookhaven National Laboratory, Upton, NY, December 23, 2002, p. 17. ADAMS Accession Number ML031700011.

discrepancy for at least two decades. In the draft "Reactor Risk Reference Document" (NUREG-1150, Vol. 1), NRC noted that for the Zion plant (a four-loop PWR), that "comparisons made between the Source Term Code Package results and MAAP results indicated that the MAAP estimates for environmental release fractions were significantly smaller. It is very difficult to determine the precise source of the differences observed, however, without performing controlled comparisons for identical boundary conditions and input data."[17] We are unaware of NRC having performed such comparisons.

The NUREG-1465 source term was also reviewed by an expert panel in 2002, which concluded that it was "generally applicable for high-burnup fuel."[18] This and other insights by the panel on the NUREG-1465 source term are being used by the NRC in "radiological consequence assessments for the ongoing analysis of nuclear power plant vulnerabilities."[19]

In light of this, it is clear that Next Era should not have used a MAAP-generated source terms in its SAMA analysis. It minimized consequences. NRC Staff is silent on this source of minimization and we request a response justifying their apparent approval of NextEra's choice of the MAAP code that has not been validated by NRC.

B. Meteorology

1. Straight-Line Gaussian Plume Model Used by NextEra is Deficient

Introduction

[17] U.S. NRC, "Reactor Risk Reference Document: Main Report, Draft for Comment," NUREG-1150, Volume 1, February 1987, p. 5-14.
[18] J. Schaperow, U.S. NRC, memorandum to F. Eltawila, "Radiological Source Terms for High-Burnup and MOX Fuels," December 13, 2002.
[19] J. Schaperow (2002), op cit.

The straight- line Gaussian plume model does not subsume all reasonably possible meteorologic patterns, and is not appropriate for Seabrook's coastal location. It did not predict site-specific atmospheric dispersion. The MACCS2 code used by NextEra could not model many *site-specific* conditions and did not determine economic costs for Seabrook's affected area that includes within its 50-mile radius densely populated areas. Appendix E (2.2) says that, "There are two metropolitan areas within 50 miles of the site; Manchester, New Hampshire (31 miles west-northwest), and Boston, Massachusetts (41 miles south-southwest)."

The Gaussian plume model assumes that a released radioactive plume travels in a steady-state straight-line, i.e., the plume functions much like a beam from a flashlight. The MACCS2 code used by NextEra was based upon this straight-line, steady-state model; it also assumed meteorological conditions that are steady in time and uniform spatially across the study region. However, the assumption of a steady-state, straight-line plume are inappropriate when complex inhomogeneous wind flow patterns happen to be prevailing in the affected region. The meteorological inputs that NextEra's Gaussian plume model ignored or minimized by use of the mean include the variability of winds, sea breeze effects, the behavior of plumes over water, and re-suspension of contaminants.

Another significant defect in NextEra's model - its meteorological inputs (e.g., wind speed, wind direction, atmospheric stability and mixing heights) into the MACCS2 are based on data collected by Applicant at a single, on-site anemometer and that the data is from only one year.

2. Deficiencies of NextEra's Use of a Straight-Line Gaussian Plume Model to Characterize Consequences in Seabrook's SAMA analysis

NextEra's straight-line, steady-state Gaussian plume model does not allow consideration for the fact that the winds for a given time period may be spatially varying, and it ignores the presence of sea breeze circulations which dramatically alter air flow patterns. Because of these failings the straight-line Gaussian plume model is not appropriate for Seabrook's coastal location. The nearby presence of the ocean greatly affects atmospheric dispersion processes and is of great importance to estimating the consequences in terms of human lives and health effects of any radioactive releases from the facility, and that the transport, diffusion, and deposition of airborne species emitted along a shoreline can be influenced by mesoscale atmospheric motions. These cannot be adequately simulated using a Gaussian plume model.

3. Sea breeze effect

The sea breeze effect, ignored by NextEra's model, is a critical feature to consider at Seabrook's coastal location. The sea breeze circulation is well documented (Slade, 1968, Houghton, 1985, Watts, 1994, Simpson, 1994).... [T]he presence of a sea breeze circulation changes the wind directions, wind speeds and turbulence intensities both spatially and temporally through out its entire area of influence. The classic reference *Meteorology and Atomic Energy*, (Section 2-3.5) (Slade, 1968) succinctly comments on the importance of sea breeze circulations as "The sea breeze is important to diffusion studies at seaside locations because of the associated changes in atmospheric stability, turbulence and transport patterns. Moreover its almost daily occurrence at many seaside locations during the warmer seasons results in significant differences in diffusion climatology over rather short distances. Further "[t]The atmospheric model included in the [MACCS2] code does not model the impact of terrain effects on atmospheric dispersion." 1997 User Guide for MACCS2.

Regarding sea breeze it is clear that:

- The meteorological data collected at the Seabrook site would not reflect the occurrence of the sea breeze in terms of wind speeds and direction is not necessarily true.
- A measurement at a single station tower will not provide sufficient information to allow one to project how an accidental release of a hazardous material would travel. Measurement data from one station will definitely not suffice to define the sea breeze.
- The sea breeze is not beneficial in dispersing the plume and in decreasing doses. In fact, the development of sea breeze flow that would transfer a release inland is the greatest danger. If the same meteorological conditions (strong solar insolation, low synoptic-scale winds) that are conducive to the formation of sea breezes at a coastal site occurred at a non coastal location, the resulting vertical thermals developing over a pollution source would carry contaminants aloft. In contrast, at a coastal site, the sea breeze would draw contaminants across the land and inland subjecting the population to potentially larger doses.

4. Behavior of Plumes over Water

NextEra's Gaussian plume model assumed that plumes blowing out to sea would have no impact. A plume over water, rather than being rapidly dispersed, will remain tightly concentrated due to the lack of turbulence. The marine atmospheric boundary layer provides for efficient transport. Because of the relatively cold water, offshore transport occurs in stable layers. Wayne Angevine's (NOAA) research of the transport of pollutants on New England's coast concluded that major pollution episodes along the coast are caused by efficient transport of pollutants from distant sources. "The transport is efficient because the stable marine boundary layer allows the polluted air masses or plumes to travel long distances with little dilution or

chemical modification. The sea-breeze or diurnal modulation of the wind, and thermally driven convergence along the coast, modify the transport trajectories." Therefore a plume will remain concentrated until winds blow it onto land. [Zager et al.; Angevine et al. 2006[20]]. This can lead to hot spots of radioactivity in places along the coast. An alternative model that NextEra did not use, CALPUFF, could provide the ability to account for reduced turbulence over water and could be used for sensitivity studies.

5. Storms

The storm cycle consists generally of northeasters in the winter and spring and hurricanes sometimes occur in the late summer and fall. The accompanying strong and variable winds would carry a plume to a considerable distance. The storm cycle is projected to increase in frequency and in severity over the license renewal period - note noted by the Staff.

6. Geographical Variations, Terrain Effects, and Distance

The topography of a coastal environment plays an important role in the sea breeze circulation, and can alter the typical flow pattern expected from a typical sea breeze along the coastline. But "[t]The atmospheric model included in the [MACCS2] code does not model the impact of terrain effects on atmospheric dispersion." [1997 User Guide for MACCS2.]

The Gaussian plume model also does not take terrain effects, which have a highly complex impact on wind field patterns and plume dispersion, into account. Wind blowing inland will experience the frictional effects of the surface which decrease speed and direction. EPA has recognized that "geographical variations can generate local winds and circulations, and modify

[20] Angevine, Wayne; Tjernström, Michael; Žagar, Mark, Modeling of the Coastal Boundary Layer and Pollutant Transport in New England, Journal of Applied Meteorology and Climatology 2006; 45: 137-154

the prevailing ambient winds and circulations" and that "a*ssumptions of steady-state straight-line transport both in time and space are inappropriate.*" [EPA Guidelines on Air Quality Models (Federal Register Nov. 9, 2005, Section 7.2.8, Inhomogeneous Local Winds, italics added EPA's November 9, 2005 modeling Guideline (Appendix A to Appendix W) lists EPA's "preferred model;" the Gaussian plume model used by NextEra (ATMOS) is not on the list. EPA recommends that CALPUFF, a non-straight-line model, be used for dispersion beyond 50 Km.[21]

The essential difference between the models that EPA recommends for dispersion studies and the two-generation-old Gaussian plume model (ATMOS) used by NextEra and the NRC is more than determining where a plume will likely to go. Major improvements in the simulation of vertical dispersion rates have been made in the EPA models by recognizing the importance of surface conditions on turbulence rates as a function of height above the ground (or ocean) surfaces. We know that turbulence rates and wind speeds vary greatly as a function of height above a surface depending upon whether the surface is rough or smooth (trees versus over water transport) (Roughness), how effectively the surface reflects or absorbs incoming solar radiation (Albedo) and the degree that the surface converts latent energy in moisture into thermal energy (Bowen ratio). These parameters are included in the AERMOD and CALPUFF models and determine the structure of the temperature, wind speed and turbulent mixing rate profiles as a function of height above the ground. NextEra's ATMOS model does not include these parameters. This is an especially important deficiency when modeling facilities located along coastlines, such as Seabrook.

[21] Appendix A to Appendix W to 40 CFR Part 51, EPA Revision to the Guideline on Air Quality Models: Adoption of a Preferred General Purpose (Flat and Complex Terrain) Dispersion Model and Other Revisions; Final Rule, November 9, 2005. http://www.epa.gov/ scram001/guidance/guide/appw_05.pdf.

7. NextEra's Inputs to the MACCS2 Code Are Deficient and Did Not Account for Site-Specific Conditions

a. Meteorological Inputs

One fundamental defect in NextEra's use of the MACCS2 code is that its meteorological inputs to that code are all based on the straight-line Gaussian plume model. This model does not allow consideration of the fact that the winds for a given time period may be spatially varying. The 1997 User Guide for MACCS2, SAND 97-0594[22] makes the point: "The atmospheric model included in the code does not model the impact of terrain effects on atmospheric dispersion."

Indeed, the MACCS2 Guidance Report, June 2004,[23] is even clearer that NextEra's inputs to the code do not account for variations resulting from *site-specific* conditions such as those present at Seabrook. (1)The "code does not model dispersion close to the source (less than 100 meters from the source);" thereby ignoring resuspension of contamination blowing offsite. (2) The code "should be applied with caution at distances greater than ten to fifteen miles, especially if meteorological conditions are likely to be different from those at the source of release." There are large potentially affected population concentrations more than 10-15 miles from Seabrook. (See LRA) (3) "Gaussian models are inherently flat-earth models, and perform best over regions where there is minimal variation in terrain." According to the Seabrook License Renewal Application, "The terrain varies from hilly to mountainous except along the coast." (ER. F, Section 2-10, pg., 2-70)

[22] Chanin, D.I., and M.L. Young, Code Manual for MACCS2:Volume 1, User's Guide, SAND97-0594 Sandia National Laboratories, Albuquerque, NM, (1997)
[23] MACCS2 Guidance Report June 2004 Final Report page 3-8:3.2 Phenomenological Regimes of Applicability

A second defect in the Applicant's inputs into the MACCS2 code lies in the data itself. NextEra input meteorological data for only a single year and the data was collected from a *single, on-site* weather station.

One year of data would have been insufficient even if more than one station had been used. Seasonal wind distributions can vary greatly from one year to the next. "*The NRC staff considers 5 years of hourly observations to be representative of long-term trends at most sites,*" although "with sufficient justification [not presented by NextEra here] of its representativeness, the minimum meteorological data set is one complete year (including all four seasons) of hourly observations." (NRC Regulatory Guide 1.194, 2003)

The simple fact is that measurements from a single onsite anemometer will not provide sufficient information to project how an accidental release of a hazardous material would travel; certainly not for cases when the sea breeze was just developing and for cases when the onshore component winds do not reach entirely from the ground to the anemometer height. The occurrence of a sea breeze would not be identified. The anemometer would likely indicate an offshore wind indication. Further basing wind direction on the single on-site meteorological tower data ignores shifting wind patterns away from the Seabrook Plant including temporary stagnations, re-circulations, and wind flow reversals that produce a different plume trajectory. Since the 1970s, the USNRC has historically documented all the advanced modeling technique concepts and potential need for multiple meteorological towers especially in coastal regions. NRC Regulatory Guide 123 (Safety Guide 23) On Site Meteorological Programs 1972, states that, "at some sites, due to complex flow patterns in non-uniform terrain, additional wind and temperature instrumentation and more comprehensive programs may be necessary."[Ibid]; and an EPA 2000 report, Meteorological Monitoring Guidance for Regulatory Model Applications,

EPA-454/R-99-005, February 2000, Sec 3.4 points to the *need for multiple inland meteorological monitoring sites.* See also Raynor, G.S.P. Michael, and S. SethuRaman, 1979, Recommendations for Meteorological Measurement Programs and Atmospheric Diffusion Prediction Methods for Use at Coastal Nuclear Reactor Sites. NUREG/CR-0936.

NextEra should have taken data from more locations over a longer period; and modified the MACCS2 code to account for the inability of the code that NextEra used to account for site-specific conditions. "The user has total control over the results that will be produced." [1997 User Guide, Section 6.10].

Finally, MACCS2 is not a state-of-the-art computer model. It does not rely upon or utilize current understandings of boundary layer meteorological parameterizations such as those adopted by the EPA in the models AERMOD OR CALPUFF (EPA, 2001). The Gaussian plume model employed in the Seabrook MACCS2 model may be the standard for NRC but it is not the basis for advanced modeling used by other US regulatory agencies. Computational time should not be a major factor in the choice of a dispersion model used for non-real time applications. The idea that randomly chosen meteorological conditions would give the same results as inputting meteorological conditions as a function of time is erroneous. To accommodate the real role of persistence in dispersion modeling EPA requires sequential modeling for all averaging times from 3 hour averages to annual averages. The fact that a model may seem to be conservative in particular applications or in limited data comparisons does not mean that the model is better or should be recommended. Models can be conservative but have incorrect simulations of the underlying physics. Sensitivity studies do not add useful information if the primary model is flawed.

b. The Affected Area

NextEra's choice of a straight-line Gaussian plume rather than a variable trajectory model drastically reduced, to a wedge, the size of the area that might potentially be impacted by a release. NextEra's analyses also assumed a "small" accident that had no real impact beyond 10 miles. NextEra did not consider the potential of the by far largest, and perhaps also the most likely, potential radiological release – from the spent fuel pool. In addition, NextEra chose to use the MACCS2 Code that, *absent site specific modifications that NextEra chose not to make*, cannot provide credible cost estimates.

The use of a variable trajectory model, rather than the straight-line Gaussian plume, would have significantly increased the area potentially affected by a released radioactive plume, and thus would also greatly increase the size of the affected population and property, and the economic effect, beyond 10 miles. For example, NextEra's MACCS2 analysis does not assume an evacuation zone of greater than 10 miles. A second major defect in the MACCS2 inputs is that NextEra apparently assumed that the only source of radiation in the event of an accident would be from the reactor within the containment. The potentially far greater source of leaked radiation, the spent fuel pool, contains far more radioactive material. It was ignored.

Absent modifications to permit inputs that address the MACCS2 code limitations discussed above, the MACCS2 code used by NextEra is incapable of providing an accurate estimate of economic consequence.

8. NEPA's Rule of Reason

In another licensing decision, CLI-10-22, pg., 9, the Commission stated that NEPA requirements are "tempered by a practical rule of reason" and an environmental impact statement

is not intended to be a "research document." If relevant or necessary meteorological data or modeling methodology prove to be unavailable, unreliable, inapplicable, or simply not adaptable for evaluating the SAMA analysis cost-benefit conclusions, there may be no way to assess, through mathematical or precise model-to model comparisons, how alternative meteorological models would change the SAMA analysis results."

The plume modeling advocated herein as appropriate for Seabrook's SAMA analysis, instead of NextEra's decision to use the straight line Gaussian model, are not techniques that require research. They are, in fact, established methods that are publically available, routinely used, and appropriate for quantifying atmospheric dispersion of contaminants. Although an effort may be required to adapt these methods for SAMA analyses, this would be very straightforward and research would not be required.

Appropriate meteorological data or modeling methodology is available. There is no shortage of appropriate meteorological data for a licensing model application. Alternative modeling methods that would use more extensive meteorological data are also available.

The applicant chose to use only one year of onsite data collected at the Seabrook's site. Meteorological data is also available from nearby airports and, importantly, processed data on a gridded basis can be obtained from NOAA to augment the onsite meteorological data relied upon for the SAMA analyses that have been provided by NextEra. For example, see Jennifer Thorpe[24] site-specific meteorological study. Also there are several publically available meteorological modeling methods that can simulate variable trajectory transport and dispersion

[24] Thorp, Jennifer E., Eastern Massachusetts Sea Breeze Study, Thesis Submitted to Plymouth State University in Partial Fulfillment of the Requirements for the Degree of Master of Science in Applied Meteorology, May 2009, Appendix A

phenomena. MM5 is one which is routinely used nationally and internationally. There are other options as well. The present state of art of an appropriate meteorological model would use multi station meteorological measurement data as input to the meteorological model. The numerical computations, based upon numerical weather prediction techniques, would compute wind fields appropriate for modeling dispersion over a much larger geographic area than the a single measurement site would be appropriate for.

A second reasonableness criterion is that the modeling method must be reliable. The outputs from such meteorological models that are used to produce inputs for the dispersion models are well accepted and form the basis for the weather predictions provided by the national weather service as well as analyses of air pollution impacts of concern to regulatory agencies. These techniques have been proven to be reliable and acceptable for air quality permitting and policy applications in complex terrain and over large distances for the US EPA , the US Park Service as well as internationally. These techniques would be *more* reliable than using the straight line Gaussian model.

The third reasonableness criterion is that the modeling methods be applicable to SAMA analyses. The methods recommended herein are applicable because with straightforward modifications to incorporate nuclear radiation decay rates, they can produce the fields of concentration values and deposition rates needed for dosage calculations.

The fourth reasonableness criterion is that the modeling methodology be adaptable for evaluating SAMA analysis cost benefit conclusions. There is nothing inherent in variable trajectory models that would prohibit the output concentration and deposition fields from being applied to SAMA analyses.

None of the criteria cited would make the use of alternative models unreasonable to apply to the Seabrook's SAMA analyses.

Further there is no basis to the argument that there may be no way to assess through mathematical or precise model to model comparisons, how alternative meteorological models would change the SAMA analysis results. Some assessments may necessarily be qualitative, based simply upon expert opinion. But this argument seems to undercut the very value of mathematical simulation models in general as a method to assess the impacts of nuclear reactor emissions.

Last, the rationale offered that the use of advanced models would be computationally too expensive and/or burdensome to use are not justified by the actual run time shown in our review of MACCS2 output files. With modern computers, the use of inappropriate models on the basis of differences of computational costs is indefensible.

Invoking the "practical rule of reason" to the most appropriate modeling methodology for application to the Seabrook SAMA analyses would be blatantly dismissive of the concept that the present methods are inappropriate and outdated and that there are indeed alternative modeling available.

There is no basis for the Staff's assurance that they "identified no new and significant information related to the postulated accidents of other available information. Therefore there are no impacts related to postulated accidents beyond those discussed in the GEIS." (Ibid, 5-3)

C. Averaging

NextEra fails to consider the uncertainties in its consequence calculation resulting from meteorological variations by only using mean values (LRA, Appendix E, 2.10) for population dose and offsite economic cost estimates. The Staff's SEIS analysis is inadequate in that it ignores (fails to justify and analyze the effect of) NextEra's choice of averaging in its SAMA.

Dr. Edwin S. Lyman, Senior Staff Scientist, Union of Concerned Scientists report commissioned by Riverkeeper, Inc., November 2007, A Critique of the Radiological Consequence Assessment Conducted in Support of the Indian Point Severe Accident Mitigation Alternatives Analysis[25] provides valuable lessons to apply to Seabrook's SAMA.

The consequence calculation, as carried out by the MACCS2 code, generates a series of results based on random sampling of a year's worth of weather data. The code provides a statistical distribution of the results. We find, based on calculations done at other reactors such as Indian Point, that the ratio of the 95th percentile to the mean of this distribution is typically a factor of 3 to 4 for outcomes such as early fatalities, latent cancer fatalities and off-site economic consequences.

NextEra admits (LRA, F.8.2- Uncertainty) that, ... the inputs to the PRA cannot be known with complete certainty, there is a possibility that the actual plant risk is greater than the mean values used in the evaluation of the SAMA described in the previous sections."

[25] Report available at NRC Electronic Library, Adams Accession Number ML073410093

Kamiar Jamali[26] (*Use of risk in measures in design and licensing of future reactors,* Reliability Engineering and Safety System 95 (2010) 935-943 www.elsevier.com/locate/ress) makes the same observation. He says that,

> It is well- known that quantitative results of PRAs, in particular, are subject to various types of uncertainties. Examples of these uncertainties include probabilistic quantification of single and common cause hardware or software failures, occurrence of certain physical phenomena, human errors of omission or commission, magnitudes of source terms, radionuclide release and transport, atmospheric dispersion, biological effects of radiation, dose calculations, and many others. (935)."

Despite warning, NextEra describes an unconvincing sensitivity analysis (ER, F.8.2-Uncertainty) that they claim resolves the issue. They report, *absent any specifics* of the study, that "to consider the uncertainty, a sensitivity analysis was performed in which an uncertainty factor was applied to the frequencies calculated by the PRA and in subsequent upper bound (UB) benefits were calculated based upon the mean risk multiplied by the this uncertainty factor. The uncertainty factor applied to the ratio of the 95th percentile value of the CDF from the PRA uncertainty analysis to the mean value of the CDF. For Seabrook Station, the 95th percentile value of the CDF is 2.75 E-05/yr; therefore the uncertainty factor is 1.90." NextEra's approach at "proof" is not convincing.

Seabrook's SAMA cost-benefit evaluation should be based on the 95th percentile of the meteorological distribution to be consistent with the approach taken in the License Renewal GEIS, which refers repeatedly to the 95th percentile of the risk uncertainty distribution as an appropriate "upper confidence bound" in order not to "underestimate potential future

[26] Kamiar Jamali, DOE Project Manager for Code Manual for MACCS2: Vol. 1, User's Guide (NUREG/CR 6613/SAND 97-0594, Vol.1; DOE Project Manager for Code Manual for MACCS2: Vol. 2, Preprocessor Codes COMIDA A2, FGRDCF, DCF2 (NUREG/CR 6613/SAND 97-0594, Vol. 2); member of the working group for DOE Standard Guidance for Preparation DOE 5480.22(TSR) and DOE 5480.23 (SAR) Implementation Plans, November 1994.

environmental impacts."[27]

Additional discussion of statistical analysis and its impact in provided above at 13. **Again, there is no basis for the Staff's assurance** in the draft SEIS that they "identified no new and significant information related to the postulated accidents of other available information. Therefore there are no impacts related to postulated accidents beyond those discussed in the GEIS" (Ibid, 5-3) because: Staff ignores the impact of NextEra's averaging choice, do not provide any justification for doing so, or justification of why the 95% would not be the appropriate choice, or show the difference using the 95% would make.

D. Economic Costs David Chanin author of the code's FORTRAN said, "If you want to discuss economic costs ... the 'cost model' of MACCS2 is not worth anyone's time. My sincere advice is to not waste anyone's time (and money) in trying to make any sense of it." (and) "I have spent many many hours pondering how MACCS2 could be used to calculate economic costs and concluded it was impossible."

The ER is required to include "a consideration of alternatives to mitigate severe accidents (SAMA)." 10 CFR 51.53(c)(30(ii)(L) That analysis depends upon an accurate calculation of the cost of a severe accident in order to have a base line against which to measure proposed mitigation measures. NextEra, instead, severely minimized decontamination and clean-up costs, health costs (that includes inaccurately modeling evacuation time estimates), and minimized and ignored a myriad of other economic costs that belong in a SAMA analysis. NRC Staff's analysis appears to be unaware of these facts.

1. **Decontamination/Cleanup Costs:** Discussed in the foregoing at11-30.

[27] U.S. NRC, "Generic Environmental Impact Statement for License Renewal of Nuclear Plants," NUREG-1437, Vol. 1, May 1996, Section 5.3.3.2.1

2. Health Costs:

a. Value of Life: Health costs are an important part of economic consequences. NextEra's "life lost" value is much too low. U.S. agencies other than NRC place a value on human life of between $5 million and $ 9 million. NRC despite the Office of Management and Budget's warning that it would be difficult to justify a value below $5 million- has continued to value human life at $3 million since 1995.[28] There is no excuse for NRC Staff to allow this valuation for a LR extension 20 years hence. Bringing the valuation in line with other agencies today would have a major effect of justifying mitigations to reduce risk that now are considered too expensive in NextEra's underestimated SAMA.

b. The population dose conversion factor of $2000/person-rem used by NextEra to estimate the cost of the health effects generated by radiation exposure is based on a deeply flawed analysis and seriously underestimates the cost of the health consequences of severe accidents.

NextEra underestimates the population-dose related costs of a severe accident by relying inappropriately on a $2000/person-rem conversion factor. NextEra use of the conversion factor is inappropriate because it (i) does not take into account the significant loss of life associated with early fatalities from acute radiation exposure that could result from some of the severe accident scenarios included in NextEra's risk analysis; and (ii) underestimates the generation of stochastic health effects by failing to take into account the fact that some members of the public exposed to radiation after a severe accident will receive doses above the threshold level for application of a dose- and dose-rate reduction effectiveness factor (DDREF).

[28] Appelbaum, B. 2011. A life's value: It may depend on the agency, NYT, Feb 17.

The $2000/person-rem conversion factor is intended to represent the cost associated with the harm caused by radiation exposure with respect to the causation of "stochastic health effects," that is, fatal cancers, nonfatal cancers, and hereditary effects.[29] The value was derived by NRC staff by dividing the Staff's estimate for the value of a statistical life, $3 million (presumably in 1995 dollars, the year the analysis was published) by a risk coefficient for stochastic health effects from low-level radiation of $7x10^{-4}$/person-rem, as recommended in Publication No. 60 of the International Commission on Radiological Protection (ICRP). (This risk coefficient includes nonfatal stochastic health effects in addition to fatal cancers.) But the use of this conversion factor in NextEra's SAMA analysis is inappropriate in two key respects. As a result NextEra underestimates the health-related costs associated with severe accidents.

First, the $2000/person-rem conversion factor is specifically intended to represent only stochastic health effects (e.g. cancer), and not deterministic health effects "including early fatalities which could result from very high doses to particular individuals."[30] However, for some of the severe accident scenarios evaluated by NextEra at Seabrook, we estimate that large numbers of early fatalities could occur representing a significant fraction of the total number of projected fatalities, both early and latent. This is consistent with the findings of the Generic Environmental Impact Statement for License Renewal of Nuclear Plants (NUREG-1437).[31] Therefore, it is inappropriate to use a conversion factor that does not include deterministic effects.

[29] U.S. Nuclear Regulatory Commission, Office of Nuclear Regulatory Research, "Reassessment of NRC's Dollar Per Person-Rem Conversion Factor Policy," NUREG-1530, 1995, p. 12
[30] U.S. NRC (1995), op cit., p. 1.
[31] U.S. NRC, Generic Environmental Impact Statement for License Renewal of Nuclear Plants, NUREG-1437, Vol. 1, May 1996, Table 5.5.

According to NRC's guidance, "the NRC believes that regulatory issues involving deterministic effects and/or early fatalities would be very rare, and can be addressed on a case-specific basis, as the need arises."[32] Based on our estimate of the potential number of early fatalities resulting from a severe accident at Seabrook Station, this is certainly a case where this need exists.

Second, the $2000/person-rem factor, as derived by NRC, also underestimates the total cost of the latent cancer fatalities that would result from a given population dose because it assumes that all exposed persons receive dose commitments below the threshold at which the dose and dose-rate reduction factor (DDREF) (typically a factor of 2) should be applied. However, for certain severe accident scenarios at Seabrook evaluated by NextEra, we estimate that considerable numbers of people would receive doses high enough so that the DDREF should not be applied.[33] This means, essentially, that for those individuals, a one-rem dose would be worth "more" because it would be more effective at cancer induction than for individuals receiving doses below the threshold. To illustrate, if a group of 1000 people receive doses of 30 rem each over a short period of time (population dose 30,000 person-rem), 30 latent cancer fatalities would be expected, associated with a cost of $90 million, using NRC's estimate of $3 million per statistical life and a cancer risk coefficient of $1x10^{-3}$/person-rem. If a group of 100,000 people received doses of 0.3 rem each (also a population dose of 30,000 person-rem), a DDREF of 2 would be applied, and only 15 latent cancer fatalities would be expected, at a cost of $45 million. Thus a single cost conversion factor, based on a DDREF of 2, is not appropriate when some members of an exposed population receive doses for which a DDREF would not be applied.

[32] U.S. NRC, "Reassessment of NRC's Dollar Per Person-Rem Conversion Factor Policy (1995), op cit., p. 13.
[33] The default value of the DDREF threshold is 20 rem in the MACCS2 code input

A better way to evaluate the cost equivalent of the health consequences resulting from a severe accident is simply to sum the total number of early fatalities and latent cancer fatalities, as computed by the MACCS2 code, and multiply by a readjusted value of life figure (> $3 million figure). Again, we do not believe it is reasonable to distinguish between the loss of a "statistical" life and the loss of a "deterministic" life when calculating the cost of health effects.

Another way to explain why NextEra's estimates of how many lives might be lost are too low is to look at the 1982 Sandia National Laboratory report, using 1970 census data, that estimated the number of cancer deaths at Seabrook in a severe accident to be 6,000; early fatalities 7,000; and early injuries 27,000. Peak fatalities were estimated by CRAC to occur within 20 miles of Seabrook; and peak injuries to occur with 65 miles of Seabrook from a core melt. (CRAC 2, Sandia, 1982[34]) The population of the affected area, no matter what model is used, has greatly increased during the intervening almost 40 years; SAMAs project forward to 2050 based on projected demographics. NextEra estimated the population within 50-miles (2050) to total 5185206. (LRA, Section F.3.4.1, Table F.3.4.1-1) Further CRAC was based on old, and now outdated, dose response models.

In the SAMA, cancer incidence was not considered; neither were the many other potential health effects from exposure in a severe radiological event (National Academy of Sciences, BEIR VII Report, 2005) and risk differentiated for women and children that BEIR VII reported were far more susceptible.

NextEra's cost-benefit analysis ignored a marked increase in the value of cancer mortality risk per unit of radiation at low doses (2-3 rem average), as shown by recent studies published on

[34] Calculation of Reactor Accident Consequences, U.S. Nuclear Power Plants (CRAC-2), Sandia National Laboratory, 1982

radiation workers (Cardis et al. 2005[35]) and by the Techa River cohort (Krestina et al (2005[36]). Both studies give similar values for low dose, protracted exposure, namely (1) cancer death per Sievert (100 rem). According to the results of the study by Cardis et al. and use of the risk numbers derived from the Techa River cohort the SAMA analyses prepared for Seabrook needs to be redone. It seems clear that a number of additional SAMAs that were previously rejected by the applicant's methodology will now become cost effective.

Cancer incidence and the other many health effects from exposure to radiation in a severe radiological event (National Academy of Sciences, BEIR VII Report, 2005) must be considered; they were not. Neither did NextEra appear to consider indirect costs. Medical expenditures are only one component of the total economic burden of cancer. The indirect costs include losses in time and economic productivity and liability resulting from radiation health related illness and death.

Examination of NextEra's **Emergency Response analysis** (LRA, Appendix E, Section F.3.4.4), approved by the SEIS, shows that the Applicant's evacuation time input data into the code were unrealistically low and unsubstantiated; and that if correct evacuation times and assumptions regarding evacuation had been used, the analysis would show far fewer will evacuate in a timely manner, increasing health-related costs.

---

[35] Elizabeth Cardis, "Risk of cancer risk after low doses of ionising radiation: retrospective cohort study in 15 countries." *British Medical Journal* (2005) 331:77. Available on line at: http://www.bioone.org/doi/abs/10.1667/RR1443.1?cookieSet=1&prevSearch=

[36] Krestinina LY, Preston DL, Ostroumova EV, Degteva MO, Ron E, Vyushkova OV, et al. 2005.Protracted radiation exposure and cancer mortality in the Techa River cohort. Radiation Research 164(5):602-611. Available on line at: http://www.bioone.org/doi/abs/10.1667/RR3452.1

NextEra failed to reference specific KLD-type actual time estimates, instead references the "paper plan," Seabrook Station Radiological Emergency Response Plan, Rev. 56, July 2008. No indication is provided, for example, that the following site-specific variables that would slow response time were taken into consideration in the analysis: shadow evacuation; evacuation time estimates during inclement weather coinciding with high traffic periods such as commuter traffic, peak commute time, holidays, summer beach/holiday traffic; notification delay delays because notification is largely based on sirens that cannot be heard in doors above normal ambient noise with windows closed or air conditioning systems operating.

The Applicant (ER E., F-160) claims that they assumed no evacuation of the population in a seismically induced severe accident and found only a small increase to the overall total accident dose risk and no change in economic risk. We find that sensitivity studies do not add useful information if the primary model is flawed, as we have shown is true. Lessons learned from Fukushima add that the 10 mile EPZ, the distance that evacuation time estimates were measured, is not an adequate distance to assume health effects extend. *Panel proposes widening nuclear evacuation perimeter to 30 km* (18 miles), Mainichi News, October 20, 2011

3. A myriad of other economic costs were underestimated or totally ignored by the applicant that when added together would in all likelihood add up collectively to a significant amount. The NRC Staff's analysis in the Draft SEIS appears oblivious to these factors.

For example, NextEra did not appear to include in their economic cost estimates the business value of property and the incurred costs such as costs required from job retraining, unemployment payments, and inevitable litigation. They used an assumed value of non-farm

wealth that appeared not justified by review of Banker and Tradesmen sales figures. NextEra appears to underestimate Farm Value, for example, by not considering the value of the farm property for development purposes as opposed to agricultural; and farm land assessments are intentionally very low to encourage farming and open space.

NextEra also appears to **ignore the indirect economic effects** or the "multiplier effects" from a delayed and incomplete cleanup. For example, depending on the business done inside the building contaminated, the regional and national economy could be negatively impacted. A resulting decrease in the area's real estate prices, tourism, and commercial transactions could have long-term negative effects on the region's economy.

For example since Fukushima some European countries have canceled orders for new nuclear reactors and decided to phase out of nuclear power completely – an indirect economic effect in NextEra's SAMA not modeled because it is outside the "50-mile area." Also reports in the Japanese press are replete with food products unsold, outside the 50-mile zone, simply for fear that they may be contaminated and distrust of Government reports. It is causing economic havoc to producers. For example: *Radiation Bankrupts Japanese Cattle Ranch With $5.6 Billion in Liabilities*, Bloomberg, 2001-08-15, reported that "Agura Bokujo, operator of a cattle ranch north of Tokyo, became Japan's biggest corporate failure this year after consumer fears over beef contaminated with radiation damaged sales, Tokyo Shoko Research said." Rice market turned upside down by radiation fears, Japan Times, Philip Brasor & Masako Tsubuku October 6, 2011 reported that, "Supposedly, the government checked much of the rice grown in the region when it was immature and decided it was safe, but a lot of people are far from being reassured by such announcements. Consequently, the market for rice has been knocked on its

head. New rice (preferred in Asia) from the Tohoku region, usually flying off shelves at this time of the year, is being avoided, while old rice from last year's stocks are in high demand."

V. CONCLUSION

A. MACCS2 Code

A fundamental problem with the SAMA missed by NRC Staff is that NextEra used the MELCOR Accident Consequence Code System (MACCS2) computer program.[37] There is no NRC regulation *requiring* the use of that code, or any other particular code. It was a choice by NextEra and the wrong choice, not appreciated by NRC Staff. The cost formula and assumptions contained in the MACCS2 underestimate the costs likely to be incurred as a result of a severe accident, most of which is explained above, and summarized below.

1. The code is not Quality Assured.[38] The MACCS & MACCS2 codes were developed for research purposes not licensing purposes – for that reason they were not held to the QA requirements of NQA-a (American Society of Mechanical Engineering, QA Program Requirements for Nuclear Facilities, 1994). Rather they were developed using following the less rigorous QA guidelines of ANSI/ANS 10.4. [American Nuclear Standards Institute and American Nuclear Society, *Guidelines for the Verification and Validation of Scientific and Engineering Codes for the Nuclear Industry*, ANSI/ANS 10.4, La Grange Park, IL (1987).
2. In addition to the meteorological inputs discussed above, important code input parameters include source, average (cumulative distribution function), probability, and a discount rate applied in CHRONC.

---

[37] ER.E E, Attachment F, F.3.4

[38] Chanin, D.I. (2005), "The Development of MACCS2: Lessons Learned," [written for:] *EFCOG Safety Analysis Annual Workshop Proceedings*, Santa Fe, NM, April 29–May 5, 2005. Full text: the development of maccs2.pdf (154 KB), revised 12/17/2009. http://chaninconsulting.com/index.php?resume. (Attachment 5, Exhibit 4)

3. Source is chosen by NextEra and input to ATMOS. ATMOS outputs, based on NextEra's chosen source, are input into both EARLY and CHRONC which determine consequences of an accident from NextEra's chosen source. NextEra chose an unrealistically low source input for the purpose of avoiding having to take mitigation steps that would have to be taken if a realistic source input was used.
4. A discount rate is chosen by NextEra and input to CHRONC, which in determining consequences applies the discount rate to property that must be condemned. A discount makes little sense. Properties appreciate over 20 years, not depreciate.
5. The type of average and probability of an accident are also chosen by NextEra. The Output file "averages" consequences from EARLY and CHRONC and permits the user to "average" using any one of several percentiles, including "mean," 90^{th} percentile, and 95^{th} percentile. NextEra chose mean for the purpose of avoiding having to take mitigation steps that would have to be taken if a higher, i.e., 90^{th} or 95^{th} percentile had been chosen.
6. NextEra failed to consider the uncertainties in its consequence calculation resulting from meteorological variations by only using mean values for population dose and offsite economic cost estimates.
7. In the License Renewal GEIS refers repeatedly to the 95^{th} percentile of the risk uncertainty distribution as an appropriate "upper confidence bound" in order not to "underestimate potential future environmental impacts."[39]
8. The consequence calculation, as carried out by the MACCS2 code, generates a series of results based on random sampling of a year's worth of weather data. The code provides a statistical distribution of the results. Based on calculations done at other reactors such as

[39] U.S. NRC, "Generic Environmental Impact Statement for License Renewal of Nuclear Plants," NUREG-1437, Vol. 1, May 1996, Section 5.3.3.2.1.

Indian Point, the ratio of the 95th percentile to the mean of this distribution is typically a factor of 3 to 4 for outcomes such as early fatalities, latent cancer fatalities and off-site economic consequences. [40]

9. The Output file also multiplies the consequences resulting from NextEra's chosen consequence percentile by an assumed probability of an accident, which is also chosen by NextEra. NextEra improperly assumed, and chose, an extremely low probability for the purpose of avoiding having to take mitigation steps that would have to be taken if a probability that was realistic and would provide protection to the public had been chosen. The probabilities (CDF) do not stand post-Fukushima.

B. NEPA

As required by NEPA, the NRC Staff should consider the new and significant information arising from the Fukushima accident brought forward and totally reassess Section 5.0.

Respectfully submitted,

(Electronically signed)
Mary Lampert
Permanent Address:
148 Washington Street
Duxbury, MA 02332
Tel. 781.934.0389
Email. Mary.lampert@comcast.net
October 26, 2011

[40] Dr. Edwin S. Lyman, Senior Staff Scientist, Union of Concerned Scientists report commissioned by Riverkeeper, Inc., November 2007, A Critique of the Radiological Consequence Assessment Conducted in Support of the Indian Point Severe Accident Mitigation Alternatives Analysis; available at NRC Electronic Library, Adams Accession Number ML073410093, Exhibit 12

Raymond Shadis
(Electronically filed)
New England Coalition
Friends of the Coast
PO Box 98
Edgecomb, Maine 04556
Tel 207-882-7801
Email: Shadis@prexar.com

David Agnew
(Electronically signed)
Cape Downwinders, Coordinator
173 Morton Road
S. Chatham, MA 02659-1334
d-agnew@comcast.net

PWA -Sea Breeze -Pollutant transport Coastal Mass.

THE EASTERN MASSACHUSETTS SEA BREEZE STUDY

by

Jennifer E. Thorp
B.S., Plymouth State University, 2007

THESIS

Submitted to Plymouth State University
in Partial Fulfillment of

the Requirements for the Degree of

Master of Science
in

Applied Meteorology

May, 2009

This thesis has been examined and approved.

Thesis Director, Dr. Samuel T. K. Miller
Professor of Meteorology
Department of Atmospheric Science & Chemistry
Plymouth State University / Plymouth, NH

Mr. Dan St. Jean
Science and Operations Officer
National Weather Service, Gray / Portland, ME

Dr. Barry Keim
Louisiana State Climatologist
Department of Geography and Anthropology
Louisiana State University / Baton Rouge, LA

Date

DEDICATION

This thesis is dedicated to my family, boyfriend, and friends who supported me through my college career and helped me pursue my dreams.

ACKNOWLEDGEMENTS

I would like to acknowledge the support of several individuals who helped me obtain archived data and gave me the technical know-how I needed to complete this study. A special thanks to Brendon Hoch (Plymouth State University), Dr. Samuel T. K. Miller (Plymouth State University), Scott Reynolds (CWSU Nashua, NH), and Plymouth State University graduate students and faculty. Without their time, knowledge, and patience, this project would not have been possible.

TABLE OF CONTENTS

LIST OF TABLES

LIST OF FIGURES

ABSTRACT

THE EASTERN MASSACHUSETTS SEA BREEZE STUDY

by

Jennifer E. Thorp

B.S., Plymouth State University, 2007

This study investigates many different aspects of the sea breeze at Logan Airport in Boston, Massachusetts (KBOS) and along the Massachusetts coastline. Part of the study adapts the method of predicting sea breeze events developed by Miller and Keim (2003) for Portsmouth, New Hampshire (KPSM) to KBOS. A nearly ten-year dataset of hourly KBOS surface observations (1998-2007) was used to identify 879 days when the sea breeze occurred or was likely to occur at the airport. These days were classified as sea breeze, marginal, or non-sea breeze events. Sea breeze events were further classified into fast and slow transitions, with a fast transition identified by a wind shift taking one hour or less to develop, and a slow transition identified by a wind shift taking two hours or more to develop. Marginal events were events that had a duration of 1 hour or less, no clear start or finish, or were interrupted by periods of "calm" or "light and variable" winds. Non-events were events in which the background conditions for a sea breeze to occur existed, but a sea breeze did not develop.

Times of onset and event durations for the sea breeze events (fast, slow, and marginal) were calculated and used to create seasonal statistics by event type. It was

found that seasonal variation did occur with both characteristics, but was more evident in the time of onset. Slow events occurred earliest in the day overall, while marginal events occurred a bit later, and fast events occurred the latest. Slow events had the longest duration overall, while marginal events, by definition, had the shortest duration. Seasonally, similar results were found for both characteristics with a few variations.

United States surface analyses for each event at the time of onset (or average time of onset, 1500 UTC, for non-events) were classified using the seven synoptic classes developed by Miller and Keim (2003), and statistics were developed to evaluate the distribution of synoptic classes amongst the different types of events and various seasons. Composite surface analyses of the different synoptic classes and types of events were then developed. There were significant differences between the composites of each event type within a synoptic class.

Wind vector plots, created from surface observations using Barnes analysis, were used to identify the position of the sea breeze front as the sea breeze airmass penetrated inland. The depth and shape of this front was examined by synoptic class. The prevailing synoptic scale flow was found to limit penetration in expected areas along the coastline.

Mesoscale calculations were used to determine the critical balance of the cross-shore temperature gradient (dT/dx) versus the cross-shore geostrophic wind component (u_G) at the surface necessary for the occurrence and non-occurrence of the sea breeze. It was found that by stratifying the events by synoptic classes, a smaller transition area (containing both sea breeze and non-sea breeze events) could be created. The method was taken further by adding a third variable, the 850 hPa geostrophic wind component. The

three dimensional plot showed a large transition area and future research may be able to reduce this area by breaking it down by synoptic class.

Finally, the effect of the sea breeze on convection was analyzed using radar reflectivity data from the Taunton, Massachusetts WSR-88D (KBOX) for 2002 through 2007 (562 events). Convection was present inland along the Massachusetts coastline for only 24 of the total 562 events (4%). This small occurrence results from a bias from the methodology used to develop the data set. However, when the sea breeze did occur convection developed or was affected by the sea breeze front.

CHAPTER 1

1. Introduction and Background

The sea breeze is a gravity current in which there is a landward flow of cool, moist marine air that develops when daytime heating results in a significant land-sea temperature difference (Miller *et al.*, 2003). Boston's General Edward Lawrence Logan International Airport is located on the shore of the Gulf of Maine, and is therefore significantly impacted by sea breezes. Unexpected changes in wind direction and speed can result in passenger delays, wasted fuel, and added expense. An effective method is needed to predict sea breeze events and behavior at Logan. Part of the goal for this study was to adapt the method of predicting sea breeze events developed by Miller and Keim (2003) to Logan Airport (KBOS). Many of the characteristics of the sea breeze at Boston were studied by Barbato (1978).

Barbato investigated the sea breeze circulation at Boston using a one-year dataset. Barbato found 40 sea breeze episodes in Boston during 1972. Explicit criteria were created to identify a sea breeze episode. The first criterion stated that there must be high pressure and anticyclonic flow in Boston. The second condition required that more than half the amount of possible sunshine for the day be received. The third and fourth criteria stipulated that the regional winds must be offshore prior to the event and that a sea breeze wind maximum must occur during the afternoon. The fifth criterion stated that a noticeable cooling in temperature at Logan Airport needed to be present just after the onset of the sea breeze. The final criterion asserted that the sea breeze must be $\geq$5 hrs in duration at Logan Airport.

In this study, standard synoptic data, upper air data, and Landsat-1 data were used to determine the various parameters of the Boston sea breeze. The upper air data came from the Massachusetts Institute of Technology (MIT) in Cambridge which deployed radiosondes twice a day between September 1971 and May 1973 at 1000 UTC and 1500 UTC. Onset was defined as the first time the wind was between 15° and 145° and the mean time of onset was 1500 UTC. The mean duration at Logan Airport was 8.1 hrs. The mean vertical depth of the sea breeze flow was 667 m with a range between 330 m and 1230 m.

Similar research was done by Miller and Keim (2003) and a one-year data-set for Portsmouth, New Hampshire for 2001 was utilized. The study defined three types of events: sea breeze event, marginal event, and non-sea breeze event. Sea breezes were defined as insolation-driven local onshore winds with marginal events representing weak sea breezes. Non-sea breeze events were those days when sufficient insolation was present but failed to produce a sea breeze at Portsmouth (Miller and Keim, 2003). Using the METARs from Portsmouth's Pease Air National Guard Base, 167 dates were identified as events. Surface analyses for each date were obtained and classified using a synoptic class system developed for the study. Using standard surface observations, a cross-shore geostrophic wind component (u_G) and a cross-shore potential temperature gradient ($\delta\theta/\delta x$) were calculated for the hour of onset. The study found that in the presence of stronger positive u_G value, a stronger negative value of $\delta\theta/\delta x$ was needed to develop a sea breeze.

An extensive look at the sea breeze was done by Miller *et* al. (2003) reviewing over 2500 years of sea breeze research. The study utilized a gridded wind vector analysis

for Portsmouth, NH using land and sea based observations to visualize the sea breeze flow. The observations were interpolated to the grid using a Barnes analysis scheme. The grouping of available data stations (particularly over land) allowed for a 10-km grid spacing. The rectangular grid was rotated 30° clockwise from north to make it shore parallel. The wind vectors created using this method were plotted allowing Miller *et al.* (2003) to analyze the location of the sea breeze front based on a shift in wind direction. The study looked at three case studies based on different synoptic scale surface flow regimes; northwesterly, southwesterly, and northeasterly. The focus of the case studies was to investigate the effect of the Coriolis force on the evolution of the sea breeze events.

McPherson (1970) also used gridded modeling to investigate the shape of inland penetration of the sea breeze front. This study sought to determine the effect of coastal irregularities on inland penetration. A three-dimensional model based off work done by Estoque (1961, 1962), was used to interpolate data to a 276 km by 56 km grid with a 4-km grid spacing integrated over an 18 hr time period. McPherson found that a bay located along an otherwise straight coastline caused the sea breeze front to bow landward compared to the straight portions of coastline to either side of the bay. This bowing creates a bulge in the sea breeze front that dampens out as the front progresses further inland.

The effect of grid spacing on the behavior of the sea breeze was studied by Colby. (2004) Colby used the Mesoscale Model (MM5) to simulate the sea breeze along the Massachusetts coastline and then compared the results to actual observations from 3 coastal weather stations and 3 inland weather stations. The results were also compared to

the NCEP Eta Model which uses a 22-km grid that is outputted onto a 40-km grid. Data from the Aviation Model (AVN) at 1200 UTC was used to set boundary and initial conditions for the MM5. The purpose of the study was to investigate the effect of using a nested grid to look at factors such as the time of onset, wind direction and speed, and the temperature and dew point. The nested grid was made up of three grids using a two-way interaction with the outer grid using a 36-km grid spacing, the middle grid using a 12-km grid spacing, and the innermost grid using a 4-km grid spacing. The model was run in 3 modes; the first mode used all three grids, the second used only the 36- and 12-km grids, and the third mode used just the 36-km grid. The model was used to simulate the sea breeze for 7 case studies. Colby found that the 4-km grid was both the best and the worst at forecasting the characteristics noted above at the given station locations. The 4-km grid performed the worst at forecasting the dew point in all 7 cases. The 36-km grid was able to develop the sea breeze but lacked detail. The 36-km and the Eta Model both were unable to resolve small scale rain showers that had actually developed while the 4-km grid produced these showers for one of the cases.

Another goal of the current study was to investigate the effect of the sea breeze on thunderstorms in Massachusetts. Little research exists concerning the sea breeze circulation's effect on convection in Massachusetts. Research has been done pertaining to this topic along coastal regions in warmer climate zones such as the Gulf of Mexico and India (Medlin and Croft, 1998, and Suresh, 2007).

Medlin and Croft (1998) used the WSR-88D radar data from Mobile, Alabama to investigate the interactions between large scale flow and the sea breeze circulation, as well as the effects of physiographic features such as elevation. The study found that

events that occurred in late spring and early summer had a stronger land-sea temperature differential which allowed for a deeper inland penetration, and therefore convection would occur farther inland. In late summer, the overall anticyclonic flow over the region is increased and the thermal gradient is reduced causing decreased inland penetration. The convective initiation occurs closer to the coastline where there is greater thermodynamic instability and more water vapor content in the lower troposphere. It was also found that Mobile Bay caused the sea breeze flow to diverge and move further inland. Most convective initiation occurred within 15 km of the coast. The initiation also occurred when thermodynamic instability and heating were at a maximum. Also, first cell development was either along a coastal boundary or near peaks in elevation (Medlin and Croft, 1998).

Research has also been done in Chennai, India using Doppler weather radar to determine many characteristics of the sea breeze. Radar data were used to identify the sea breeze front as well as the depth of the inland penetration of the sea breeze circulation, the speed of the propagation inland, the vertical depth of the sea breeze, and the occurrence of the convection along the front. The radar echoes appeared as a "thin line of enhanced reflectivity." This line is due to inhomogeneities in the refraction index. In regards to inland penetration, the study found that the most common depth was 10-20 km (34.6% of all cases) while distances less than 10 km came in second with 16% of all cases, and distances greater than 50 km came in a close third with 15.7% of all cases. Penetration depths of 20-30 km, 30-40 km, and 40-50 km, made up the remaining cases with fairly even distribution (Suresh, 2007).

An interesting characteristic of the sea breeze at Chennai was that sometimes the sea breeze would penetrate into the region north of the radar before the region to the south. Of the 248 days in the study, 57% of the time the sea breeze penetrated north first, 14% of the time the sea breeze penetrated south first, and the remaining 29% of the time the penetration was simultaneous on both sides of the radar. The reason for this behavior can be attributed to the land-use of these two regions. The area north of the radar is much more industrialized causing the necessary land-sea temperature differential to occur earlier. The southern region has more forests, vegetation, and parks. For Chennai, the study found that the depth of the sea breeze circulation ranged from less than 200 m to over 1000 m. The mean depth for the location varied between 490 and 765 m with the modal depth being between 400 and 600 m. This study found that the sea breeze moved inland at the slow pace of 4 km h^{-1} for the first 30 km and that between 30 to 80 km the speed increased to about 12-15 km h^{-1}. The speed of the sea breeze propagation is at its greatest at a height between 300 to 600 m (Suresh, 2007).

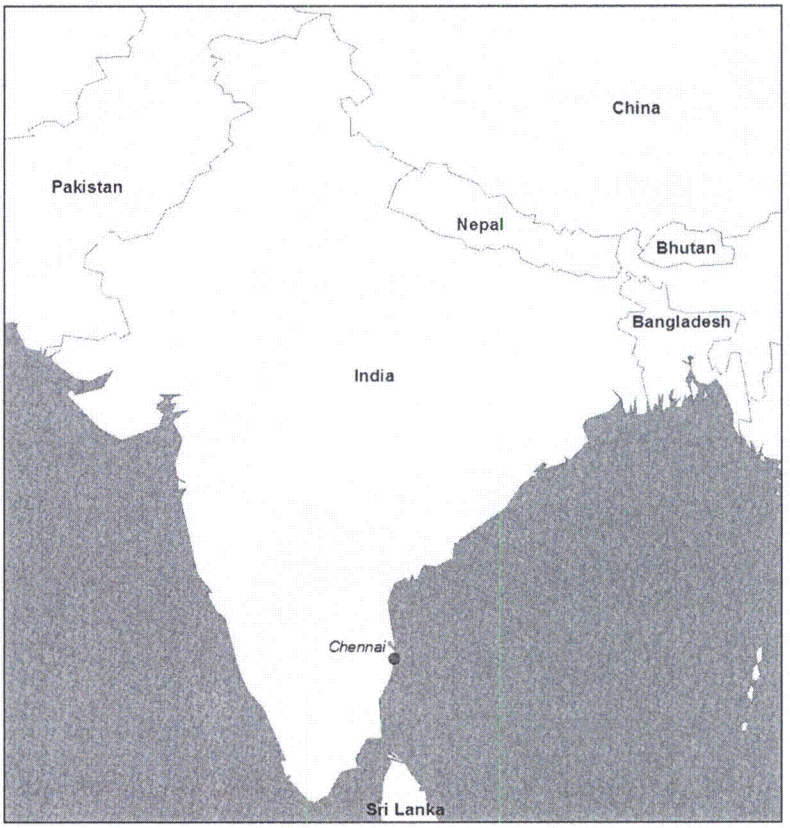

Figure 1.1: Map showing Chennai, India which is indicated by the purple circle.

Suresh (2007) also examined sea breeze-initiated convection. Overall, 37.1% of all cases showed no convection. Of the cases that did have convection, 7.3% had convection occurring within 50 km of the coastline, 31.4% had convection occurring between 50-100 km from the coast, and the remaining 24.2% noted convection at a distance greater than 100 km. (Suresh, 2007)

The initial goal of the current study was to develop a 9-year climatology of sea breeze occurrences at Logan International Airport (Fig. 1.2). The events were classified into four event type sub-categories and seven synoptic flow regimes. Statistics were generated in regards to the event type and the synoptic flow regime. As part of continuing research, more statistics were developed for the time of onset and the duration of the

event. The shape of the inland penetration of the sea breeze circulation was mapped using a vector analysis, similar to that of Miller *et al.* (2003). The mesoscale forcing for the events was examined using cross-shore temperature and geostrophic wind components. The study also includes an investigation into the effect of the sea breeze on convection in Massachusetts, by comparing cases where a sea breeze occurs to cases where a sea breeze does not occur.

It is hypothesized that behavior of the sea breeze (as revealed by the statistical results and vector analyses) will be similar to results of Miller and Keim (2003). The shape of the inland penetration is expected to vary with the different flow regimes; for example, with a southwesterly flow regime, the sea breeze should not penetrate as far inland along the coastline south of Boston as one associated with a northwesterly or northeasterly regime. As for convection, a significant connection between the sea breeze and thunderstorms is hypothesized. Results of other studies (Medlin and Croft, 1998 and Suresh, 2007) show that convection can be associated with the sea breeze in tropical and sub-tropical locations. Research has indicated this connection can occur at mid-latitudes, specifically in Maine (*See Appendix A*).

Figure 1.2: Map of Massachusetts showing the location of Logan Airport which is denoted by the airplane.

Results are separated into four chapters (chapters 3 through 6). The data and methodology for this study can be found in chapter two. Chapter three will focus on the results of the synoptic classes and inland penetration as a function of synoptic class. In chapter four, statistics for the time of onset and the duration of the event will be discussed. Chapter five contains results of the mesoscale calculations (cross-shore components). Finally, chapter six will include results of the convective analyses, and chapter seven will contain the summary and conclusions.

CHAPTER 2

2. Data and Methods

It was first necessary to define a sea breeze event at Logan International Airport. Using Miller and Keim (2003) as a reference, the following event types were defined for Logan:

1.) A *sea breeze event* occurs when the surface wind in the study area is from some westerly direction at the beginning of the day, then shifts to a direction between 10° and 190° midday, and then returns to some westerly direction at the end of the day. This wind shift must not be associated with a synoptic-pressure system. The cloud cover must remain less than "broken" (BKN). The exception to this rule is when the ceiling height is equal to or greater than 18,000 feet. It was decided that any cloud cover above 18,000 feet would be high cirrus clouds and not significantly diminish daytime heating. The final stipulation was that no precipitation could occur in the study area within six hours of the onset and the end of the event.

a.) A *fast transition* is when the wind shift to a direction between 10° and 190° occurs in an hour or less.

b.) A *slow transition* is when the wind shift to a direction between 10° and 190° occurs in two or more hours.

2.) A *non-sea breeze event* is an event in which the same conditions as a sea breeze event exist, except no wind shift is observed at Logan Airport.

3.) A *marginal event* is one in which a sea breeze event occurs but either is short lived (less than 2 hours), interrupted by periods of "calm" or "light and variable" winds, or has no clear start and/or finish.

These definitions were necessary to create a non-biased data set that could be used in this study. There were many days not included in this study where the sea breeze occurred and the cloud cover and/or precipitation criteria were not met.

After defining the different event types, a nearly ten-year data set (1998-2007) was obtained from the Plymouth State Weather Center (PSU Weather Center, 2008). METAR observations from KBOS were examined to identify dates when sea breeze events could occur based on the definitions noted above. The dates were then classified as fast, slow, marginal, or non-sea breeze events. There were 171 fast sea breeze events, 60 slow sea breeze events, 78 marginal events, and 570 non-sea breeze events for a total of 879 events over the nearly ten-year period (Tables 2.1 and 2.2).

Table 2.1: Summary of the data set used in this study by synoptic class.

Synoptic Class	*No. of cases*	*Percentage of total*
1	168	19.1
2	232	26.4
3	144	16.4
4	191	21.7
5	22	2.5
6	61	6.9
7	61	6.9
All	879	

Since this study was an expansion of previous research, the original 5-year dataset (2001-2005) was quality controlled (Thorp, 2007). An improvement was made to the time of onset for the slow sea breeze events. Originally, the time of onset was more

subjective and was chosen based on when it seemed like the wind was beginning to turn into the sea breeze. To make this study more objective, the time of onset was adjusted to be the time at which the wind direction was first within the 10° to 190° window.

Table 2.2: Summary of the data set used in this study by event type and synoptic class.

Synoptic Class	*Fast Transition SB*	*Slow Transition SB*	*Marginal Events*	*Non-sea breeze events*	*All Events*
1	42	14	26	86	168
2	36	11	8	177	232
3	4	2	6	132	144
4	53	7	23	108	191
5	0	0	0	22	22
6	13	21	11	16	61
7	23	5	4	29	61
All	171	60	78	570	879

a. Time of Onset and Event Duration

The hour of onset for each event was recorded during the initial parts of the study. This time is defined to be the first time that the wind direction was greater than 10° and less than 190°. The time of onset was used to create statistics by event type (fast, slow, and marginal only) and season. The seasons used were winter (December, January, February), spring (March, April, May), summer (June, July, August), and fall (September, October, November).

The duration of each event was the calculated difference between the time of onset and the end time of the event. The end time of the event was the first time the wind direction was greater than or equal to 190° and less than or equal to 10°. Hourly observations were used for this calculation. Event duration was stratified using the same method of statistics as the time of onset.

b. Synoptic Classification

The surface analysis for each date was obtained using the nearest analysis time prior to the time of onset (example, time of onset 1400 UTC, analysis time 1200 UTC). In the case of non-sea breeze events, the average time of the onset for sea breeze events was used, which is 1500 UTC. The surface analyses were obtained from the National Climatic Data Center's Service Records Retention System (NESDIS, 2008). The surface charts were then stratified into the synoptic classes defined by Miller and Keim (2003).

There were six synoptic classes and one miscellaneous class. Synoptic classes one, two, and three represent an overall northwesterly surface flow regime. Class one had anticyclonic flow, class two had neutral flow, and class three had cyclonic flow. Class four was anticyclonic southwesterly flow while class five was cyclonic southwesterly flow. Synoptic class six corresponded to northeasterly surface flow and synoptic class seven was the miscellaneous class (*Appendix B*).

Statistics were then generated for each event type and synoptic class to identify any trends and patterns. After creating statistics, the individual surface charts were used to create composite analyses for each event type and synoptic class (example, fast transition sea breeze synoptic class one). The composites were generated using the National Climatic Data Center's North American Regional Reanalysis composite website (ESRL PSD, 2008).

c. Inland Penetration

During the initial process of building the data set of events, information about the maximum sustained wind that occurred during the event was recorded including the time of occurrence, speed, and direction. The speed and direction were converted to u and v

components and the averages and standard deviations were calculated for the three major synoptic flow patterns. Northwesterly flow included synoptic classes one through three. Southwesterly only included synoptic class four since only non-events occurred with synoptic class five. The northeasterly flow was represented by synoptic class six.

The fast sea breeze events were used since they represent a stronger sea breeze flow. Dates were chosen at random based on the number of standard deviations from the mean. For one and two standard deviations, both the u and v component had to be within the same standard deviation. For three standard deviations, either the u or the v component needed to be within the third standard deviation. This was because there was never an occurrence of both components being three standard deviations from the mean.

Two dates were chosen from each standard deviation category resulting in six dates for each of synoptic class one, two, and four. Synoptic class three only included four dates which is the total number of events for that class. Of those four dates, one event was within two standard deviations while the remaining three were within one standard deviation. Since synoptic class six only had 14 events in total there was only one observation that fell within the three standard deviations range. A total of 27 events were used in this portion of the study.

To examine the depth of inland penetration, vector wind analyses were employed. These analyses were then created using a Barnes Analysis over a gridded area with the northwest corner at 43°N 71.75°W and a grid spacing of 5 km. The grid extends 180 km toward the east and 165 km toward the south from the northwest point (*See Appendix C*). Data from 40 different weather stations (both nautical and land based) were used to create these analysis (*See Appendix C*). The vector wind analyses were created using the hourly

wind speed and directional data which were converted to u and v wind components. The location of the sea breeze front was used to measure how far inland the sea breeze flow was extending from the coastline. An average mid-event plot was created for each of the classes by averaging the mid-event u and v components (interpolated values) of the chosen dates for each synoptic class.

d. Mesoscale Calculations

Mesoscale calculations were made for the cross-shore *in situ* temperature gradient (dT/dx) and geostrophic wind component (u_G) for all event types to determine a relationship between these variables and the occurrence or non-occurrence of a sea breeze at Logan Airport (*See Appendix D*). Calculations were performed using observations recorded at four neighboring stations to estimate both parameters for Logan, at either the time of onset (for sea breeze and marginal events), or the mean time of onset (1500 UTC, for non-sea breeze events). The station north of Boston was Lawrence, Massachusetts (KLWM) and the southerly station was Taunton, Massachusetts (KTAN) (Fig 2.1). Worcester, Massachusetts (KORH) was used as the western site and buoy 44013 was used as the eastern site (Fig 2.1).

The cross shore components were used to create a two-dimensional plot with dT/dx on the y-axis and u_G on the x-axis. A three-dimensional plot was also developed using the u_G component of the wind at 850 hPa. Sounding data from Chatham, MA (KCHH) were interpolated to the hour of onset using a simple linear equation (*See Appendix C*). Marginal events were not included in the three-dimensional plot and fast and slow sea breezes were grouped together. The sea breeze events were plotted in comparison to the non-sea breeze events.

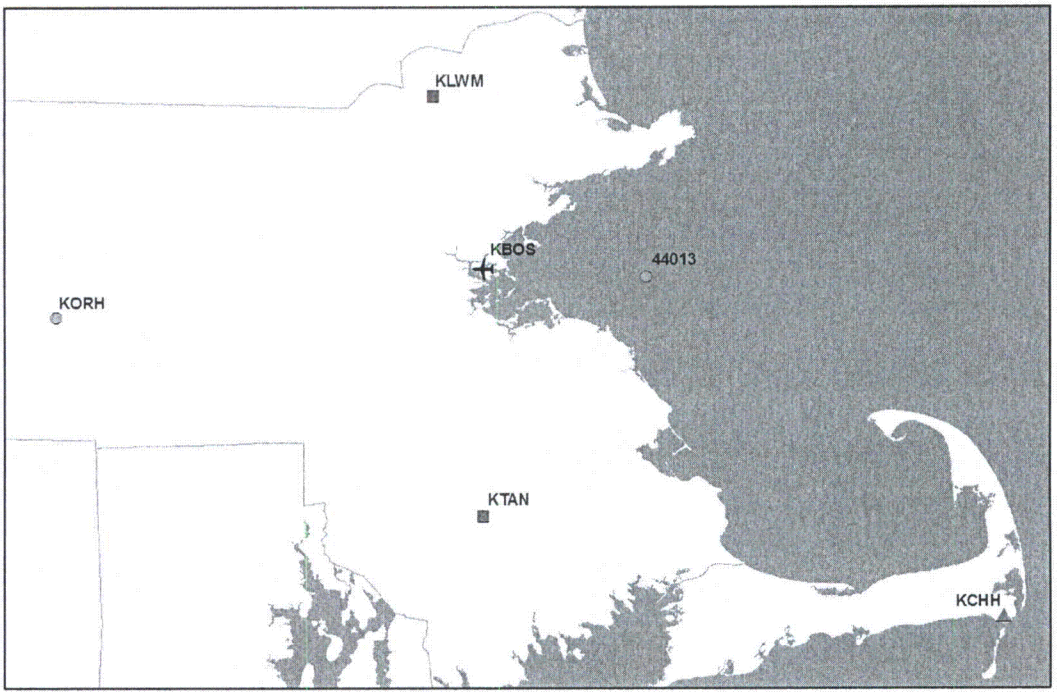

Figure 2.1: Map of Massachusetts showing the location of ASOS stations used for the cross shore component analyses. Purple squares represent stations used for uG and green circles represent stations used for dT/dx. The red triangle indicates the site used for sounding data in the three dimensional analysis. Logan Airport is denoted by the airplane.

e. Radar Analysis of Convection

Level II reflectivity data were obtained from the National Climatic Data Center (NCDC, 2008). Radar data from Taunton, MA (KBOX) were used for this part of the study. Each event and non-event date was queried and graphed showing data availability and the operational mode of the radar was produced (Fig. 2.2). If the radar was in precipitation mode at anytime between 1200 UTC and 2359 UTC the data were downloaded for further analysis. The 0.5° reflectivity data were then examined to determine whether convection was occurring in or entering into the coastal region in which the sea breeze front could exist. A threshold of greater than or equal to 30 dBZ was used to distinguish convective cells from non-convective cells (Bedka and Mecikalski, 2004).

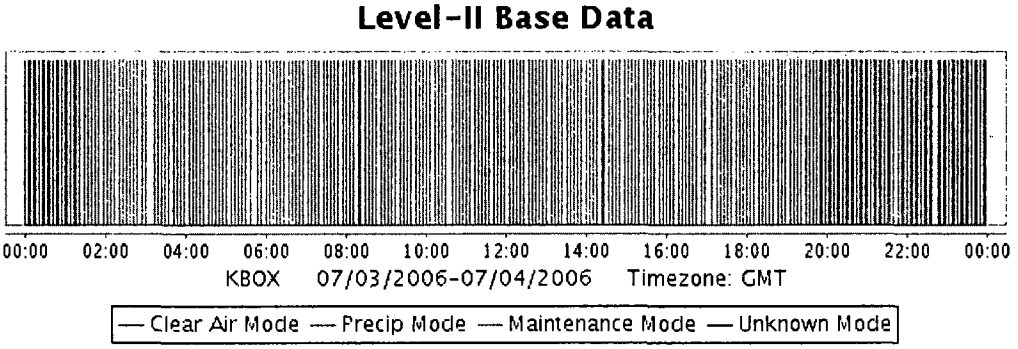

Figure 2.2: Example of the NCDC data availability graph.

Using this method for warm season months (April to September) from 2002 through 2007, 26 dates were chosen. Vector wind analyses were created using the same method described in the inland penetration section. The purpose of these analyses was to

locate the sea breeze front indicated by wind shift. This location can then be compared to the reflectivity data to determine whether convection was developing, weakening, or remaining the same along the sea breeze front.

CHAPTER 3

3. Time of Onset and Event Duration

a. Time of Onset

The time of onset for each event (fast, slow, and marginal) was recorded as described in the previous chapter. The possible times of onset for each event type were then plotted alongside the mean with an error bar of three standard deviations (Fig. 3.1). There were 171 fast sea breeze events, 60 slow sea breeze events, and 78 marginal sea breeze events. Only one data point (2300 UTC, slow events) does not fall within the range of the error bar. For the time of onset of 2300 UTC for slow events, there is only one observation of this time in the data set (shown in Fig. 3.2b).

A dual midday peak is evident for both slow and marginal events (Fig. 3.2b and 3.2c). There is a suggestion of this trend in the fast events at 1700 UTC (Fig. 3.2a), but it is not as strong a signal as with the slow and marginal events. It seems that the *weaker* the event, the *stronger* this signal is; the second peak is weaker than the first in both the fast and slow events and then equal to the first for the marginal events. Perhaps if another event type existed between marginal and non-events the second peak would be larger than the first. There is a third peak present for all events that occurs in the early evening. This peak gets increasingly later as one transitions from the fast events to the marginal events.

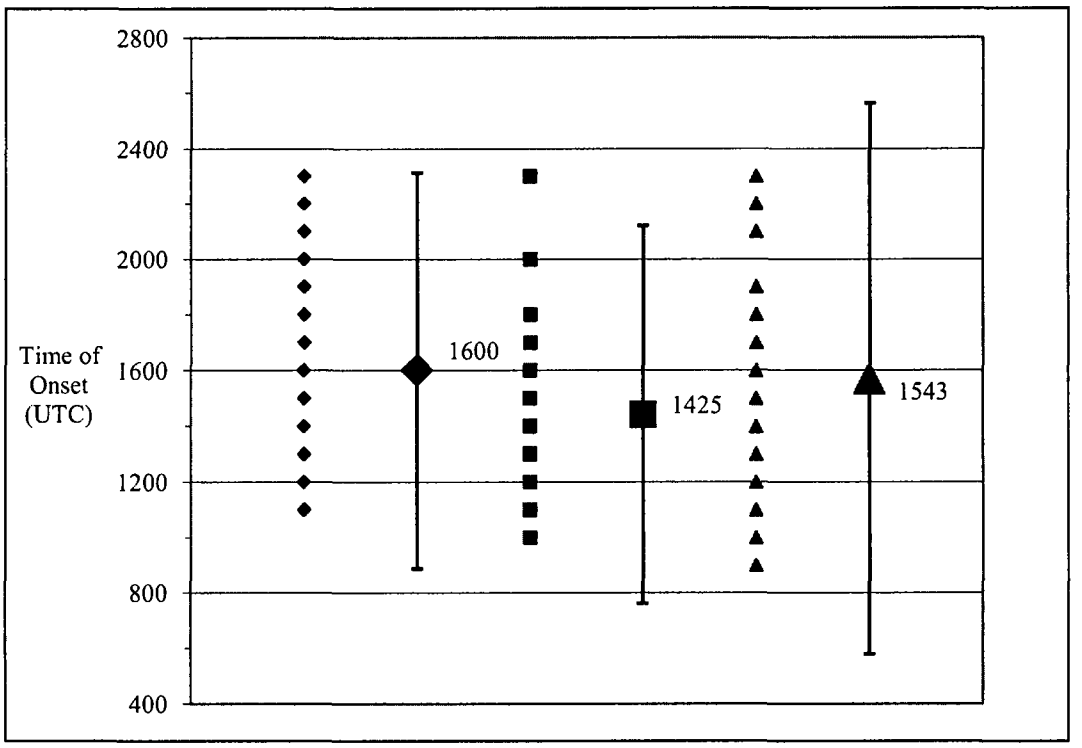

Figure 3.1: Plot of times of onset by event type alongside the mean with error bars of three standard deviations. The fast events are the blue diamond, the slow events are the purple square, and the marginal events are the green triangles.

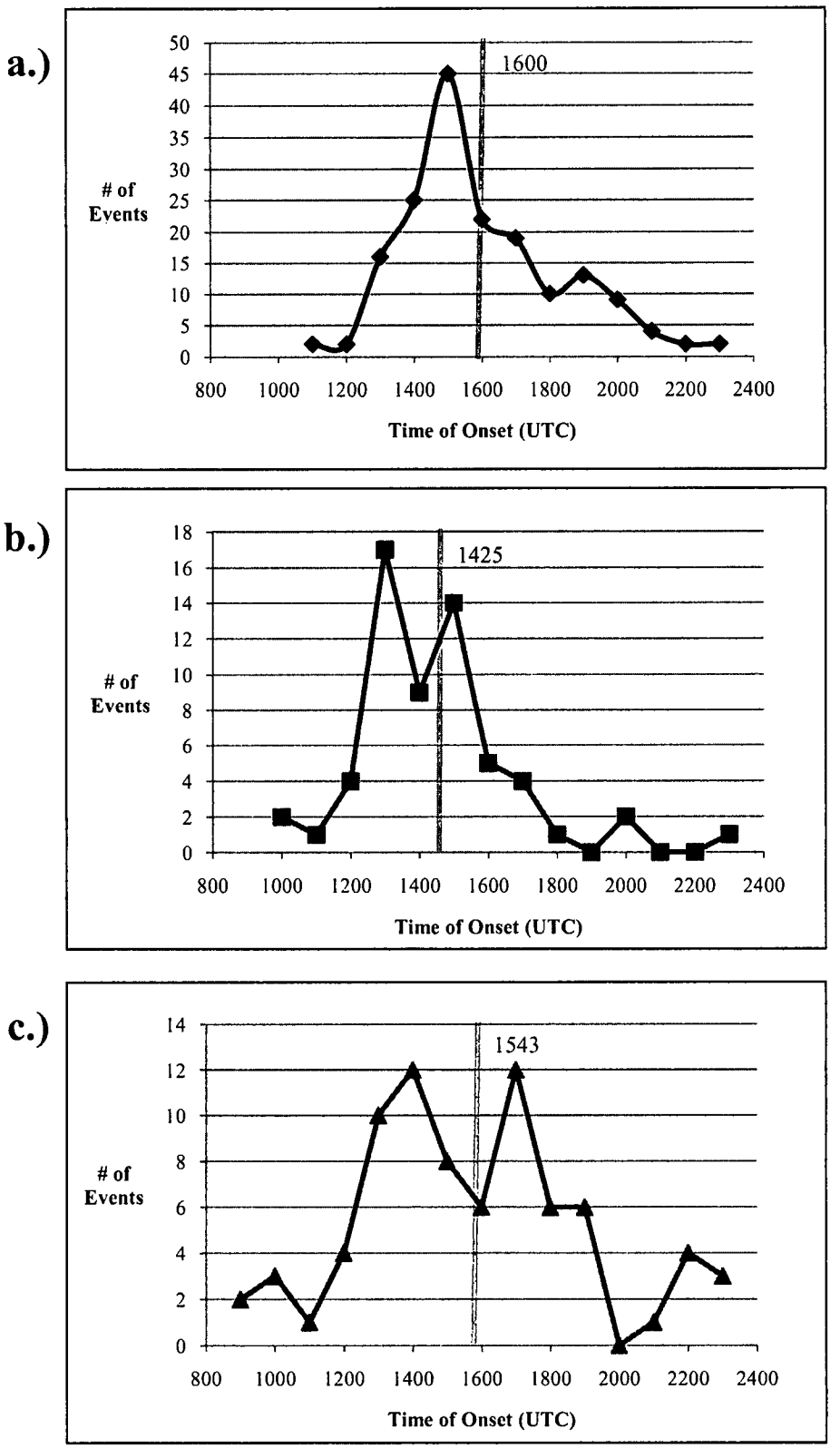

Figure 3.2: Time of onset distributions by event type. a.) fast, b.) slow, and c.) marginal. Vertical line indicates mean.

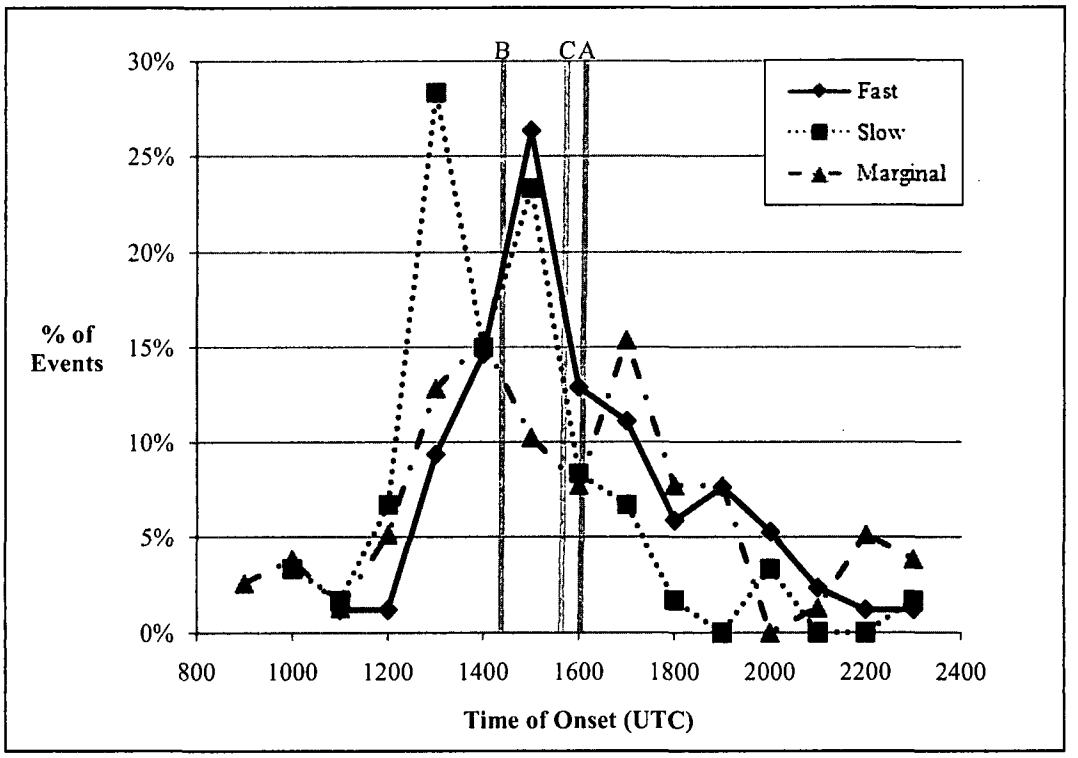

Figure 3.3: Time of onset distributions overlaid based on percentage of events. Line A is fast event mean, line B is slow event mean, and line C is marginal event mean.

Figure 3.3 shows all of the event types as an overlay. The position of each event type's mean time of onset shows slow events starting earliest (1425 UTC), with the marginal events occurring slightly later (1543 UTC), and the fast events the latest (1600 UTC). Fast events show a swift change in wind direction which could require the extra hour of daytime heating in order to occur. Slow events exhibit a more gradual change in wind direction which may not need as much daytime heating to initiate as the fast events. The marginal events contain weaker sea breezes that exhibit both fast and slow transitions and therefore it is natural for the mean time of onset to fall in between the two. Also, since the mean is shifted more towards the fast event mean, perhaps the marginal events are slightly more influenced by fast sea breeze characteristics.

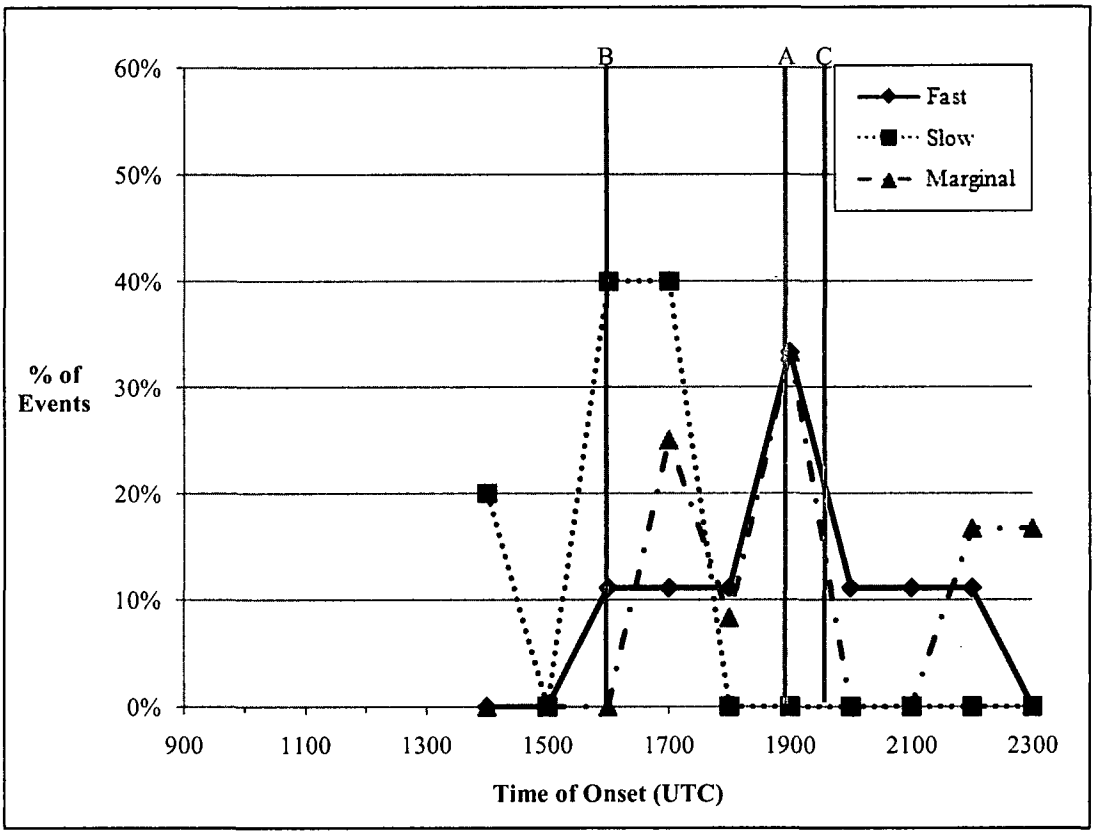

Figure 3.4: Time of onset distributions for the winter overlaid based on percentage of events. Line A is fast event mean, line B is slow event mean, and line C is marginal event mean.

These distributions can be broken down further by plotting them seasonally. The distribution for winter shows the times of onset shifted to later hours of the day (Fig. 3.4). This is expected since it would take longer for sufficient daytime heating to occur in winter. There were 9 fast sea breeze events, 5 slow sea breeze events, and 12 marginal sea breeze events in this distribution making the statistical significance of the winter data questionable. Notice that the order of the onset means has changed from the overall plot in Figure 3.3. The marginal events have the latest mean at 1935 UTC which is 35 minutes later than that of the fast events at 1900 UTC. This suggests that in winter, marginal

events tend to behave more like a fast sea breeze than a slow sea breeze. The mean for the slow events is much earlier, at 1600 UTC.

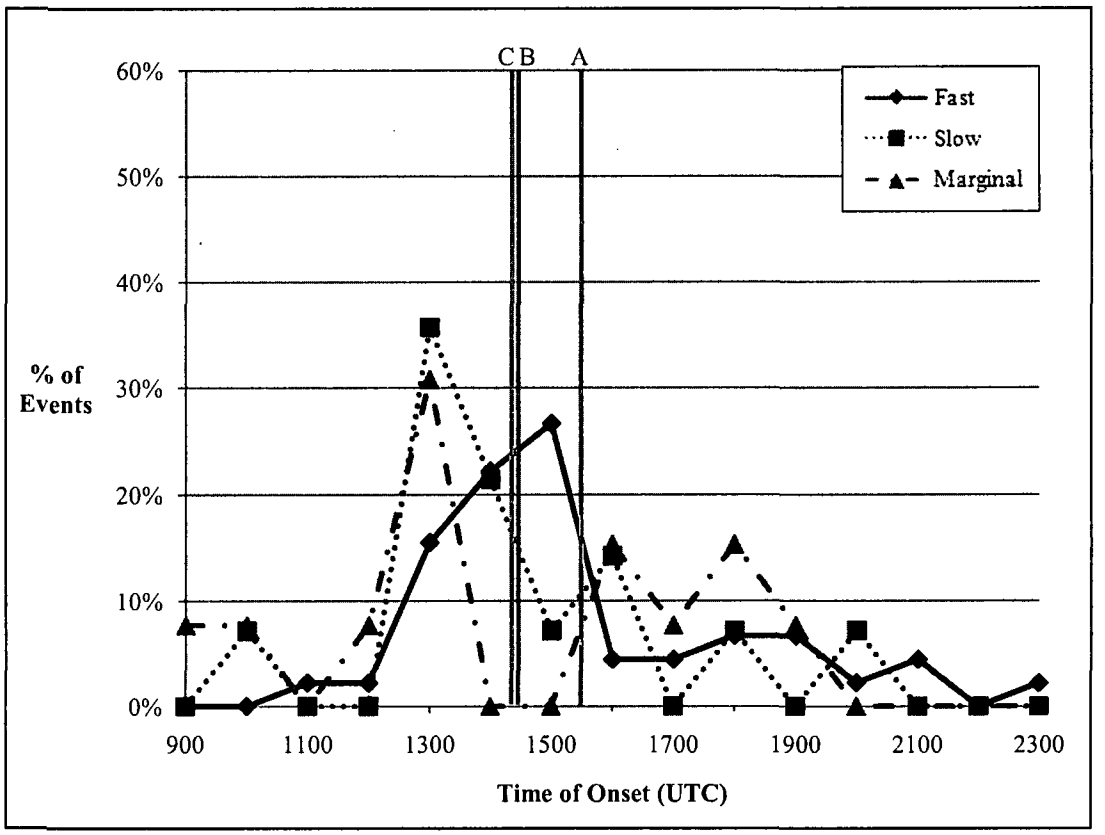

Figure 3.5: Time of onset distributions for the spring overlaid based on percentage of events. Mean lines same as in Fig. 3.4.

The spring distribution is shown in Figure 3.5. There again is a change in the order of the mean time of onset for each event. The marginal events seem to be influenced more by the slow events during spring. The marginal and slow events also share the same maximum for the time of onset at 1400 UTC. The time of onset for all events has become much earlier than it was in winter. The mean time of onset for the fast events is 1528 UTC with a sample size of 45 events. With 15 events, the mean of the slow sea breeze events is 1426 UTC. Lastly, the marginal events had a mean time of

onset of 1423 UTC with 13 events, which is the earliest mean onset of this event type. The duel maxima noted in the overall plot (Fig. 3.3) can be seen evidently in the spring distribution.

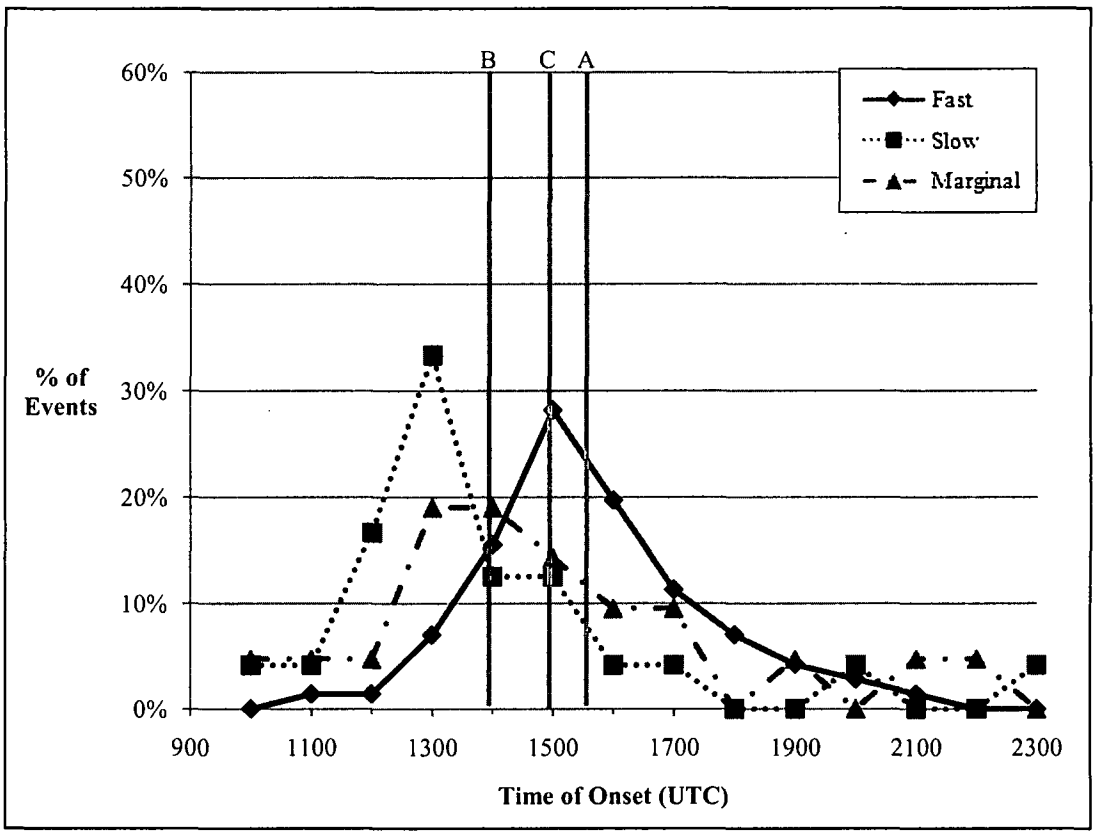

Figure 3.6: Time of onset distributions for the summer overlaid based on percentage of events. Mean lines same as in Fig. 3.4.

The distribution for summer (Fig. 3.6) has the mean times of onset in the same order as the overall distribution. Again, the mean time of onset for the marginal events is back between the fast and slow events. The summer months show a maximum in sea breeze events, which has a heavy influence on the overall plot. There were 71 fast sea breezes, 23 slow sea breezes, and 21 marginal sea breezes in summer for this study. The

mean time of onset for the fast events was at 1538 UTC which is the earliest mean time of onset for fast events overall. The same is true for the slow events which had a mean time of onset at 1400 UTC. The mean time of onset for the marginal sea breezes was at 1457 UTC. These early times of onset are clearly attributed to the abundant daytime heating available in the summer. The slow and marginal distributions seem to be right-skewed while the fast distribution is less skewed and almost a normal bell-curve. Although the mean onset of the marginal events falls slightly closer to that of the fast sea breezes, the distribution seems more similar to the distribution of the slow sea breezes.

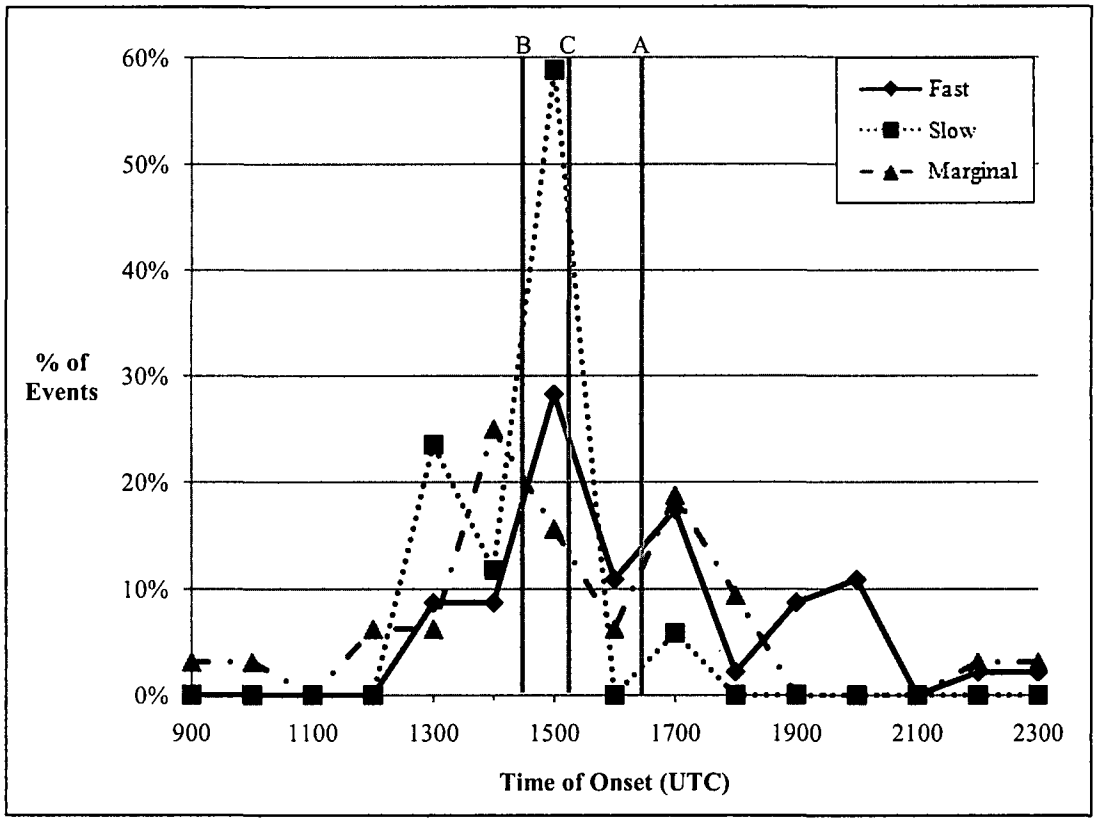

Figure 3.7: Time of onset distributions for the fall overlaid based on percentage of events. Mean lines same as in Fig. 3.4.

In the fall, the distributions for each event type show similar features (Fig. 3.7). There are three main peaks for the fast and slow events. The marginal events have two major peaks although there is a hint of another maximum at 1200 UTC. Both the fast and marginal events show an additional crest during the evening hours. The order of the mean time of onset is again like the overall plot with slow events being the earliest at 1432 UTC, followed by marginal events at 1517 UTC, and the fast events coming in the latest at 1629 UTC. There are 46 fast events, 17 slow events, and 32 marginal events for the data set in fall. There is a strong maximum at 1500 UTC for slow sea breezes with nearly 60% of all events occurring at this time. The range of the time of onset for slow events is also small (1300 UTC to 1700 UTC). The mean time of onset for the marginal sea breezes fall slightly closer to the slow events, however, the marginal events distribution seems to follow the fast event distribution.

The time of onset shows expected variation by season. The latest times of onset occur in winter when it takes longer for adequate daytime heating to develop. The overall results showed that the fast events occur the latest and the slow events occur the earliest with the marginal events falling in between. The seasonal distribution showed that this was true for summer and fall. In winter, marginal events tended to occur slightly later than the fast events while in spring marginal events occurred slightly earlier than the slow events. Since these two seasons have the lowest number of marginal events, it's arguable that with a larger sample size the marginal events may fall in between the fast and slow events like the overall plot shows.

b. Event Duration

The time of onset and the end time of each event type (fast, slow, and marginal) were recorded in the initial acquisition of the data set. The possible event durations for each type were then plotted alongside the mean with an error bar of three standard deviations (Fig. 3.8). All of the observed event durations fall within the three standard deviations for each event type. Notice that the standard deviation values for the fast and slow events are almost the same; 3.17 hrs and 3.09 hrs respectively. The marginal events have a significantly larger standard deviation at 5.11 hrs. Marginal events were defined as events that lasted one hour or less, had no clear start or finish, or had periods of "calm" or "light and variable" winds during the event. Marginal events were not further categorized by the transition into the sea breeze like the fast and slow sea breeze events and therefore contain both types of transitions. The diversity of events categorized as marginal events may have lead to this variance in the standard deviation.

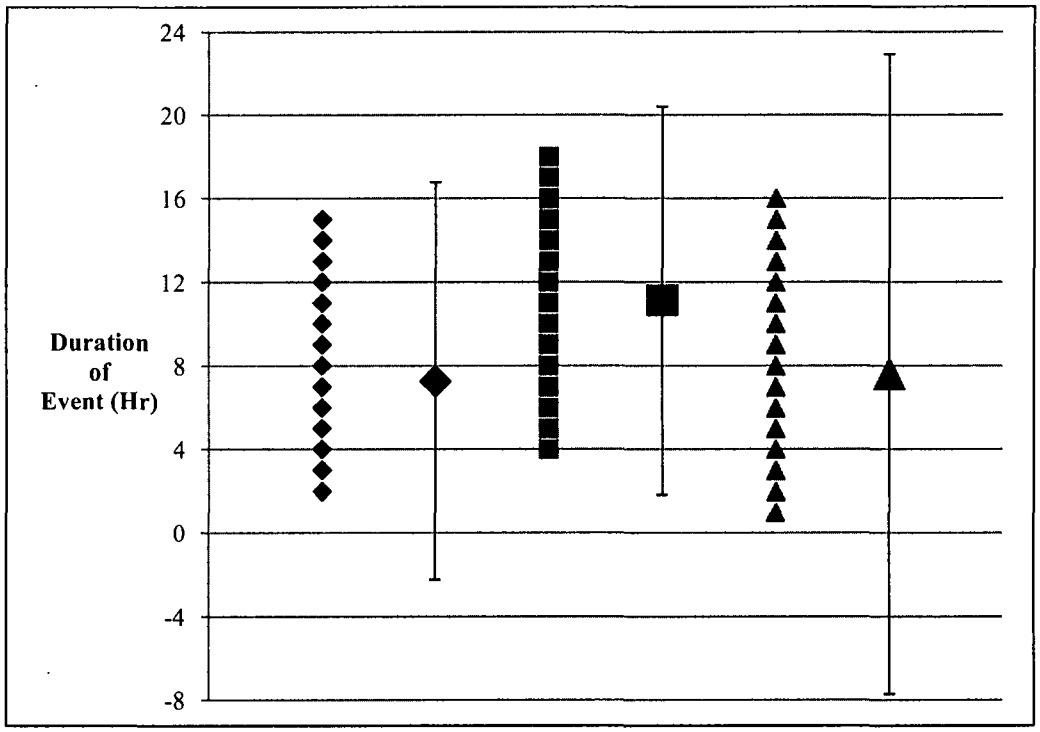

Figure 3.8: Plot of event durations by event type alongside the mean with error bars of three standard deviations. The fast events are the blue diamond, the slow events are the purple square, and the marginal events are the green triangles.

The overall distribution of event durations is shown in Figure 3.9. Most of the fast events have duration 10 hrs or less as shown in Figure 3.9a. The mean fast event duration is 7.26 hrs. Distribution of the slow event durations (Fig. 3.9b) appears to be more normal than that of the fast event durations. The majority of the events have a duration between 9 and 14 hrs and the mean duration is 11.13 hrs. With marginal event durations there seem to be no discernible pattern present in the distribution (Fig. 3.9c). The most notable feature in this distribution is that there is a strong peak for an event duration of 1 hr which is to be expected as it is one part of the definition of the event type. The mean duration for marginal events is 7.6 hrs. Figure 3.10 shows the three event types overlaid on one plot.

The long duration of the slow sea breezes is an aspect of the definition of the event. This type of sea breeze shows a gradual transition into a sea breeze and the duration starts once it passes into the sea breeze direction (10° to 190°). The strongest sea breeze winds generally are between the directions of 100° and 130° for the sea breeze at KBOS. Slow sea breezes eventually settle at these directions after the longer transition has occurred. Fast sea breeze events do not contain a long transition period which results in a shorter duration. The marginal events contain a strong outlier, by definition, with numerous one hour events skewing the mean towards a shorter duration.

To break down the distributions further, the event durations were plotted by season as well. Figure 3.11 shows the distribution for winter (December, January, and February) plotted as an overlay for the three event types. Notice that the order of the means remains the same as in the overall plot (Fig. 3.10). The mean duration of the fast events is the shortest at 4.90 hrs and that of the marginal events is the next shortest at 5.08 hrs. Slow events have the longest mean duration at 10 hrs. Also, the pattern from the overall distribution (Fig 3.10) is apparent in the winter plot for both the fast and marginal events. The marginal event duration shows the expected peak at 1 hr. The distribution of the slow events is not quite the same which is likely related to sample size issues as there were only 5 slow sea breeze events in the winter. There were also 9 fast sea breeze events and 12 marginal sea breeze events in this distribution. As stated earlier in the time of onset section, the statistical significance of the winter data is questionable.

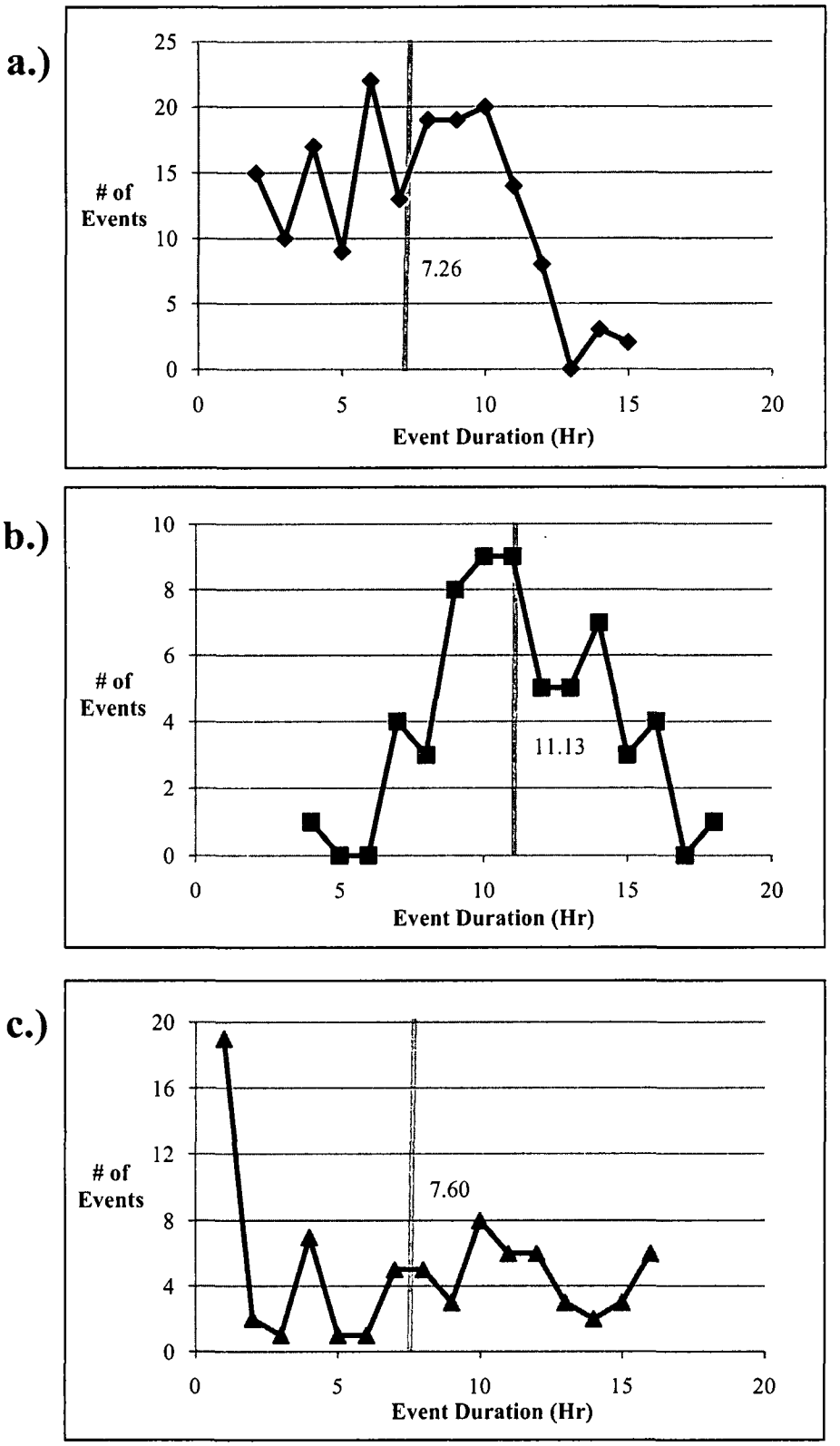

Figure 3.9: Event duration distributions by event type. a.) fast, b.) slow, and c.) marginal. Vertical line indicates mean.

The spring (March, April, and May) distribution for the three event types is shown as an overlaid plot in Figure 3.12. Again, the expected duration peak of 1 hr for the marginal events is present. There are multiple secondary peaks for the marginal events making the spring distribution similar to the overall distribution for marginal events (Fig. 3.10). The main peak of the fast event durations is 9 hrs and the spring distribution looks different from the overall distribution (Fig. 3.10). The spring distribution of the slow event durations has comparable peaks to the overall distribution of the slow event durations. The slow event durations peak at 9 and 10 hrs. The mean durations show a slightly different order in the spring distribution compared to the overall distribution. Marginal events now have the shortest mean duration at 7.46 hrs. Fast events have the next shortest mean duration at 8.04 hrs indicating that fast events become longer in spring. Slow events still have the longest mean duration at 10.93 hrs which is about an hour longer than the winter duration and just under the overall mean duration. There were 45 fast sea breeze events, 15 slow sea breeze events, and 13 marginal sea breeze events in this distribution.

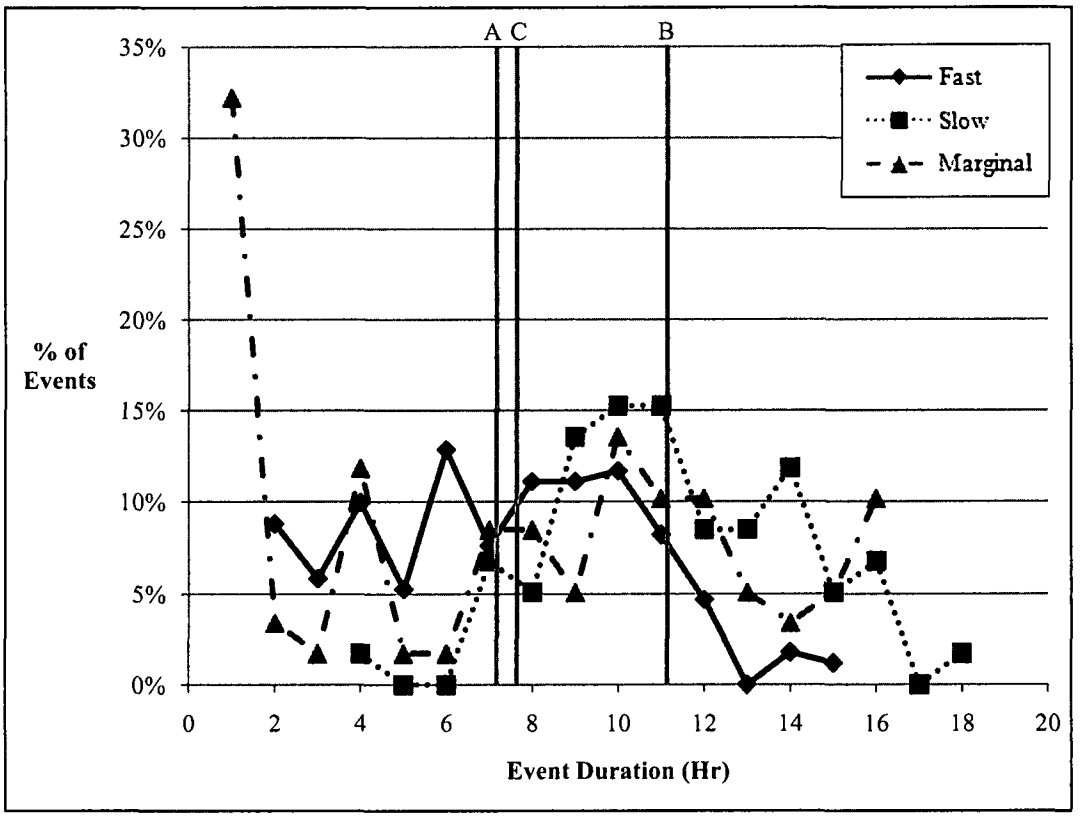

Figure 3.10: Event duration distributions overlaid based on percentage of events. Line A is fast event mean, line B is slow event mean, and line C is marginal event mean.

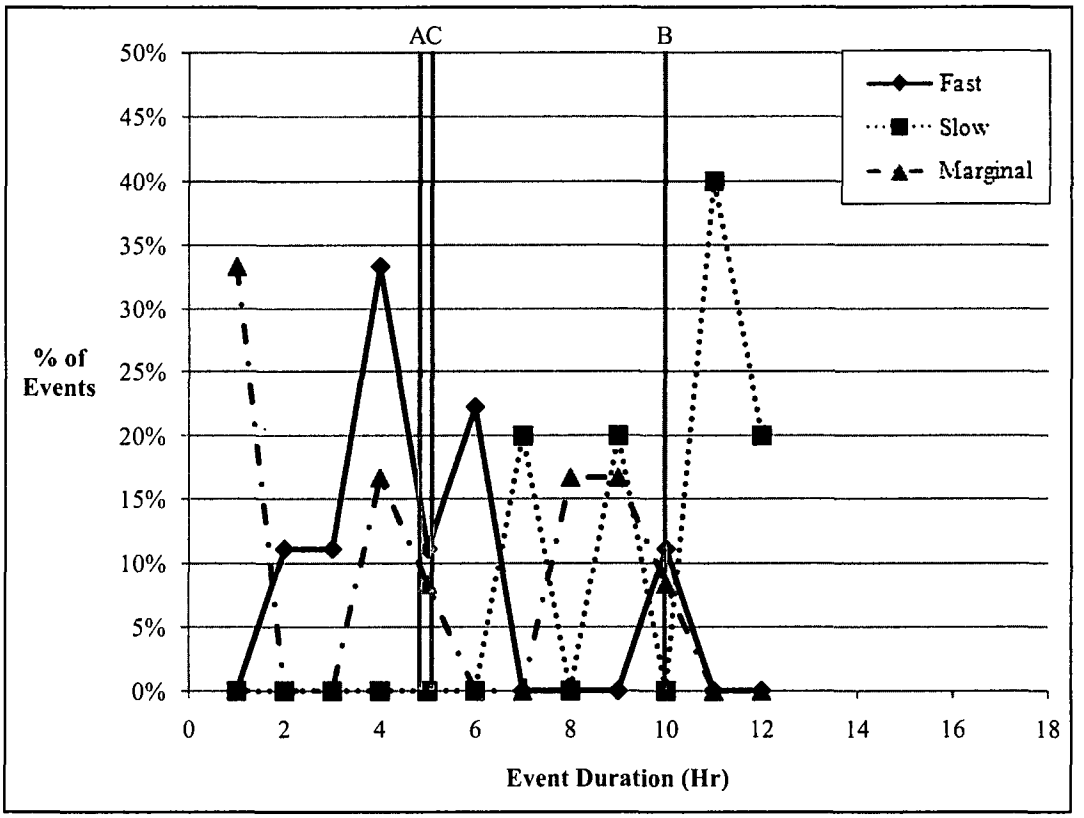

Figure 3.11: Event duration distributions for the winter overlaid based on percentage of events. Line A is fast event mean, line B is slow event mean, and line C is marginal event mean.

The distribution of the three event types for summer (June, July, and August) is depicted as an overlay in Figure 3.13. The 1 hr peak duration for the marginal events is not prominent in summer. There were 21 marginal events during the summer months. This minimum in 1 hr events supports the idea that sea breezes are stronger during summer with greater daytime heating available. There were 71 fast sea breezes and 23 slow sea breezes for this season. Arrangement of the mean durations is the same as with the overall plot (Fig. 3.10) with fast events being the shortest at 7.37 hrs, followed by marginal events at 8.38 hrs, and slow events being the longest at 11.50 hrs.

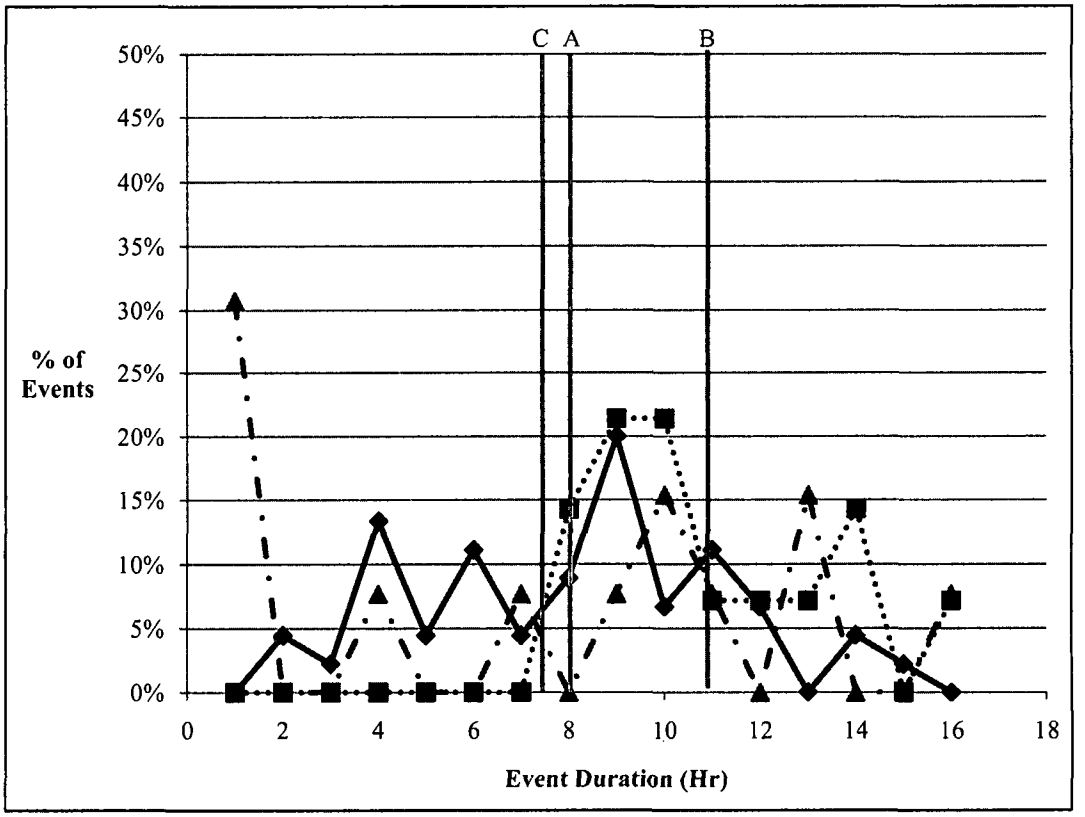

Figure 3.12: Event duration distributions for the spring overlaid based on percentage of events. Line A is fast event mean, line B is slow event mean, and line C is marginal event mean.

The fall distribution (Fig. 3.14) carries similar characteristics to the overall distribution (Fig. 3.10) for both fast and marginal events. The earlier peaks of 4 and 6 hrs for fast events are more prominent in the fall distribution that the later peaks of 8, 9, and 10 hrs compared to the overall distribution. Again, the 1 hr duration peak is present for the marginal events. Mean durations follow the same order as the overall with fast at 6.78 hrs, marginal at 8.09 hrs, and slow at 11.12 hrs.

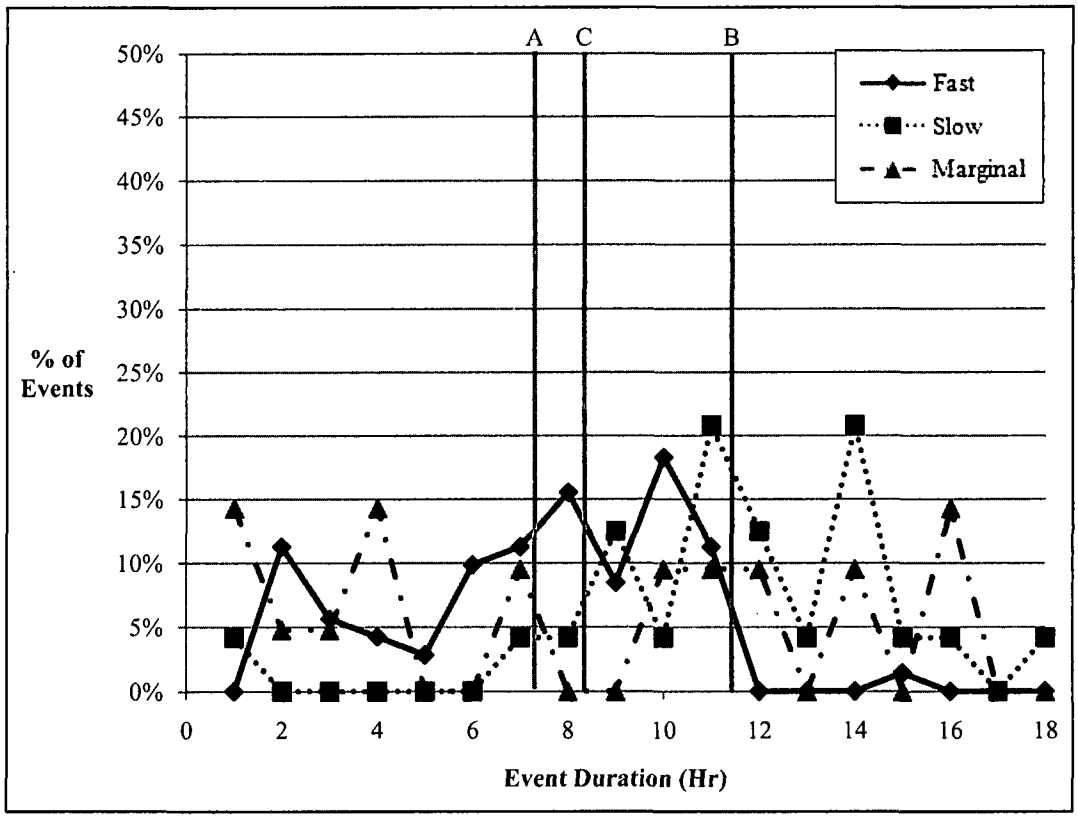

Figure 3.13: Event duration distributions for the summer overlaid based on percentage of events. Line A is fast event mean, line B is slow event mean, and line C is marginal event mean.

The duration varies between event types and shows some variance between seasons. The shortest event mean durations for all event types occurred during winter. The longest mean duration for the fast events occurred in spring while that of the slow and marginal events occurred during summer. These minima and maxima are logical as there is less daytime heating available in winter compared to spring and summer. It is interesting that the maximum mean duration for fast events occurred in spring while the maximum for slow and marginal events occur in summer. More research is needed to determine a cause of this.

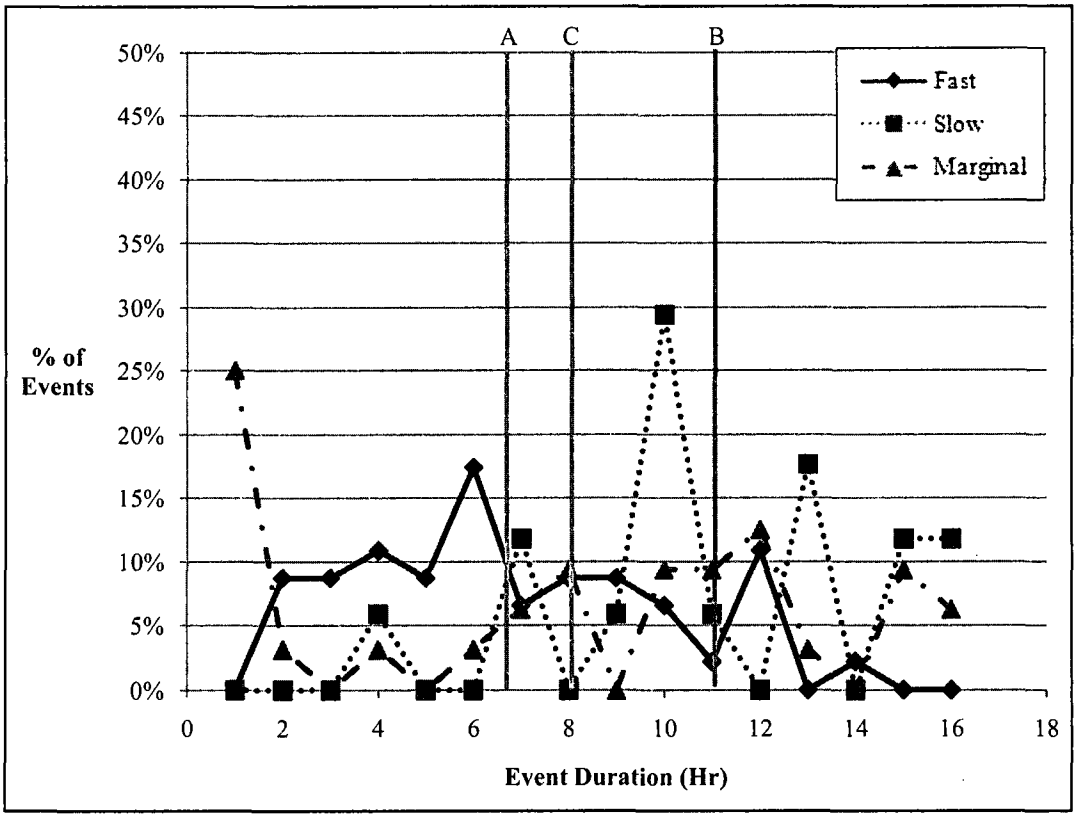

Figure 3.14: Event duration distributions for the fall overlaid based on percentage of events. Line A is fast event mean, line B is slow event mean, and line C is marginal event mean.

CHAPTER 4

4. Synoptic Classes & Inland Penetration

a. Synoptic Classes

To compare the variation in synoptic class for classes one through three for each event type, a conceptual schematic was created. The schematic (Fig. 4.1) shows the location of the composite high pressure center and measures the pressure gradient along a line perpendicular to the isobars over the study area. The perpendicular line varies in length with the different event types and synoptic classes. The line is drawn from the centermost isobar to the outermost isobar of the pressure system. Composites were generated from a list of dates and times for each event as described above.

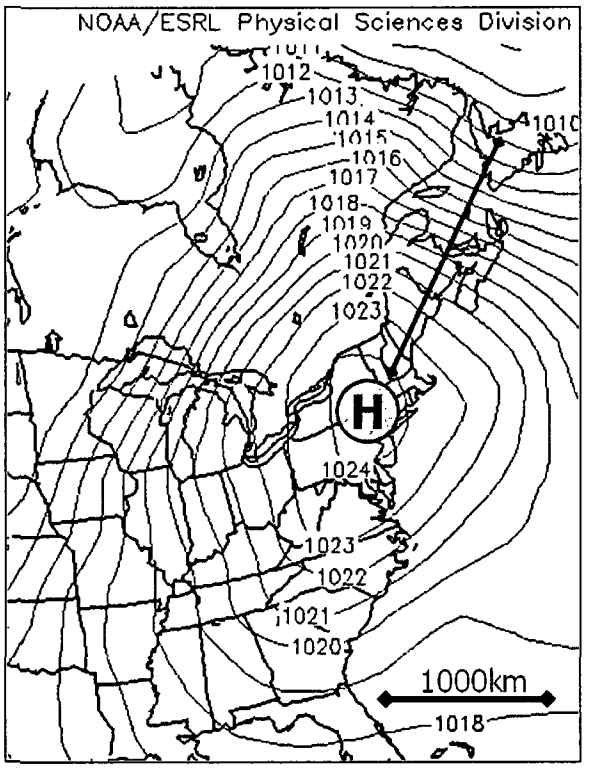

Figure 4.1: Example of how conceptual schematics were created. Fast transition sea breeze synoptic class 1.

For synoptic class 1, the composite high centers for fast, slow, and marginal events are almost colocated over eastern New York State with the slow event's high being slightly further north (Fig. 4.2). The center of the composite high pressure system with the non-sea breeze events is located further south over West Virginia and Maryland, creating a stronger gradient over the study area, and increasing the strength of the synoptically-driven offshore wind resisting the landward movement of the sea breeze. The mean gradient for the non-sea breeze events is also higher at 1.22 hPa/100km, which supports this reasoning (Table 4.1).

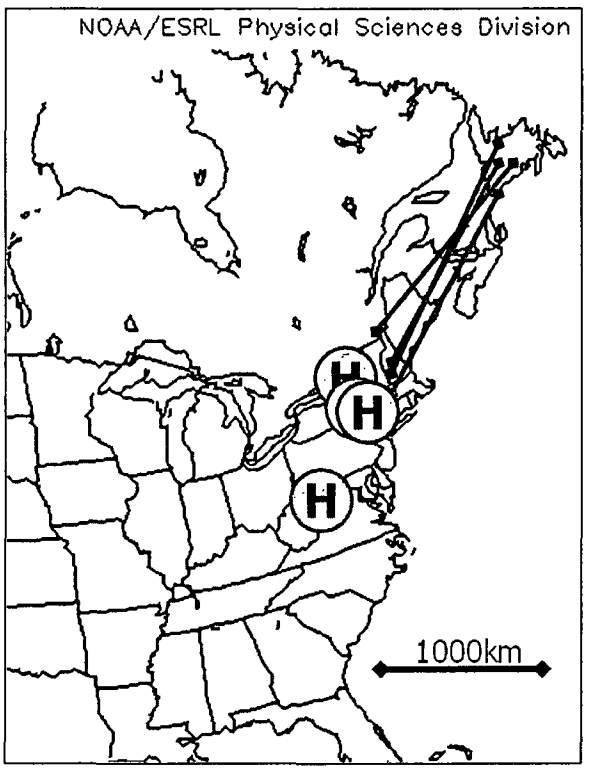

Figure 4.2: Conceptual schematic for synoptic class 1. Blue is fast event, purple is slow event, green is marginal event, and red is non-event.

Table 4.1: Gradients calculated along gradient lines in Figure 4.2.

Event Type	*Gradient (hPa/100km)*	*No. of Events*
Fast SB	0.83	42
Slow SB	0.89	14
Marginal	0.86	26
Non-Event	1.22	86

For synoptic class 2, the composite high pressure centers are somewhat more spread out; however, the non-sea breeze events' composite high center is the still farthest south (Fig. 4.3). The pressure gradient for the non-sea breeze event is 1.36 hPa/100km (Table 4.2), again making the gradient strongest for these events.

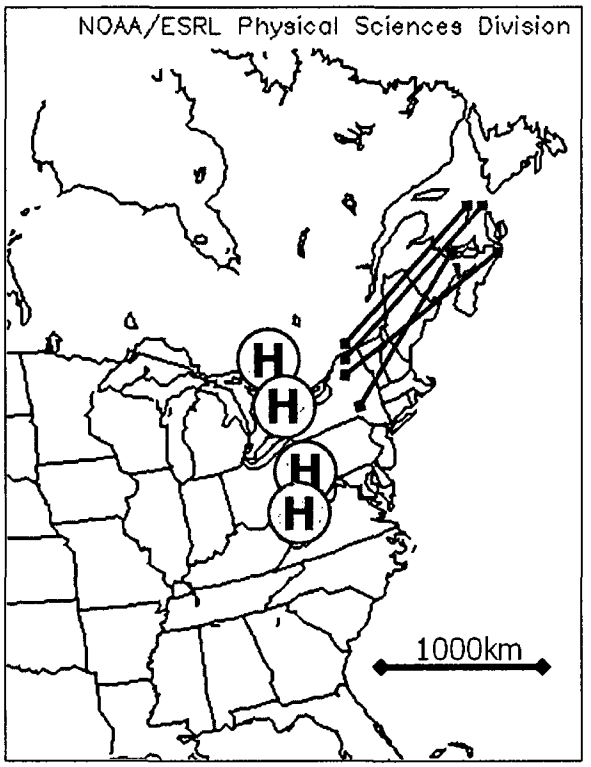

Figure 4.3: Conceptual schematic for synoptic class 2. Labeling is the same as Figure 4.2.

Table 4.2: Gradients calculated along gradient lines in Figure 4.3.

Event Type	*Gradient (hPa/100km)*	*No. of Events*
Fast SB	0.70	36
Slow SB	0.74	11
Marginal	0.71	8
Non-Event	1.36	177

For synoptic class 3, results were not as clear. Although non-sea breeze events still have the strongest composite pressure gradient at 1.39 hPa/100km (Table 4.3), the composite high center is not the farthest south (Fig. 4.4). There are *two* high centers for the marginal events, one of which represents the most southerly high center. These irregularities may be attributed to the small sample size. For synoptic class 3, there were only 4 fast sea breeze events, 2 slow sea breeze events, and 6 marginal events. Compared to the 132 non-sea breeze events, a larger sample size for the sea breeze events is needed to get a more statistically-meaningful composite analysis of the sea breeze with synoptic class 3.

A pattern can be found in the seasonal variation of each event type within these three synoptic classes (Fig. 4.5). Figure 4.5a (class 1) shows a peak in sea breeze events occurring in late spring and early summer. It also shows that synoptic class 1 non-sea breeze events happen least during the late spring and early summer. In Figure 4.5b (class 2), the peak of sea breeze events occurs closer to midsummer than with synoptic class 1. Again, the minimum for non-sea breeze events occurs at the same time as the sea breeze event peak. Finally, in Figure 4.5c (class 3), the peak appears similar to class 2 only there is much less variation between seasons.

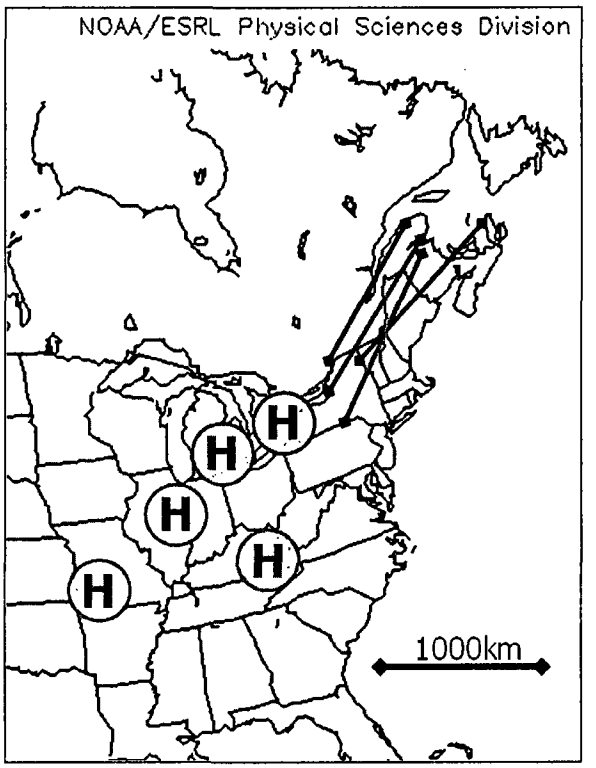

Figure 4.4: Conceptual schematic for synoptic class 3. Labeling is the same as Figure 4.2.

Table 4.3: Gradients calculated along gradient lines in Figure 4.4.

Event Type	*Gradient (hPa/100km)*	*n=No. of Events*
Fast SB	0.95	4
Slow SB	0.79	2
Marginal	0.64	6
Non-Event	1.39	132

Classes 1 through 3 behave as if they are along a single spectrum of class, with one and three at opposite extremes, and two in the middle. The same general trend for individual event types is evident in each class. Moreover, in moving along the continuum, the number of non-sea breeze events becomes greater; 15.4% for class 1, 38.2% for class

2, and 81.8% for class 3. The sample size of sea breeze events (fast, slow, and marginal) is small for synoptic class 3 which takes away from the statistical significance of the distribution. A larger data set is necessary to improve the worth of this distribution.

The composite analyses of synoptic class 4 for each event type (Fig. 4.6) show a noticeable increase in pressure gradient between fast sea breeze events and non-sea breeze events. There is also a clear rotation of the orientation of the isobars. For a fast sea breeze event the flow at the top of the boundary layer is shore parallel, making it easier for the sea breeze front to move inland. For the non-sea breeze event, the isobars are oriented shore-perpendicular, causing a stronger wind component at the top of the planetary boundary layer opposing the landward movement of the sea breeze.

The location of the low pressure system in Canada varies between fast and slow sea breeze events. For a fast sea breeze event, the low is centered farther north into Hudson Bay. This causes the pressure gradient over the study area to be much weaker. For a slow sea breeze event the low is centered farther south over James Bay, causing a slightly stronger pressure gradient over the study area.

a.)

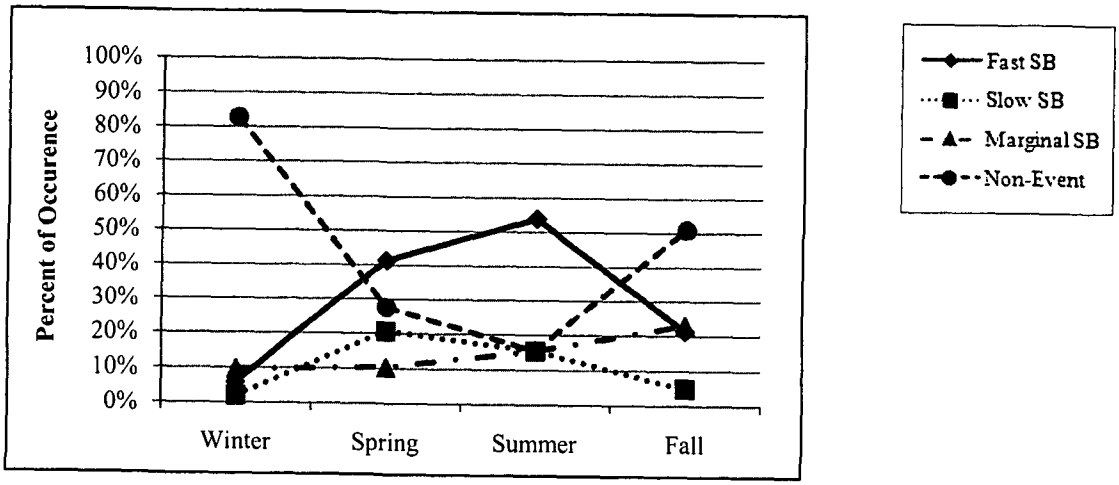

b.)

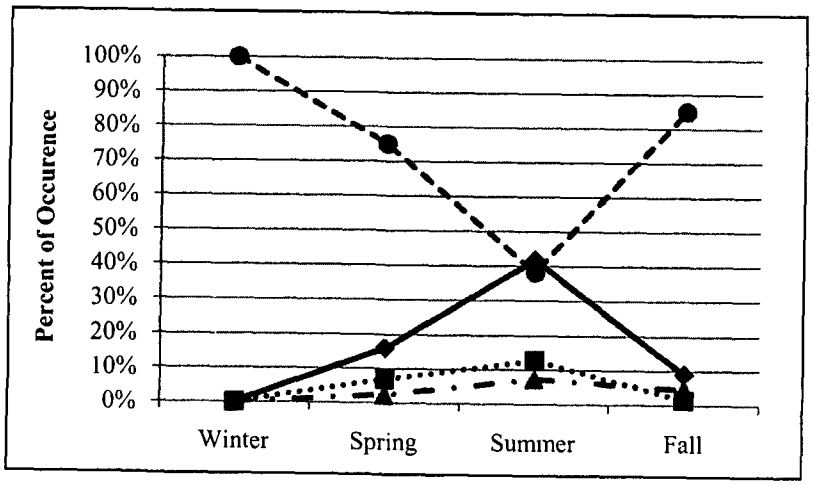

c.)

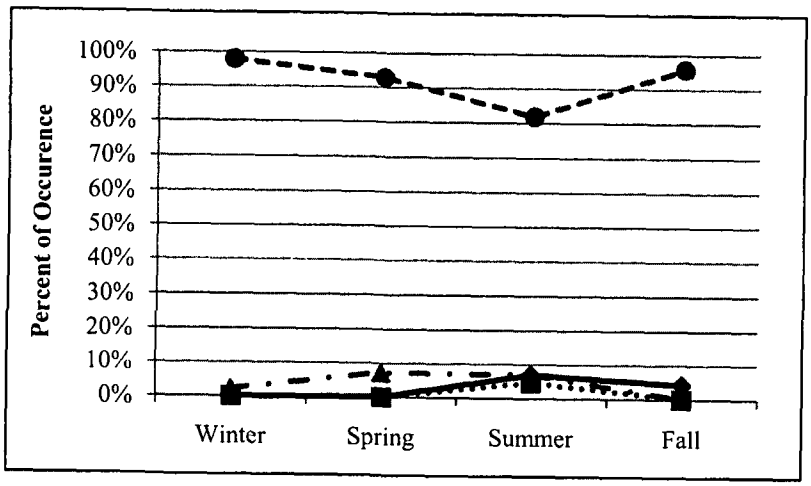

Figure 4.5: Seasonal variation of event type occurrence for a.) synoptic class 1, b.) synoptic class 2, and c.) synoptic class 3.

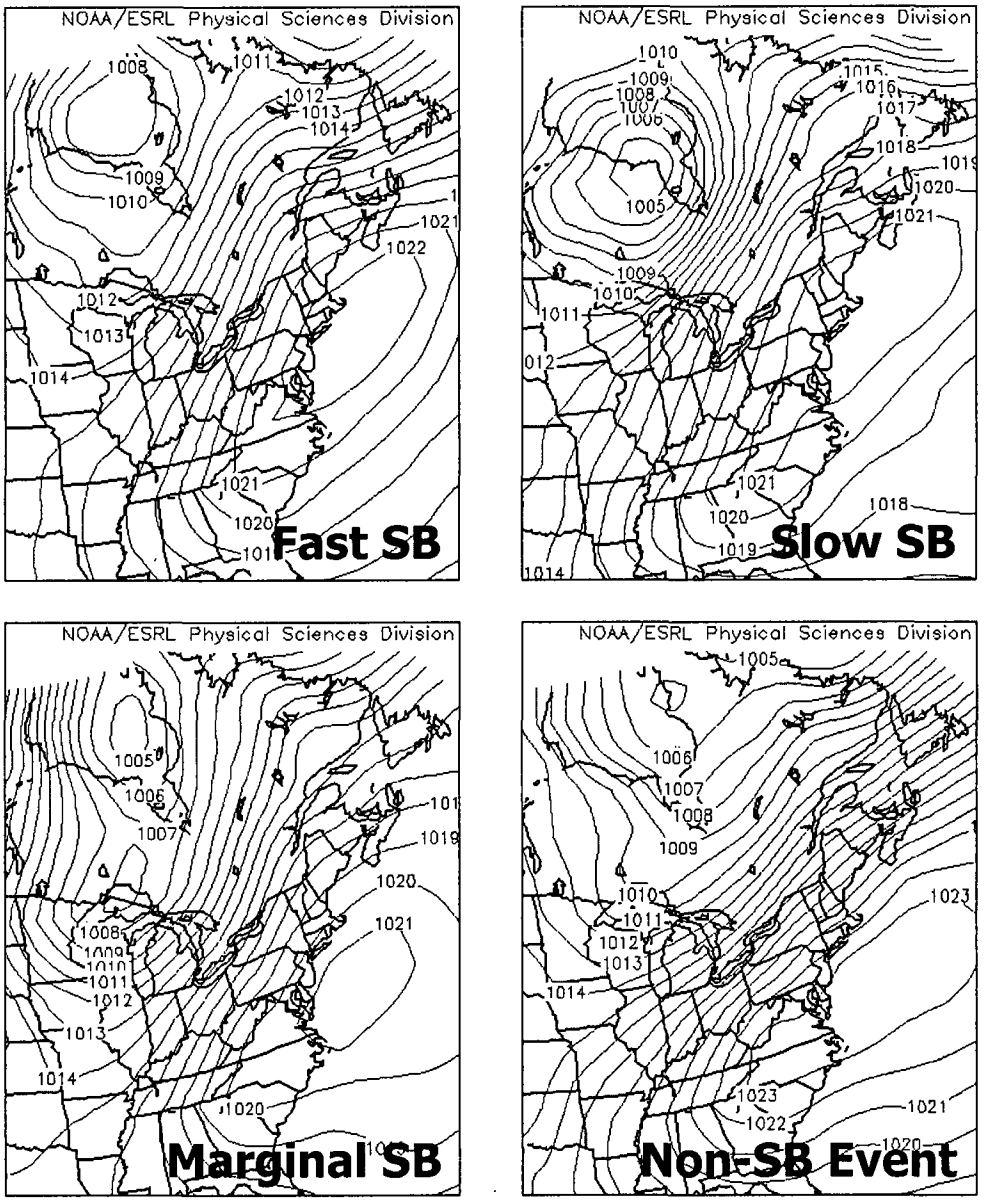

Figure 4.6: Composite analyses of synoptic class 4 for each event type.

The seasonal variation of synoptic class 4 is shown in Figure 4.7. Notice that the fast events are inversely related to non-events, increasing when the non-events decrease and vice versa. The same can be seen with the slow and marginal events. Similar characteristics beyond synoptic class seem to exist between these pairs. There seems to

be an unknown determining factor governed by season that distinguishes whether a fast event will occur versus a non-event. The factor could be as simple as the available daytime heating from season to season, but further research is needed to establish the cause. There were a total of 53 fast events, 7 slow events, 23 marginal events, and 108 non-events.

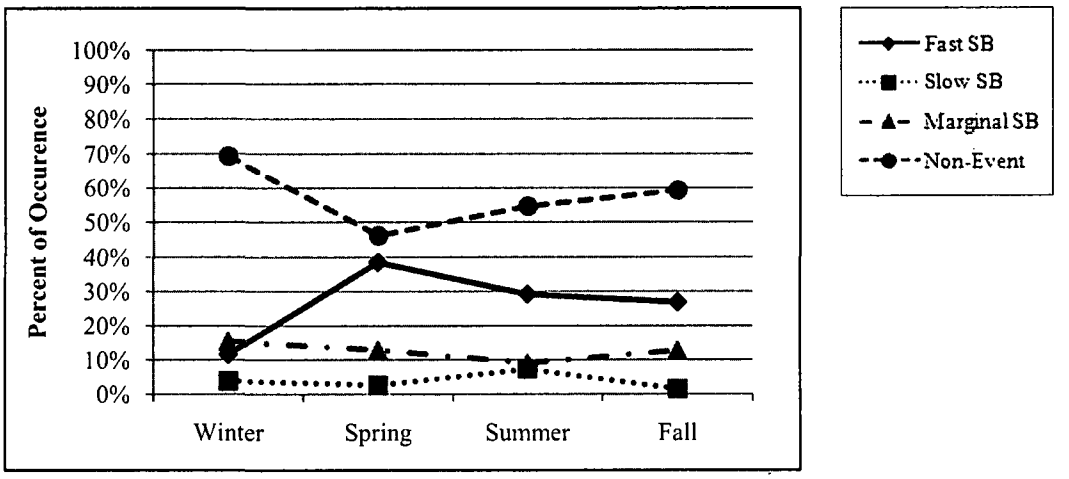

Figure 4.7: Seasonal variation of event type occurrence for synoptic class 4.

For synoptic class 5 (Fig. A-5), only non-sea breeze events occurred, confirming the findings of Miller and Keim (2003). There were a total of 22 non-events.

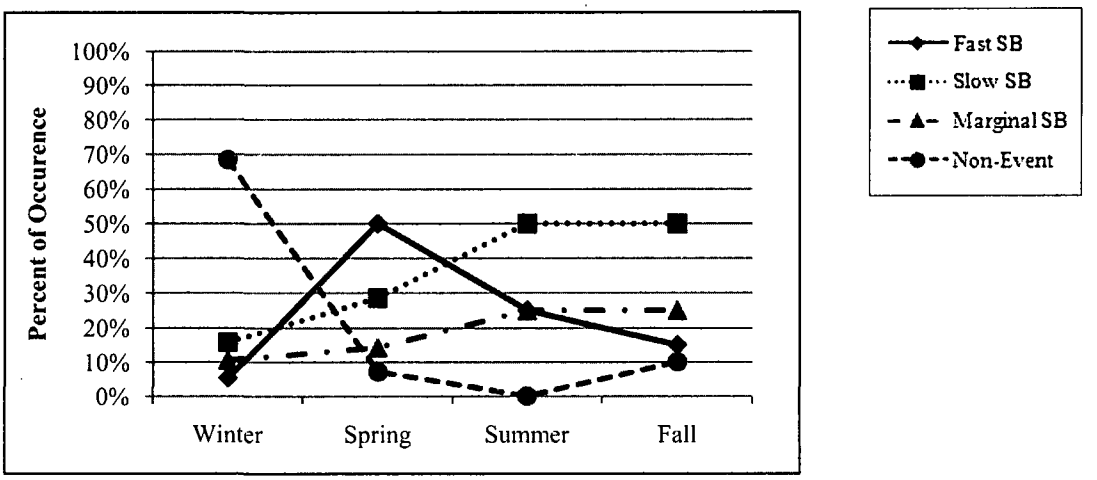

Figure 4.8: Seasonal variation of event type occurrence for synoptic class 6.

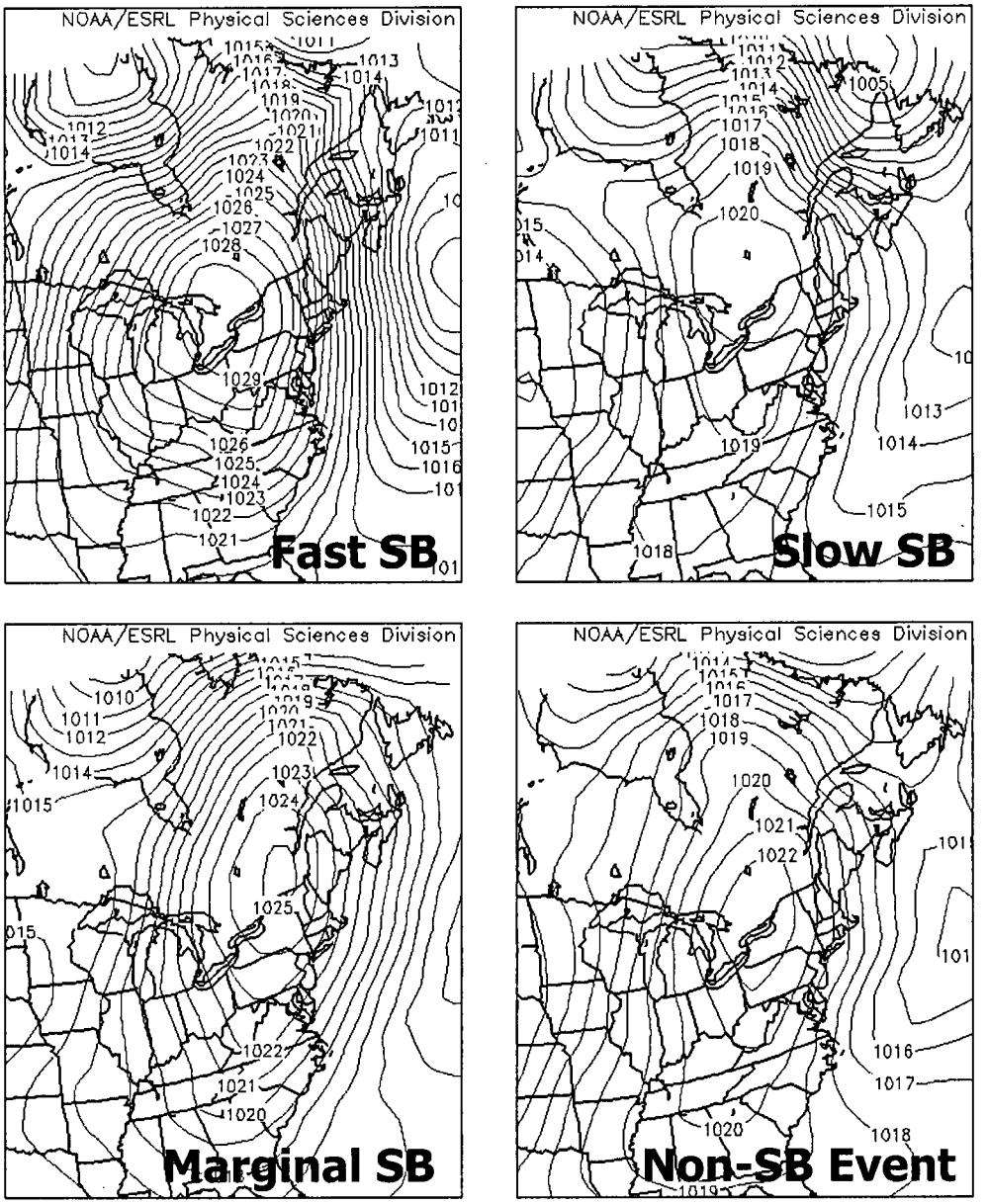

Figure 4.9: Composite analyses of synoptic class 6 for each event type.

For synoptic class 6 it is interesting to note that the seasonal variation of event type shows each event peaking in a different season (Fig.4.8). Non-sea breeze events peak in winter, fast sea breeze events peak in spring, and the slow and marginal events peak together in summer and fall. These peaks are likely related to the variations in

daytime heating available to initiate the sea breeze. There were 13 fast events, 21 slow events, 11 marginal events, and 16 non-events. The composite analyses for synoptic class 6 showed an increase in pressure gradient over the study area between fast sea breeze events and non-sea breeze events (Fig. 4.9). The center of the high is located farthest west in the non-sea breeze event which creates the stronger gradient over the study area.

b. Inland Penetration

Wind vector plots were generated to help visualize the extent and shape of the inland penetration of the sea breeze circulation. Gridded data generated using the Barnes analysis was plotted using MATLAB. The location of the sea breeze front was then subjectively analyzed based on wind shift to determine the shape and depth of penetration. The front was only analyzed based on the eastern coastline of Massachusetts and sea breezes from the south were ignored. Plots were made for the 5 major synoptic classes for fast sea breeze events (class 1 to 4, 6).

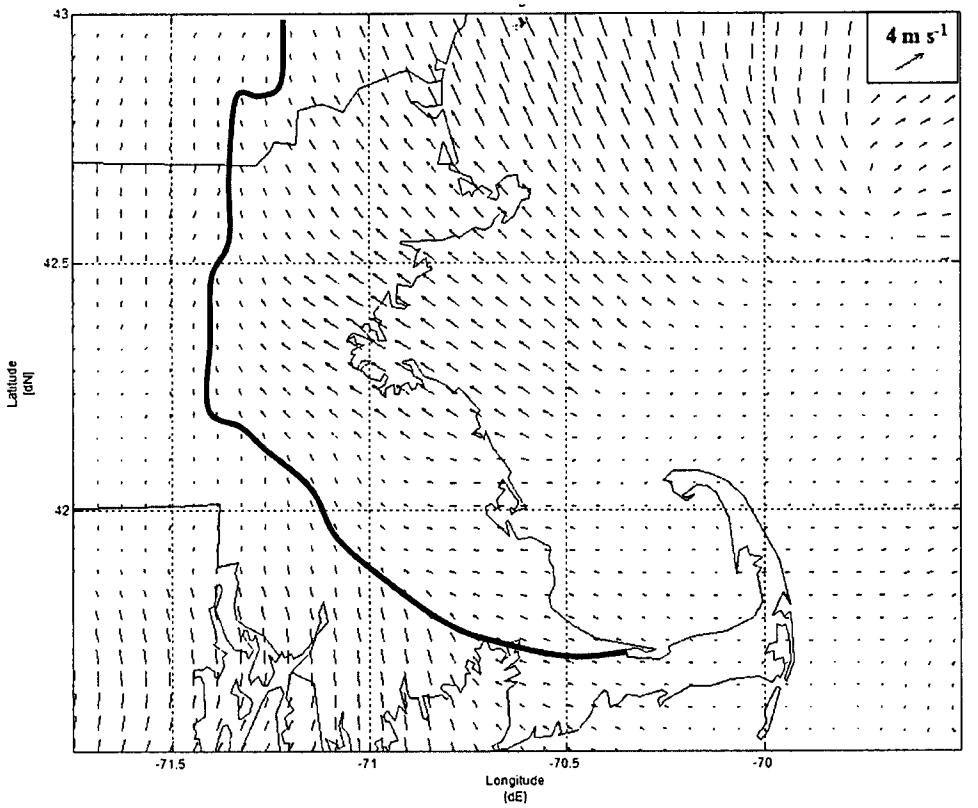

Figure 4.10: Plot of the mid-event average wind vectors for synoptic class 1. Solid black line represents the analyzed location of the sea breeze front.

Synoptic class 1, northwesterly anticyclonic flow, is shown in Figure 4.10. The wind vectors in this plot represent the average mid-event flow pattern for the 6 chosen dates described in chapter 2. Notice the depth of penetration relative to the coastline remains almost the same overall. The northern portion of the sea breeze seems to penetrate slightly further inland than the southern portion. This is clearly related to the strong southeasterly winds in the northern portion of the sea breeze flow compared to the much weaker east-southeasterly flow in the southern portion.

Figure 4.11 shows the wind vector plot of the mid-event average for synoptic class 2. The depth of inland penetration remains at a constant for the Massachusetts coastline. There is very little inland progression in New Hampshire with this synoptic

class. Synoptic class 2 has a neutral (neither anticyclonic nor cyclonic) northwesterly flow over the study area. The sea breeze from the Rhode Island Sound and Buzzard's Bay seems to be stronger with synoptic class 2 and can be seen further into Massachusetts than with synoptic class 1 (Fig. 4.10).

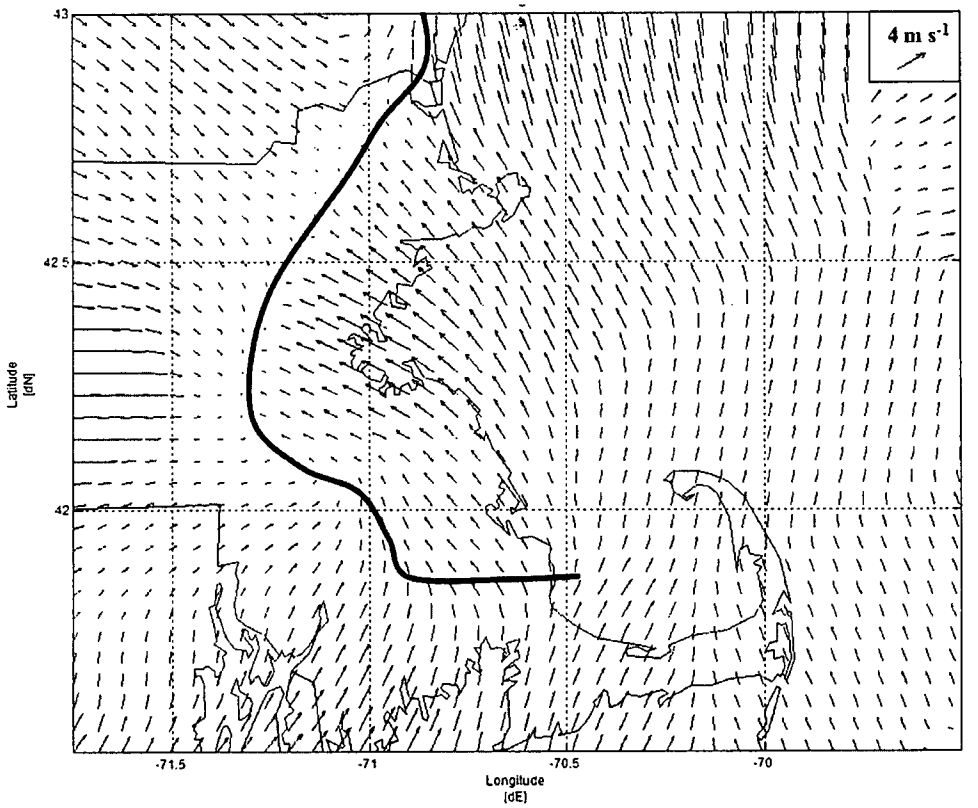

Figure 4.11: Plot of the mid-event average wind vectors for synoptic class 2. Same as Fig. 4.12.

The plot for cyclonic northwesterly flow, synoptic class 3, is shown in Fig. 4.12. This plot is only the average of 4 events unlike classes 1 and 2 which were 6 events. There were only 4 fast events in synoptic class 3 in the study overall. The inland progression of the sea breeze seems to be more limited with synoptic class 3 which is to be expected as the cyclonic winds would be stronger than the winds with classes 1 and 2.

The sea breeze also seems to push farther into New Hampshire compared to synoptic class 2 which is unexpected.

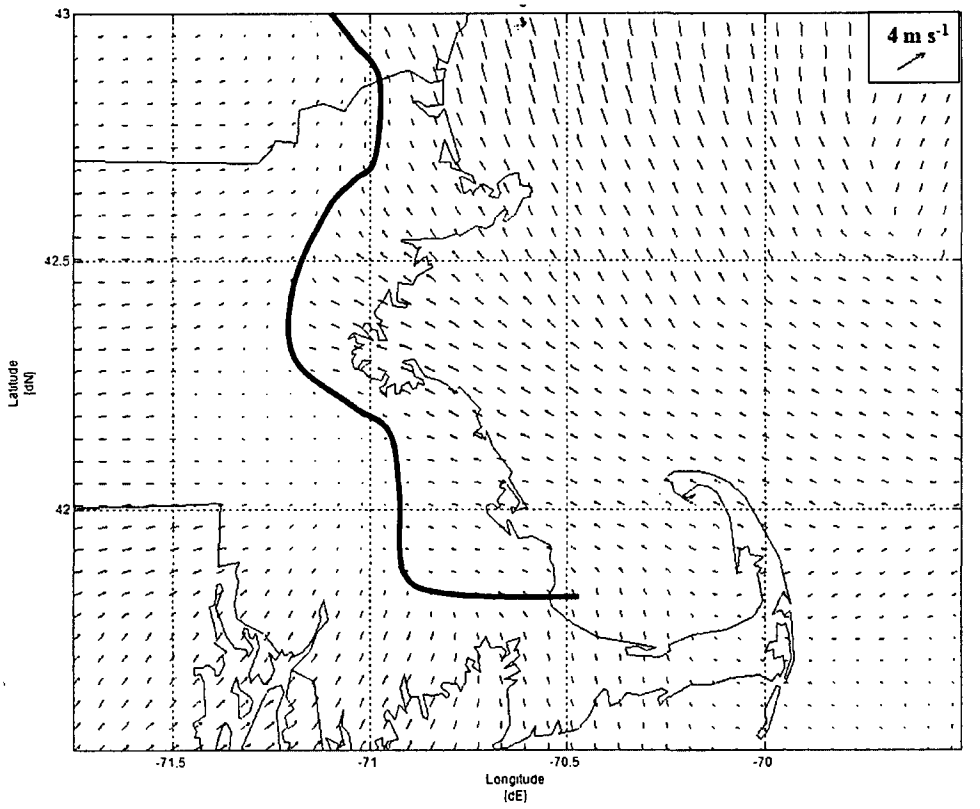

Figure 4.12: Plot of the mid-event average wind vectors for synoptic class 3.

The mid-event average wind vector plot for synoptic class 4, southwesterly flow, is shown in Figure 4.13. Inland propagation of the sea breeze is extremely limited south of Boston due to the strong effect of the southwesterly flow. The flow also somewhat limits inland penetration north of Boston as the sea breeze front is not as far inland as with synoptic class 1. The effect of the southwesterly flow is much more distinct than with the other flow regimes. I hypothesize that the southwesterly synoptic flow regime is

enhancing the sea breeze flow from the Rhode Island and Long Island Sounds thus vastly reducing the inland penetration of the Massachusetts Bay sea breeze flow.

Figure 4.14 shows the mid-event average wind vector plot for synoptic class 6. This class is characterized by shore-parallel, northeasterly surface wind flow. There were only 5 events used in this plot as mentioned in chapter 2.

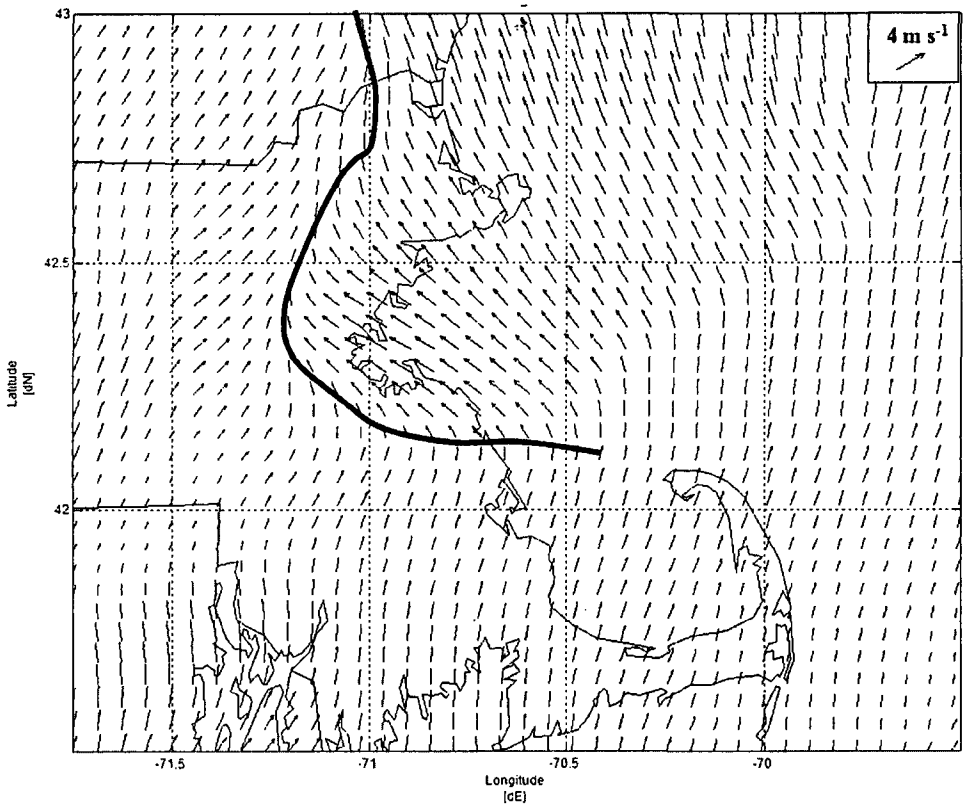

Figure 4.13: Plot of the mid-event average wind vectors for synoptic class 4.

Note that the greatest inland penetration occurs north of Boston. The sea breeze flow south of Boston also seems to progress further south compared to synoptic classes 2, 3, and 4. A slight enhancement of the sea breeze circulation by the synoptic scale flow may be the cause of this difference.

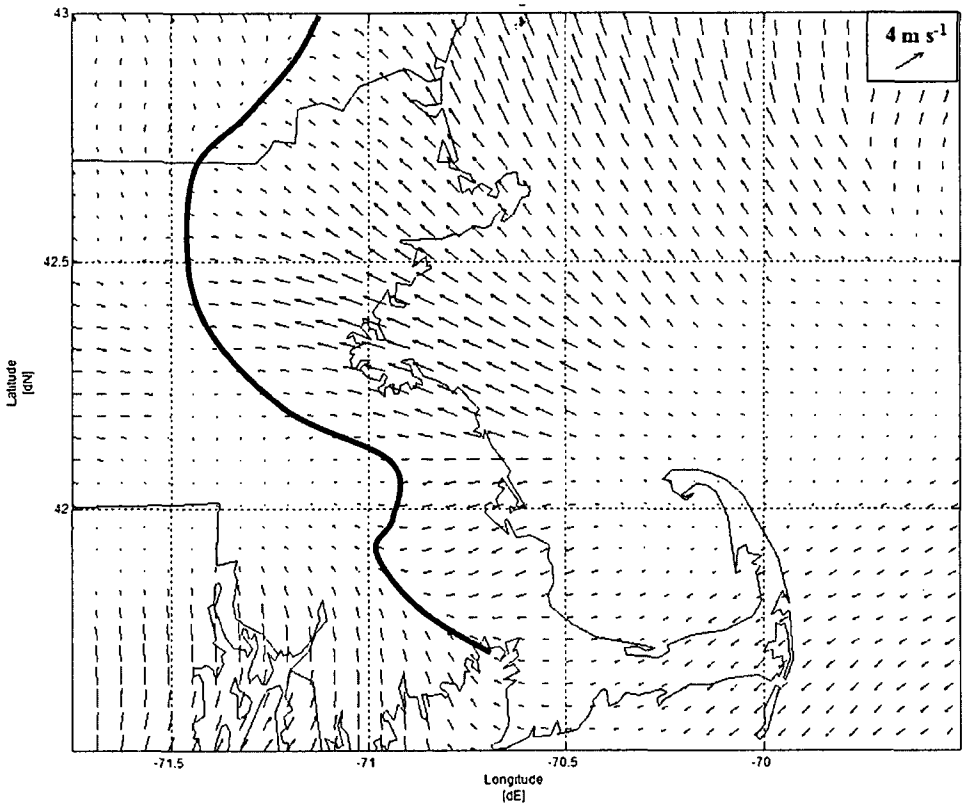

Figure 4.14: Plot of the mid-event average wind vectors for synoptic class 6.

A combined plot showing the location of each of the mid-event average sea breeze fronts is shown in Figure 4.15. This plot shows the decreasing inland penetration of the sea breeze circulation as the flow progresses from anticyclonic to neutral to cyclonic with classes 1 through 3. Synoptic class 4 seems to have the overall shallowest depth of propagation compared to all other classes. There are only subtle difference between the sea breeze fronts for classes 1 and 6. This indicates that northeasterly flow (class 6) and anticyclonic northwesterly flow (class 1) have nearly the same effect of the inland penetration of the sea breeze circulation.

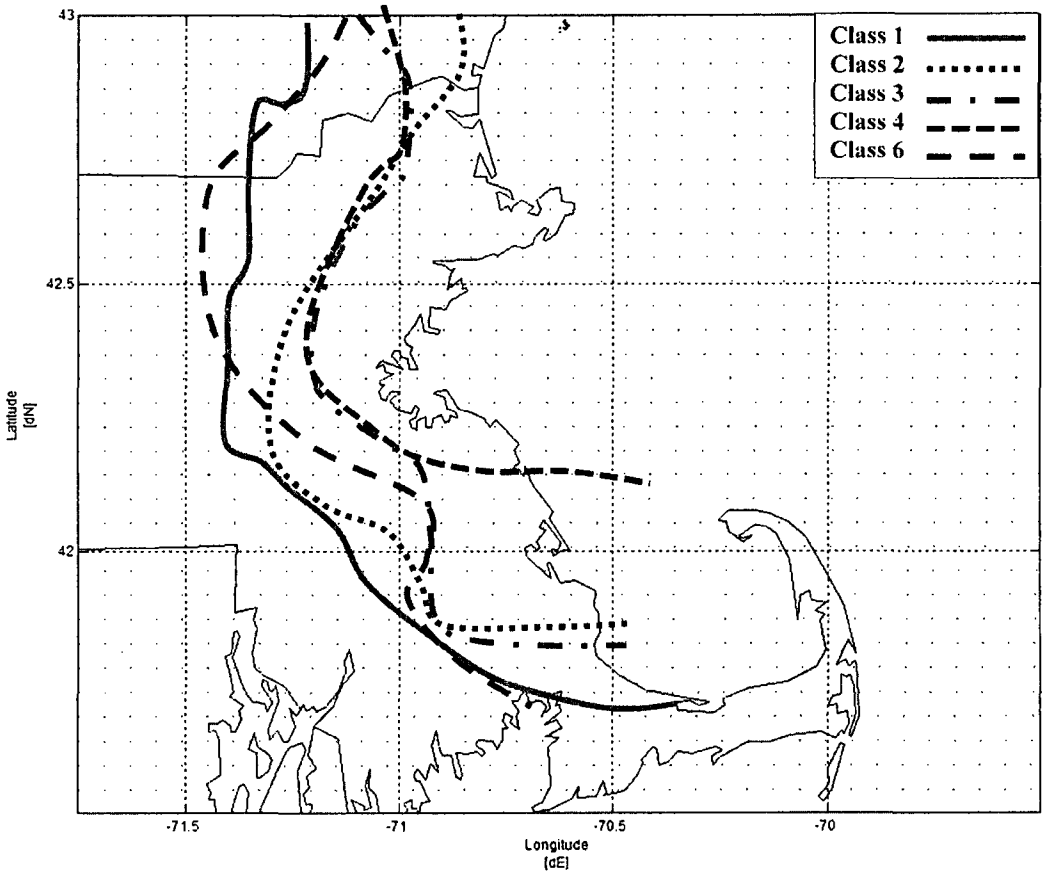

Figure 4.15: Combined plot of the mid-event average wind vectors for synoptic class 1 to 4 and 6. The lines represent the sea breeze front by synoptic class (See legend in upper-right corner).

More research is needed to explain these results. To reduce subjectivity, all of the fast events could be incorporated into the mid-event averages. This idea would prove to be computationally intensive but the resulting plots may have cleaner wind shifts. Also, including and comparing other event types beyond the fast sea breeze events may also introduce some interesting results.

CHAPTER 5

5. Mesoscale Calculations

a. 2-D Calculations

Results of the mesoscale calculations are shown in Figure 5.1, which are similar to the mesoscale results shown by Miller and Keim (2003) for Portsmouth, New Hampshire (*See Appendix E*). A total of 654 events are included in the overall diagram. There were missing data for 76 events and bad data for 149 of the non-events.

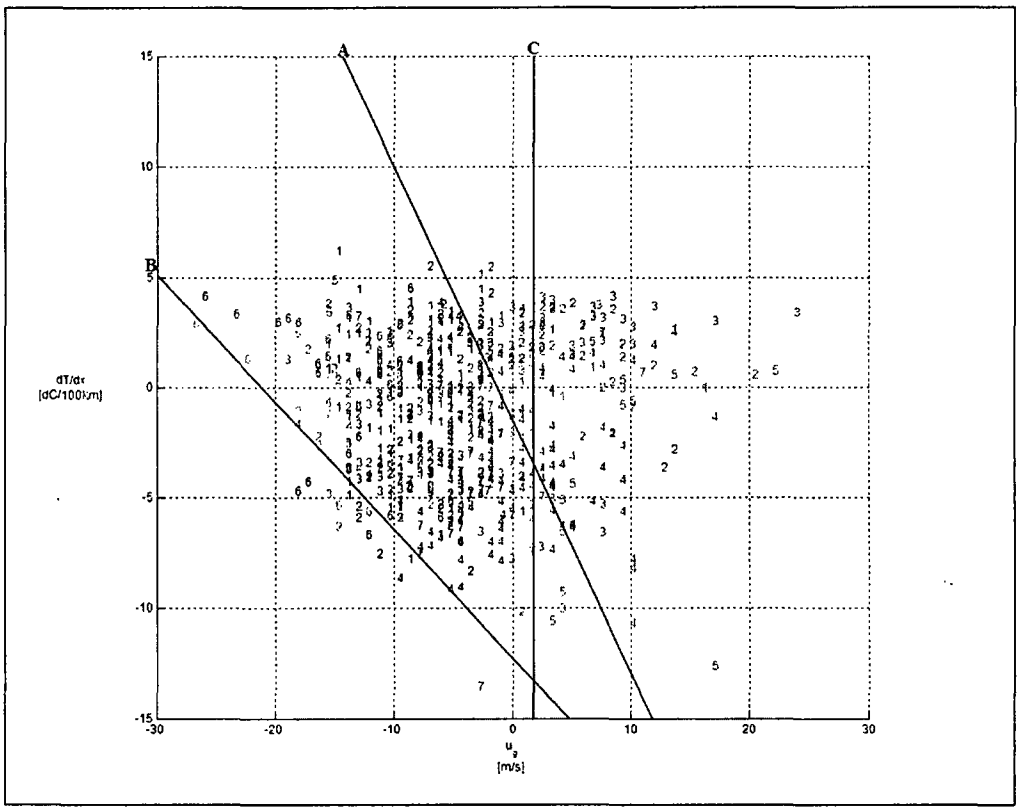

Figure 5.1: All sea breeze, marginal, and non-sea breeze events as a function of their associated cross-shore temperature gradients and geostrophic wind components. The numbers represent the synoptic class of the event. Fast sea breezes are blue (•), slow sea breezes are cyan (○), marginal sea breezes are black (•), and non-sea breezes are red (•).

The area enclosed by lines A, B, and C represents a transition area in which any type of event may occur. The lines represent critical limits between a sea breeze event (fast, slow, and marginal) and a non-sea breeze event. All events to the right of line A (Eq. 5.1) are non-sea breeze events. The area to the right of line C (Eq. 5.2) is also entirely non-sea breeze events, as the resisting u_G component is too strong for a sea breeze event to occur. All events to the left of line B (Eq. 5.3) are sea breeze events. It is evident that proportionally, more non-events fall to the right of the transition area compared to the number of sea breeze events that fall to the left of the transition area. Since the transition area is so large and includes more sea breeze events than non-events, the diagram was further broken down by synoptic class. No plots were created for synoptic class five as it only occurred with non-events, and for class 7 which was the miscellaneous class which contains a mixture of different synoptic patterns.

Line A: $y = -0.67x - 11.99$ (5.1)

Line B: $y = -1.12x - 1.82$ (5.2)

Line C: $x = 1.5$ (5.3)

Figure 5.2 shows only synoptic class 1 events using the same diagram style as described above. The transition area has been noticeably reduced and lines A and B (Eq. 5.4 and 5.5, respectively) are almost parallel. The position of line C (Eq. 5.6) moved slightly to the left. This indicates that synoptic class 1 sea breeze events require slightly less resistance from the seaward u_G component to develop compared to the limit set by line C for all events (Fig. 5.1). The distribution of the events in regards to the transition area has improved somewhat from the overall plot. A higher percentage of the sea breeze events fall to the left of the transition area compared to the plot of all synoptic classes.

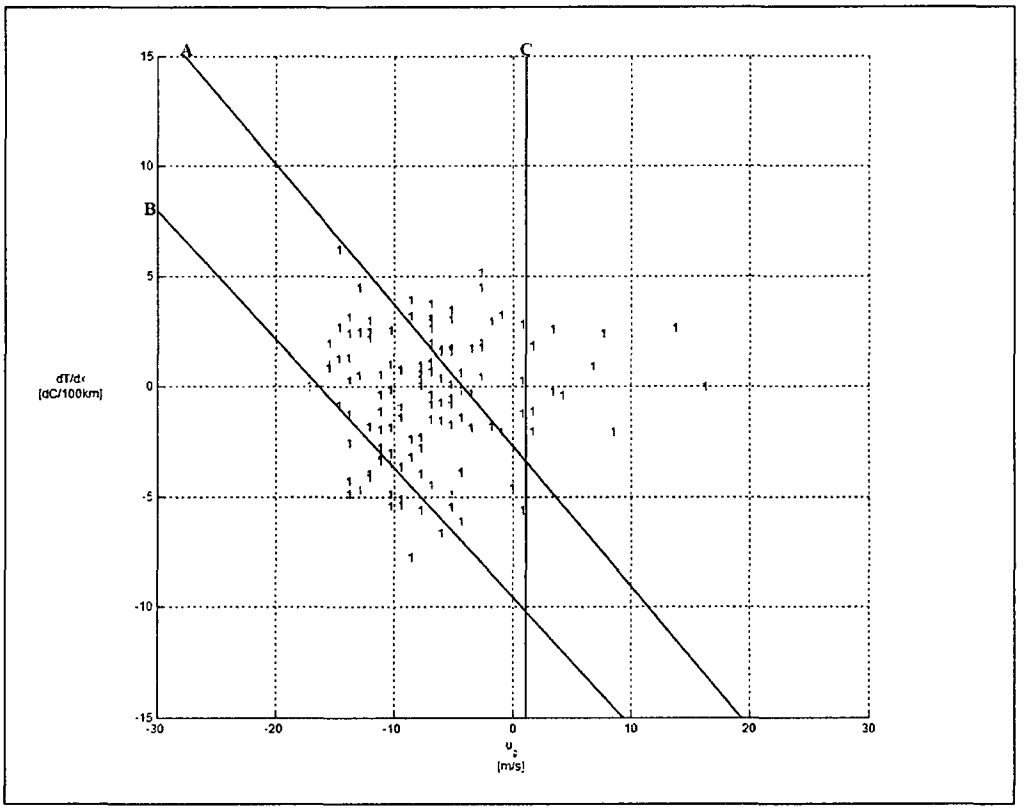

Figure 5.2: Same as Fig. 5.1 for synoptic class 1 only.

Line A: $y = -0.62x - 3.05$ (5.4)

Line B: $y = -0.57x - 9.67$ (5.5)

Line C: $x = 1$ (5.6)

The plot for synoptic class 2 is shown in Figure 5.3. The transition area shrinks compared to synoptic class 1 as lines A and B (Eq. 5.7 and 5.8, respectively) actually meet at the bottom of the diagram. Line C (Eq. 5.9) has become negative indicating that for a synoptic class 2 sea breeze to occur, a weak onshore u_G component is necessary. If any seaward u_G component exists under a synoptic class 2 flow regime, the sea breeze will not occur. The dispersion of events in this plot shows slightly more than half of the

sea breeze events falling to the left of the transition area which is an improvement from the overall plot (Fig. 5.1).

Line A: $y = -1.12x - 6.64$ (5.7)

Line B: $y = -0.60x - 10.55$ (5.8)

Line C: $x = -2.25$ (5.9)

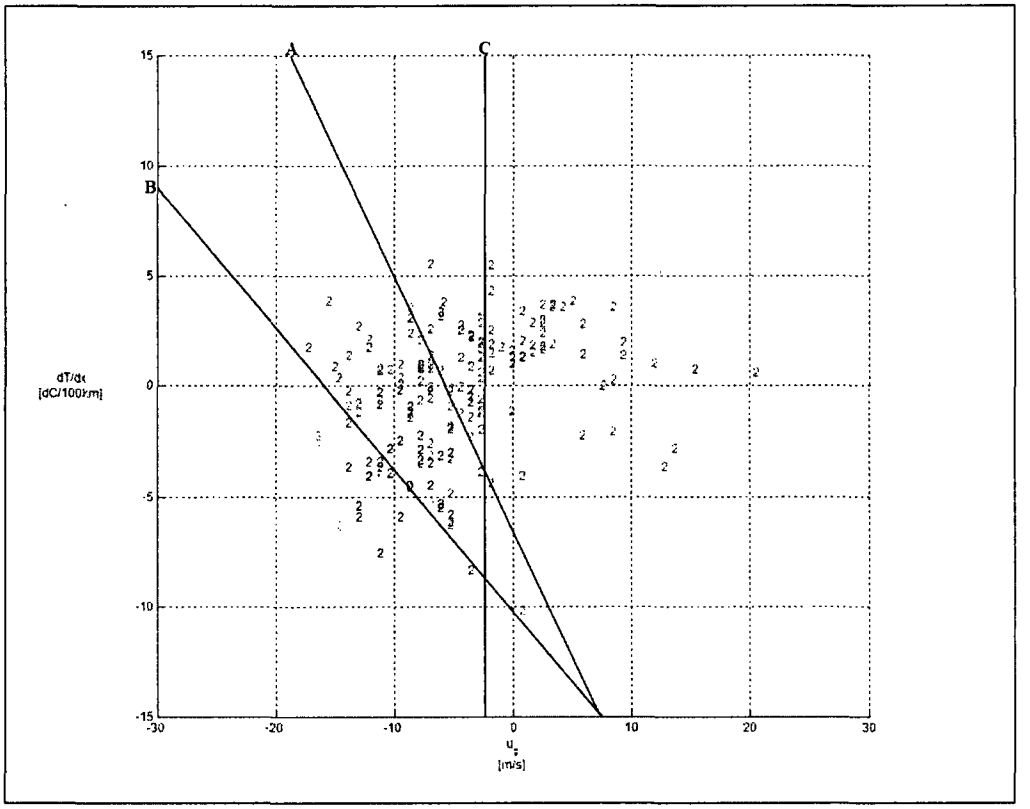

Figure 5.3: Same as Fig. 5.1 for synoptic class 2 only.

In Figure 5.4, the cross-shore components for synoptic class 3 are plotted. The transition area seems to have same width as synoptic class 2. Lines A and B (Eq. 5.10 and 5.11, respectively) meet in a point at the bottom of the plot like with synoptic class 2. Only one sea breeze event falls to the left of Line B which is believable as there were few sea breeze events with synoptic class 3. Of the overall 12 sea breeze events (4 fast, 2 slow, and 6 marginal), there were 3 events with missing data (2 fast and 1 marginal) that

were not plotted. This leaves only 9 events to be plotted versus the available 91 of 132 non-sea breeze events. Line C (Eq. 5.12) is -6.5 m s^{-1} indicating that a moderately strong onshore wind is necessary for a sea breeze to occur with synoptic class 3.

$$\text{Line A:} \qquad y = -1.67x - 17.08 \qquad (5.10)$$

$$\text{Line B:} \qquad y = -0.83x - 15.22 \qquad (5.11)$$

$$\text{Line C:} \qquad x = -6.5 \qquad (5.12)$$

If classes 1, 2 and 3 are examined as a single spectrum of synoptic class as was done in the synoptic scale analysis in Chapter 4, there is a noticeable progression from class 1 to class 3. Note the position of line C moves from 1.5 m s^{-1} with class 1 to -2.0 m s^{-1} with class 2 to -6.5 m s^{-1} with class 3. A stronger onshore mesoscale u_G component is necessary for class 3 sea breeze events to occur. Since class 3 is characterized by cyclonic northwesterly synoptic scale flow, a stronger onshore u_G component is needed to help the sea breeze overcome this opposing force.

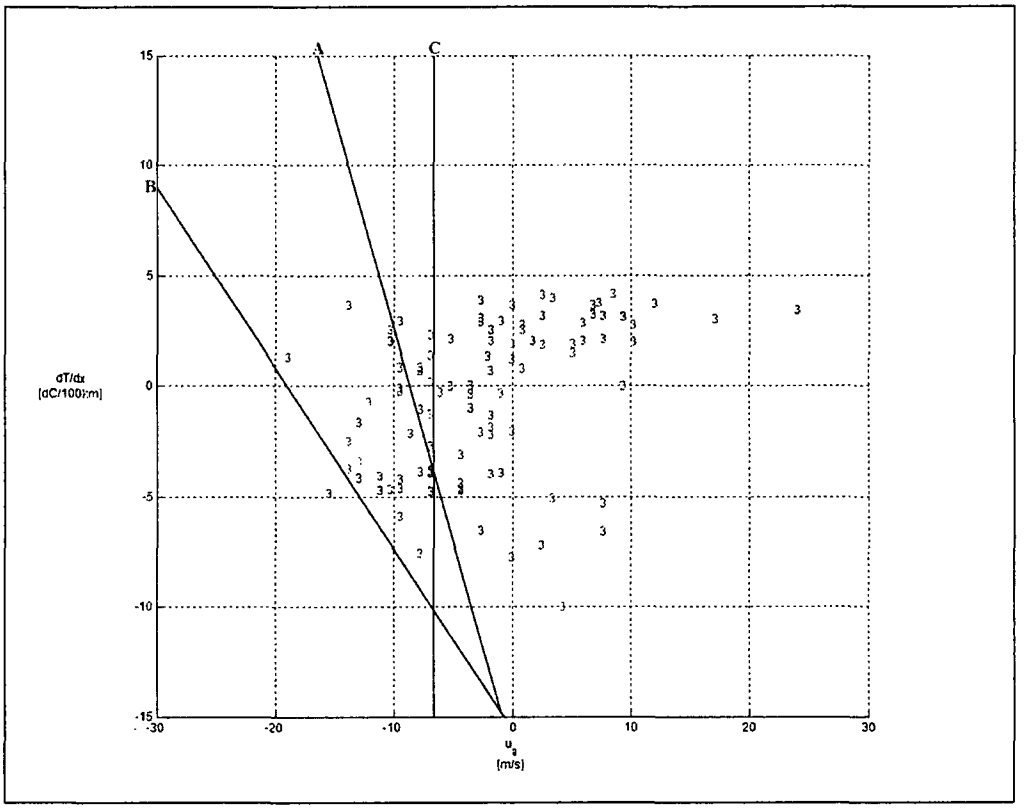

Figure 5.4: Same as Fig. 5.1 for synoptic class 3 only.

The plot of the cross-shore components for synoptic class 4 is depicted in Figure 5.5. Compared to classes 2 and 3, the shape of the transition area has reversed. Lines A and B (Eq. 5.13 and 5.14, respectively) nearly meet at the top of the plot. The transition area is also a little larger with synoptic class 4 compared to classes 1 through 3; though it is still smaller than the area in the overall plot (Fig. 5.1). About half of the sea breeze events fall to the left of the transition area, which is again an improvement compared to the plot of all synoptic classes. There also seems to be more non-events in the transition area than there are to the right of lines A and C (Eq. 5.15).

Line A: $y = -0.63x + 0.05$ (5.16)

Line B: $y = -1.07x - 9.115$ (5.14)

Line C: $x = 1.5$ (5.15)

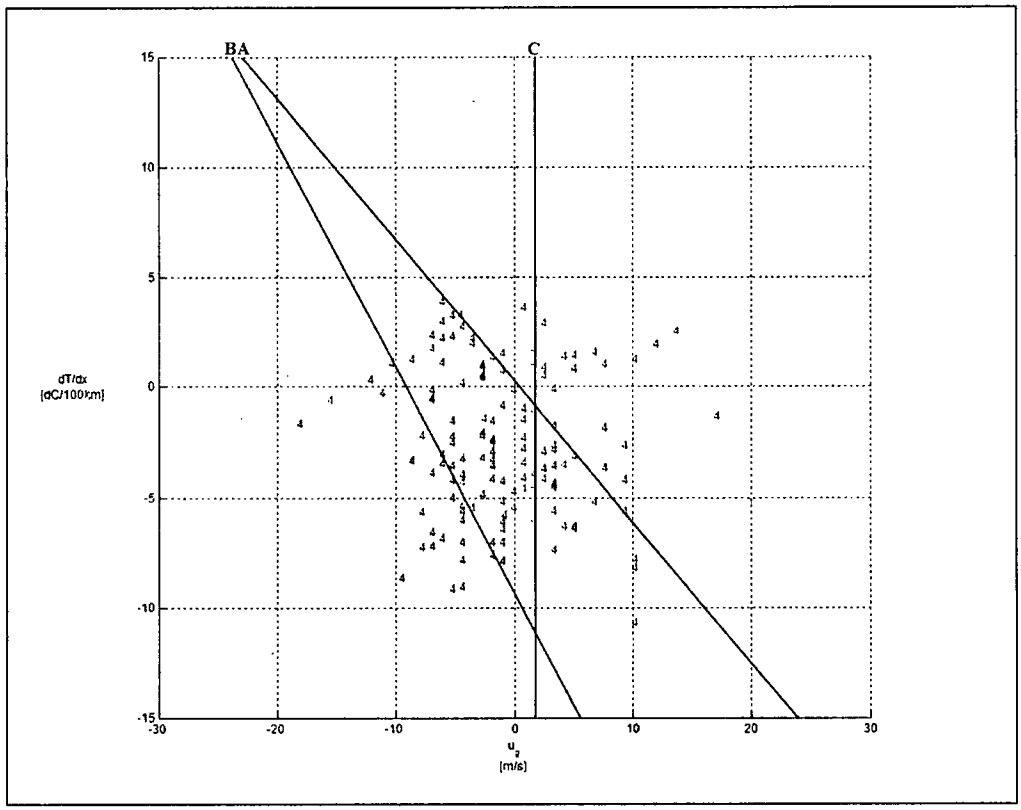

Figure 5.5: Same as Fig. 5.1 for synoptic class 4 only.

Figure 5.6 is the plot of the cross-shore components for synoptic class 6. As with synoptic classes 2 and 3, lines A and B (Eq. 5.16 and 5.17, respectively) meet at a point. The transition area is smallest with class 6; with most of the sea breeze events falling to the left of line B. Non-events make up about 25% of synoptic class 6 events. There was missing data for 1 of the non-event dates so only 15 non-events are plotted. This makes the positioning of line A questionable and makes line C (Eq. 5.18) a theoretical limit at which only non-events would occur. Line C is hypothetical since it is only derived from sea breeze event data and has no non-events to help verify its position. A larger data set could help position the critical limits of synoptic class 6 better.

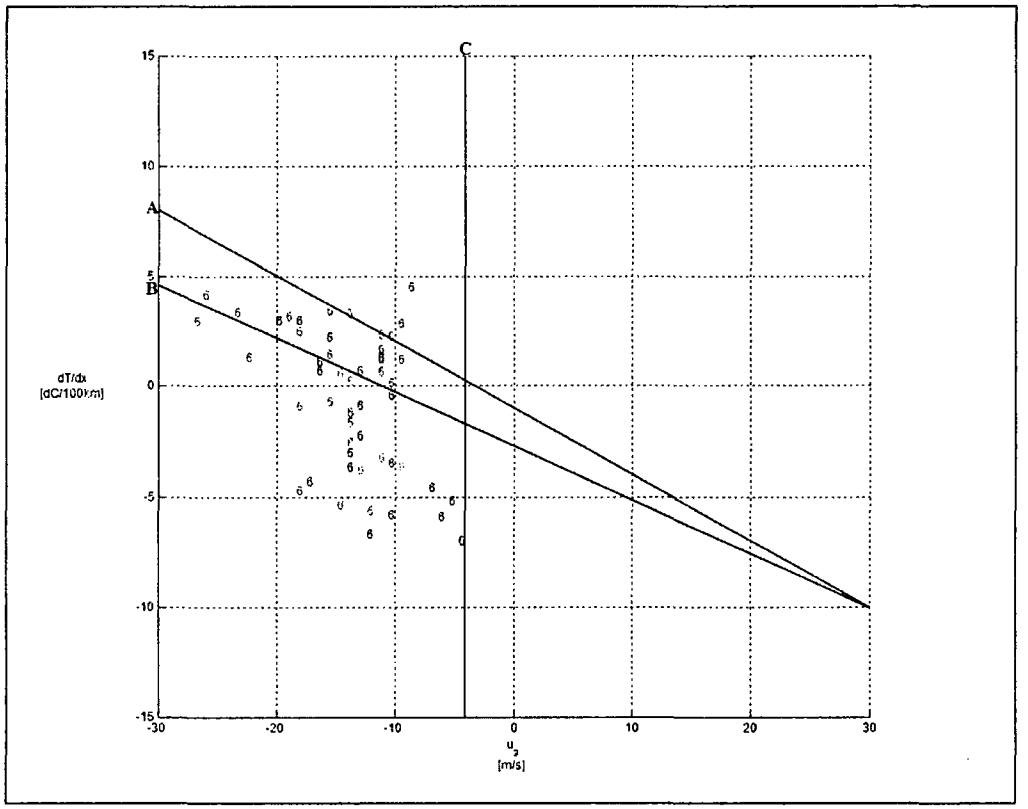

Figure 5.6: Same as Fig. 5.1 for synoptic class 6 only.

$$\text{Line A:} \qquad y = -0.30x - 1 \qquad (5.16)$$

$$\text{Line B:} \qquad y = -0.25x - 2.50 \qquad (5.17)$$

$$\text{Line C:} \qquad x = -4 \qquad (5.18)$$

Figures 5.7 shows line A for each synoptic class and for all events as an overlay. Figures 5.8 and 5.9 are the same as Figure 5.7 except for line B and line C, respectively. Notice the slope of line A becomes steeper between class 1 to class 2 and class 2 to class 3. Line A for classes 1 and 4 seem almost parallel. Line A from the plot of all events is almost parallel to that of synoptic class 2. Synoptic class 6 line A has the most gradual slope of all, although it may be slightly skewed due to a lack of non-events as mentioned before.

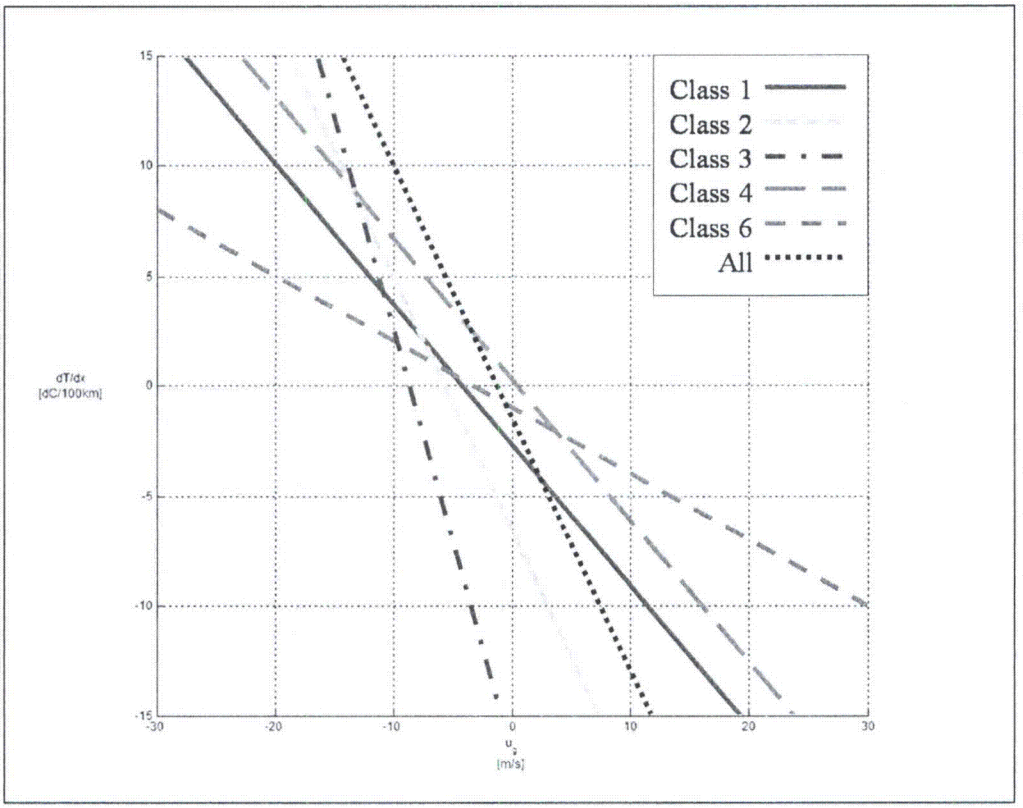

Figure 5.7: Overlay of line A for each synoptic class and for all events.

In Figure 5.8, line B for synoptic classes 1 and 2 are almost the same and they run somewhat parallel to line B for all events. Synoptic class 4 has the steepest slope for line B and synoptic class 6 has the most gradual slope like with line A. The increasing slope seen with line A for classes 1 to 3 (Fig. 5.7) is not present with line B (Fig. 5.8).

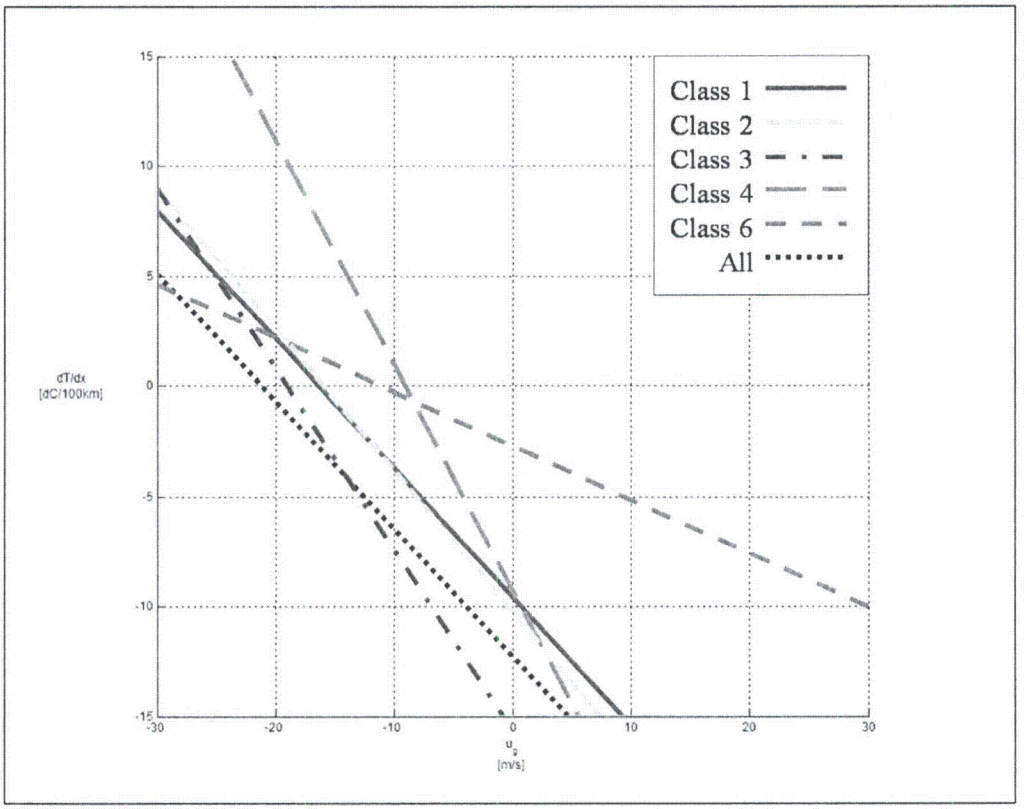

Figure 5.8: Same as Fig. 5.7 only for line B.

Line C gives a good idea how strong of an opposing wind the sea breeze can overcome with any given synoptic class or overall, in the case of the plot of all events. In Figure 5.9, line C for each class is plotted along with the line C from the overall plot (Fig. 5.1). The strongest offshore u_G wind component that events as a whole could overcome was approximately 2.0 m s^{-1}. This limit is set by synoptic class 4 as line C for class 4 is in the same place as line C for all events (Fig. 5.9). Synoptic class 1 is very close to this limit at about 1.5 m s^{-1}. Synoptic classes 2, 3, and 6 all require an onshore u_G wind component to develop.

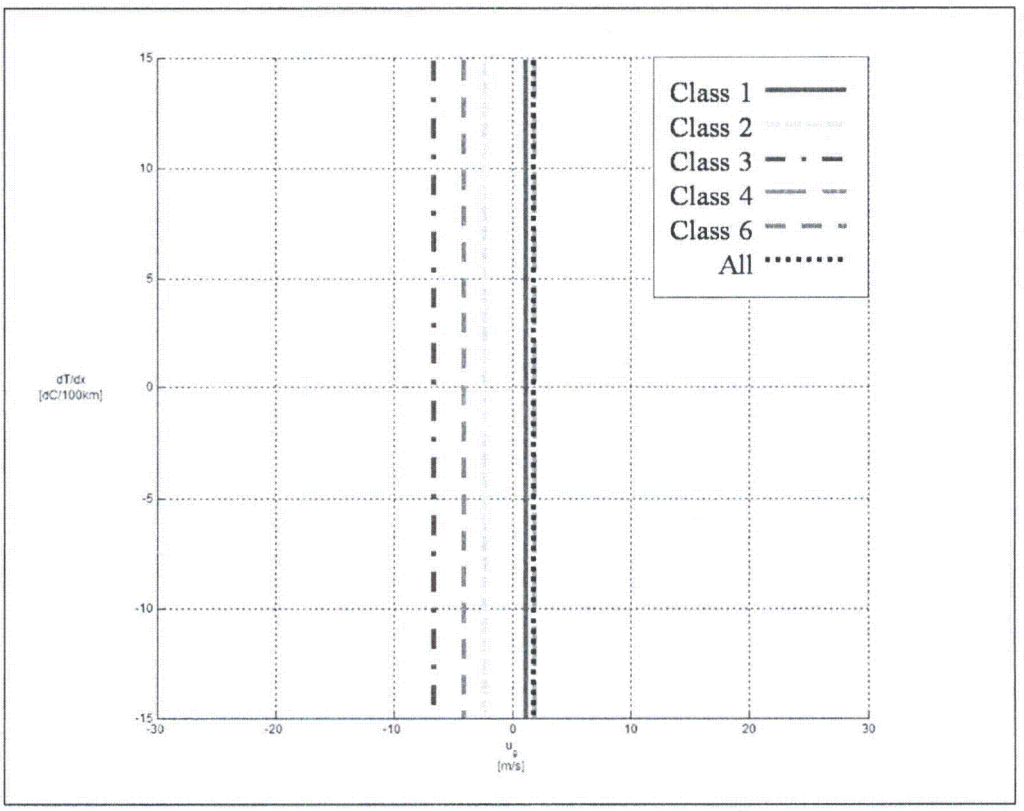

Figure 5.9: Same as Fig. 5.7 only for line C.

Figures 5.8 and 5.7 suggest a similarity in the way the sea breeze develops with synoptic classes 1 and 4. Lines B and C were almost the same for these two classes. For lines A and B, synoptic class 6 seemed to be the greatest outlier which is due to the lack of non-events. A larger data set may help to refine the critical limits for class 6. Synoptic class 3 seemed to need the largest onshore u_G wind component to develop which may be due to a lack of sea breeze events with this class. On the other hand, synoptic class 3 features the strongest northwesterly winds so a larger onshore u_G wind component is a plausible necessity for development.

b. 3-D Calculations

Sea breeze events (fast and slow only) were plotted against non-sea breeze events on a three-dimensional plot (Fig. 5.10). The variables used were the surface u_G wind component (m s^{-1}), the cross-shore temperature gradient (°C/100 km), and the 850 hPa u_G wind component (m s^{-1}). There are a total of 321 non-events on this plot and 127 sea breeze events.

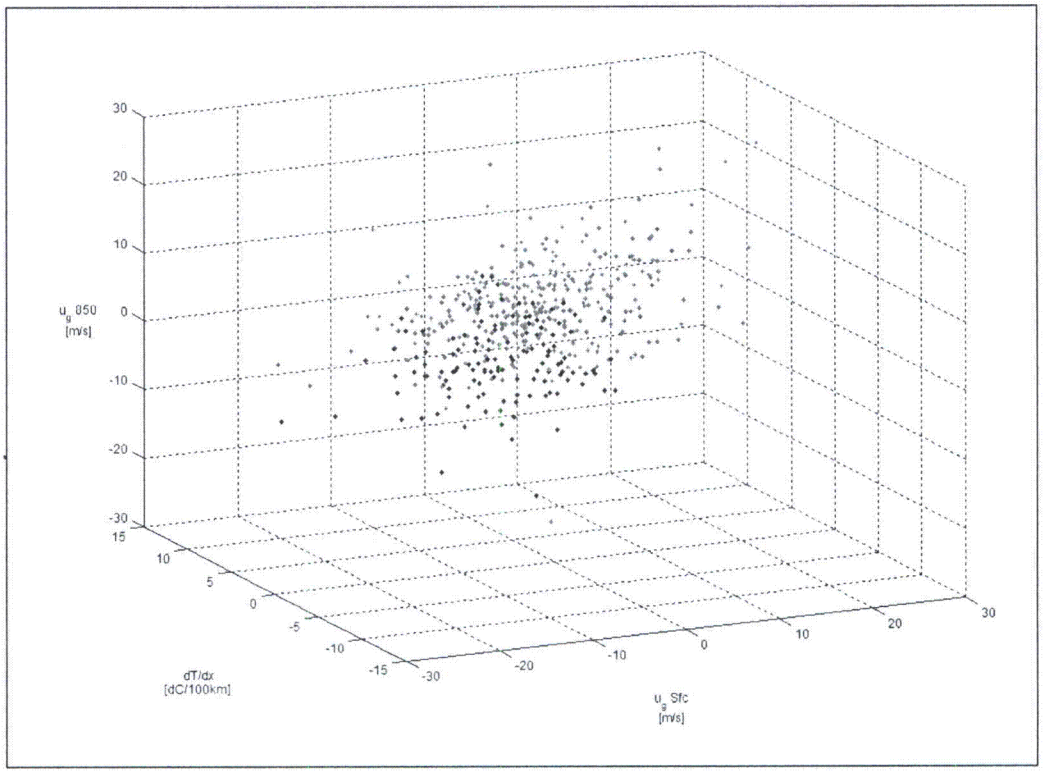

Figure 5.10: 3-D plot of surface uG wind component, cross-shore temperature gradient, and 850 hPa uG wind component. Black dots represent sea breeze events and red dots represent non-sea breeze events.

Some separation does exist between the sea breezes and the non-sea breezes, though there is a large transition area. One of the non-events, Sept. 26, 2006, has an 850 hPa u_G wind component of -25.1 m s^{-1} which is major outlier in comparison to all the other points. A low-level jet was present over Cape Cod at 0000 UTC on Sept. 27, 2006,

which is influencing the interpolated 850 hPa u_G wind component at 1500 UTC. The strongest opposing u_G wind component at 850 hPa that sea breeze events could overcome was 13.6 m s^{-1}, which can be seen in Figure 5.11.

Figure 5.11 shows a two-dimensional plot of the 850 hPa u_G wind component versus the cross-shore temperature gradient (at the surface). There is a large transition area containing both sea breeze and non-sea breeze events.

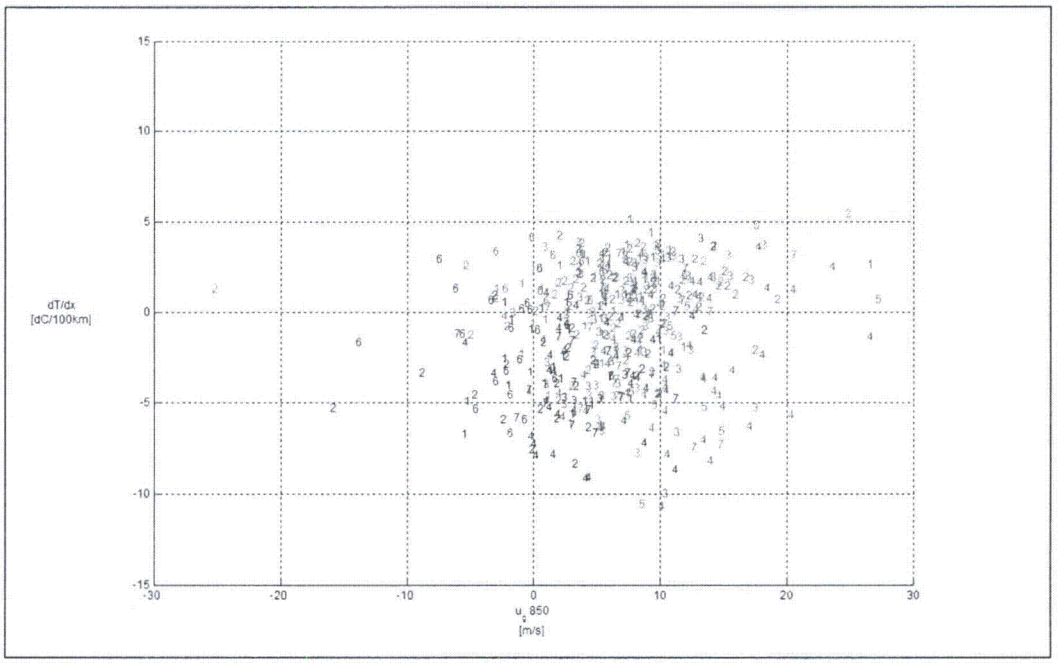

Figure 5.11: 2-D plot of the 850 hPa u_G wind component versus the surface cross-shore temperature gradient. The numbers represent the synoptic class of the event. The blue numbers are sea breeze events and the red numbers are non-sea breeze events.

Perhaps if the three-dimensional plot is broken down by synoptic class, as was done with the two-dimensional plot, a clearer separation between sea breeze and non-sea breeze events will emerge. It may also be useful to look at the u_G wind component at 925 hPa which would be deeper within the sea breeze. The sea breeze circulation only extends vertically to about 900 hPa and this depth can vary (Miller *et al.*, 2003). The

difference between 850 hPa and 925 hPa might mean being outside versus inside the circulation.

CHAPTER 6

6. Radar Analysis of Convection

Between 2002 and 2007, 24 dates were chosen that showed convection in a favorable region for the Massachusetts sea breeze. The favorable region was determined by examining the possible inland penetration of the sea breeze front in chapter 4. All event types were evaluated for existence of convection which included 110 fast events, 32 slow events, 48 marginal events, and 372 non-events; a total of 562 events. When conditions are favorable for a sea breeze to develop along the Massachusetts coastline, convection occurs about 4% of the time. The majority of the cases where convection passed near the Massachusetts coastline occurred on non-sea breeze event days. The non-event is defined based on observations at KBOS and therefore is only representative of that location; therefore, a sea breeze can still occur at other coastal locations despite the event type. Of the 24 days, there were only 5 fast events and no slow events. The remaining 19 events consisted of 4 marginal events and 15 non-sea breeze events.

The 24 dates were initially separated into two groups by whether or not the convection was affected by or caused by the sea breeze front. These two groups were further divided to create four total groups. The cases where convection was affected by the sea breeze were broken into two groups. One group contained cases where the sea breeze along the Massachusetts coastline was involved in the convective interaction (12 cases) and the other group was for cases where convection that was affected by a sea breeze along the Rhode Island or New Hampshire coastlines (2 cases). The cases not related to the sea breeze were classified into the other two groups, one for cases in which the sea breeze did not exist and convection still developed or was enhanced (7 cases), and one for cases where the sea breeze did not exist and no enhancement occurred (3 cases).

In the following subsections, two examples of each group (not including the non-Massachusetts cases) will be discussed.

a. Sea Breeze, Effect on Convection

On August 17, 2002, convective cells both develop along and interact with the sea breeze front (SBF). The SBF is visible in the radar imagery at 1925 UTC (Fig. 6.1), indicated by the "thin line" in reflectivity near the coast. By 2015 UTC, two convective cells can be seen at 41.75°N -70.75°E and 41.85°N -70.60°E (Fig. 6.2). The sea breeze is still visible in the reflectivity. The cells move northwest and at 2049 UTC, the first cell has moved to 42.85°N -70.7°E (into SBF) and has been enhanced (Fig. 6.3). By 2118 UTC this cell has weakened and begun to dissipate (Fig. 6.4). The wind vector plots for 1900 UTC and 2000 UTC are shown in Figures 6.5 and 6.6 respectively. Notice the position of the sea breeze front is the relatively the same as the "thin line" in the reflectivity.

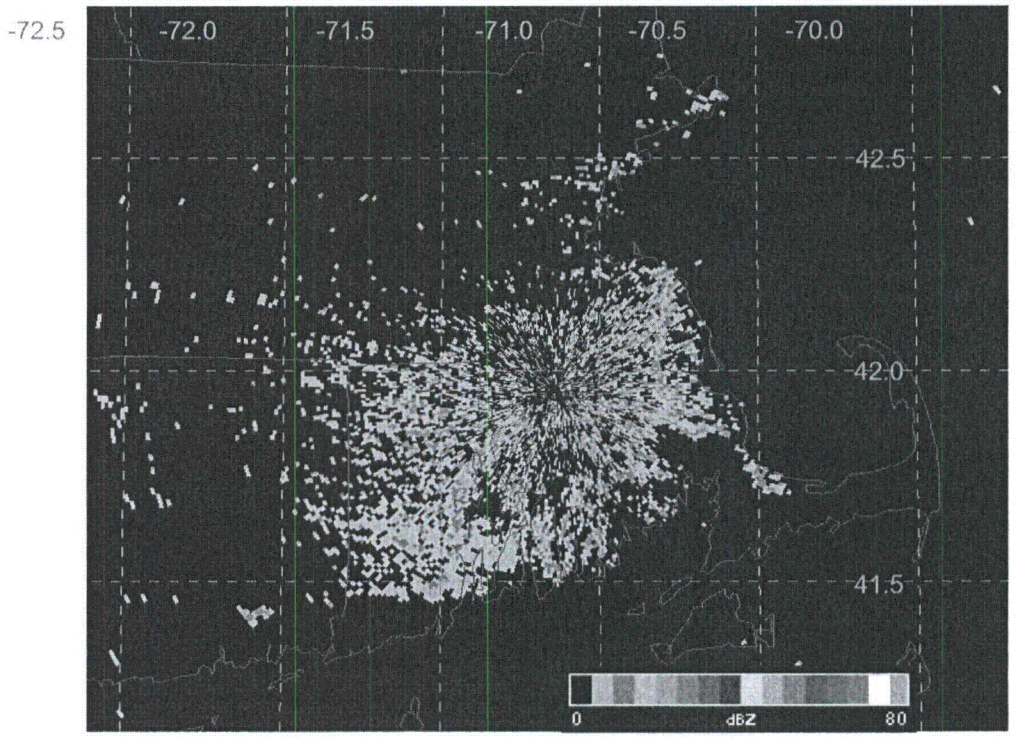

Figure 6.1: Base reflectivity at 1925 UTC from Taunton, MA (KBOX) radar on Aug. 17, 2002. Magenta dashed lines represent latitude and longitude (labeled in degrees N and E). The blue lines are state borders. Refer to legend at bottom-right for reflectivity values.

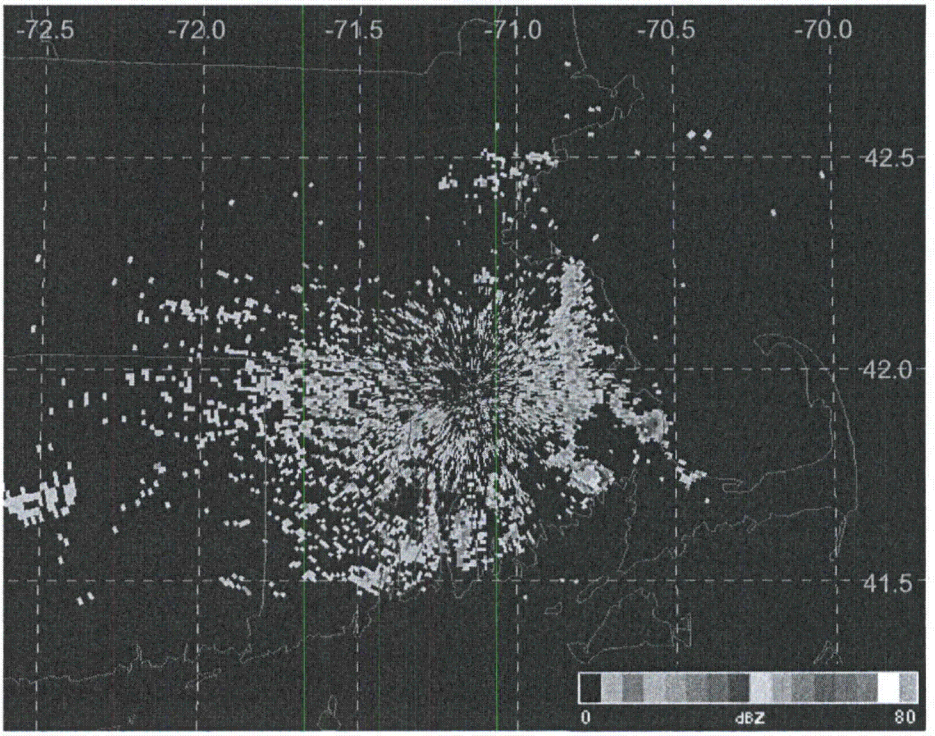

Figure 6.2: Same as Fig. 6.1 above except valid at 2015 UTC.

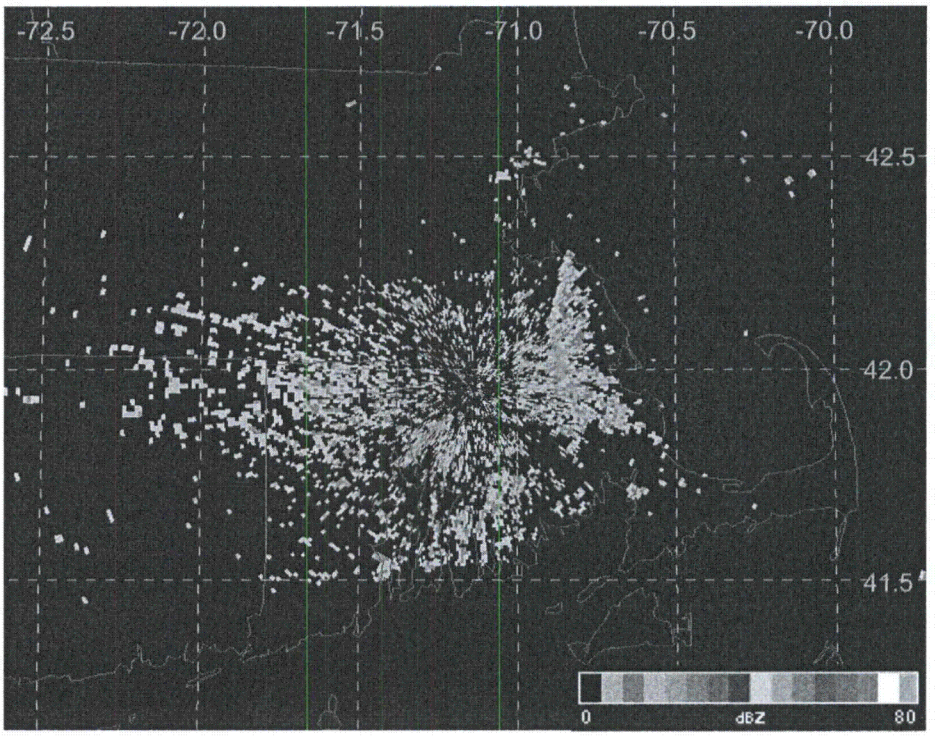

Figure 6.3: Same as Fig. 6.1 above except valid at 2049 UTC.

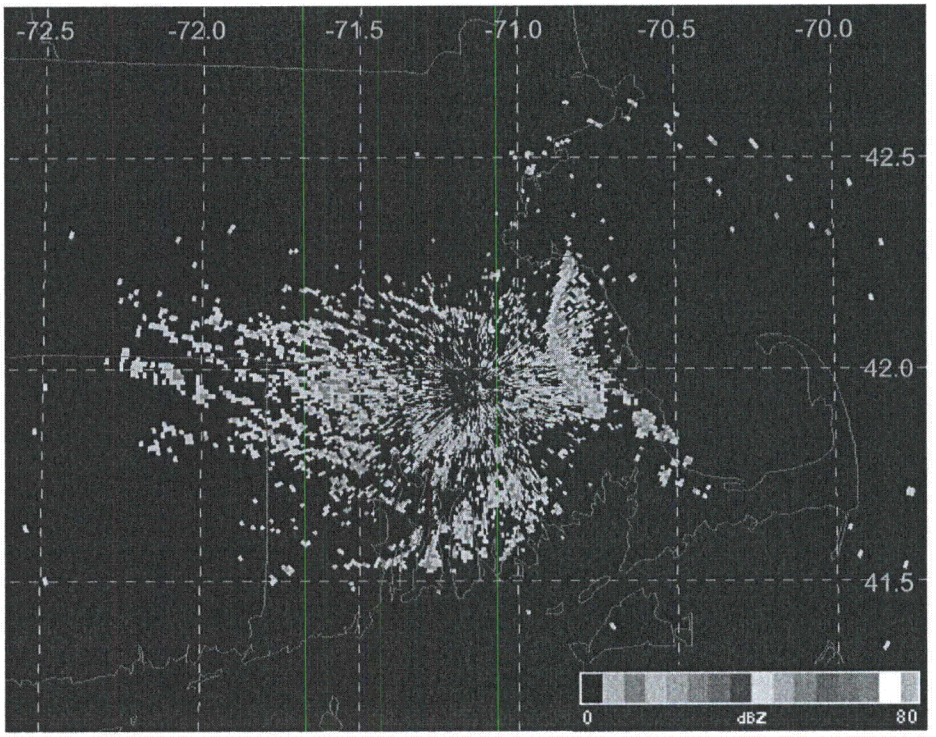

Figure 6.4: Same as Fig. 6.1 above except valid at 2118 UTC.

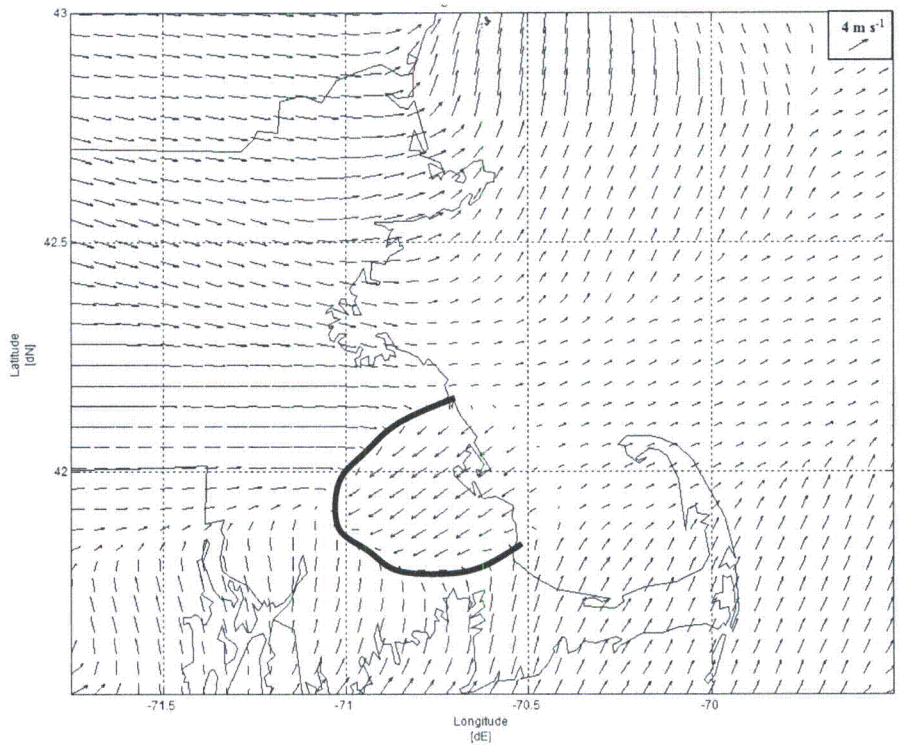

Figure 6.5: Wind vector plot for Aug. 17, 2002 at 1900 UTC. Solid black line indicates analyzed position of sea breeze front.

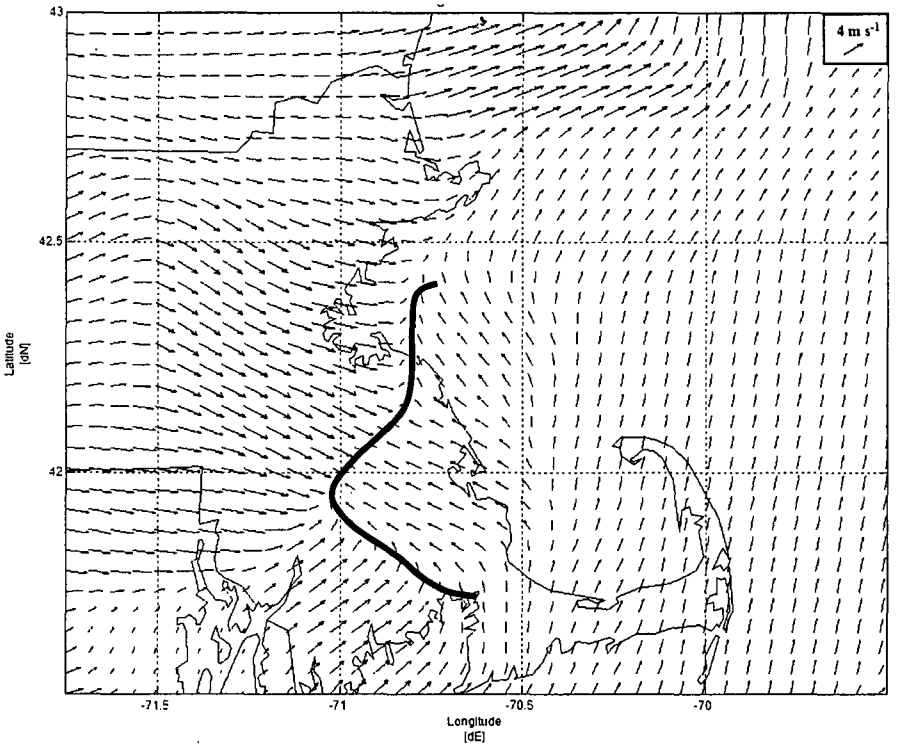

Figure 6.6: Same as Fig. 6.5 above except valid for 2000 UTC.

On August 29, 2004, a pre-existing cell interacts with the SBF and is enhanced. In Figure 6.7, the SBF is visible just northeast of the intersection of 42.50°N and -71.00°E. A cell has begun to develop at 42.40°N -71.25°E. The cell pushes northeast towards the SBF and at 1810 UTC shows no real enhancement (Fig. 6.8). At 1820 UTC, the cell has just encountered the SBF and has intensified to about 45 dBZ (Fig. 6.9). The cell reaches a maximum intensity of 50 dBZ at 1825 UTC (Fig. 6.10) and begins to weaken by 1845 UTC (Fig. 6.11). The wind vector plot for 1800 UTC (Fig. 6.12) shows the sea breeze front in the same location as the reflectivity "thin line".

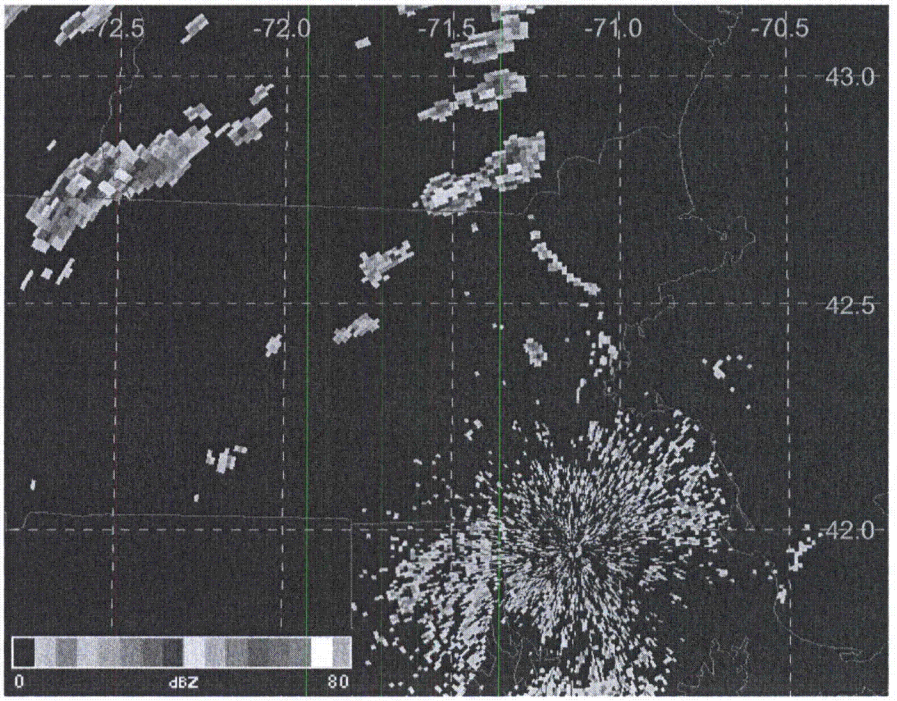

Figure 6.7: Base reflectivity at 1750 UTC from Taunton, MA (KBOX) radar on Aug. 29, 2004. Magenta dashed lines represent latitude and longitude (labeled in degrees N and E). The blue lines are state borders. Refer to legend at bottom-left for reflectivity values.

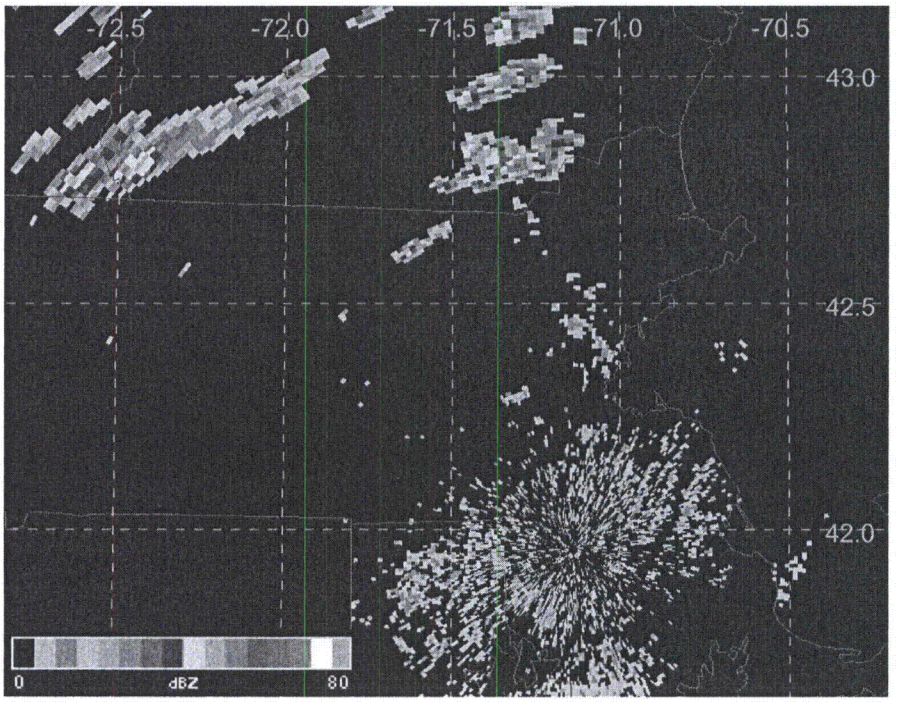

Figure 6.8: Same as Fig. 6.7 above except valid 1810 UTC.

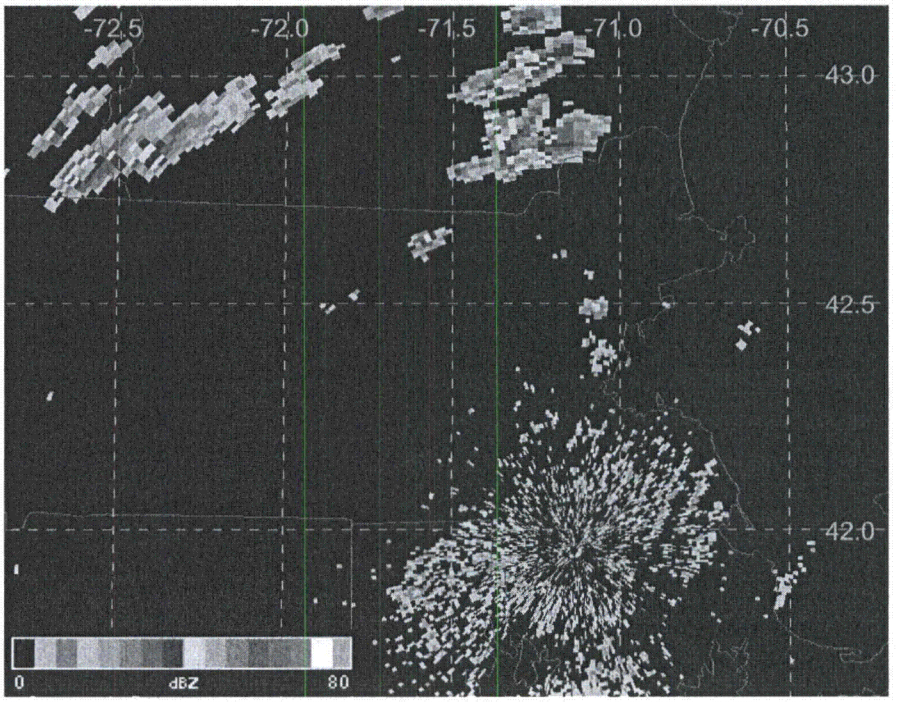

Figure 6.9: Same as Fig. 6.7 above except valid 1820 UTC.

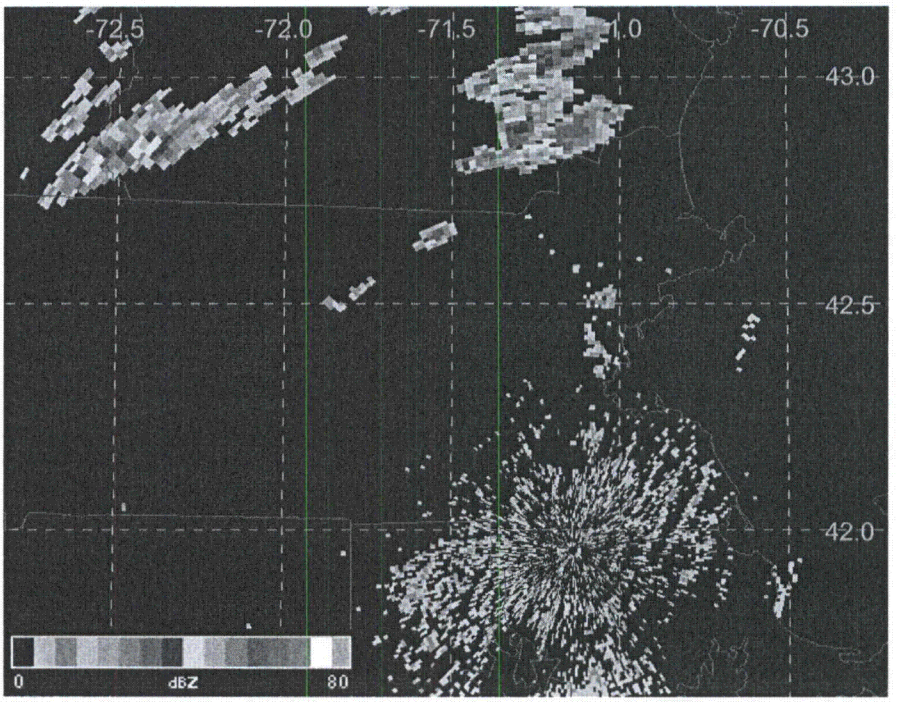

Figure 6.10: Same as Fig. 6.7 above except valid 1825 UTC.

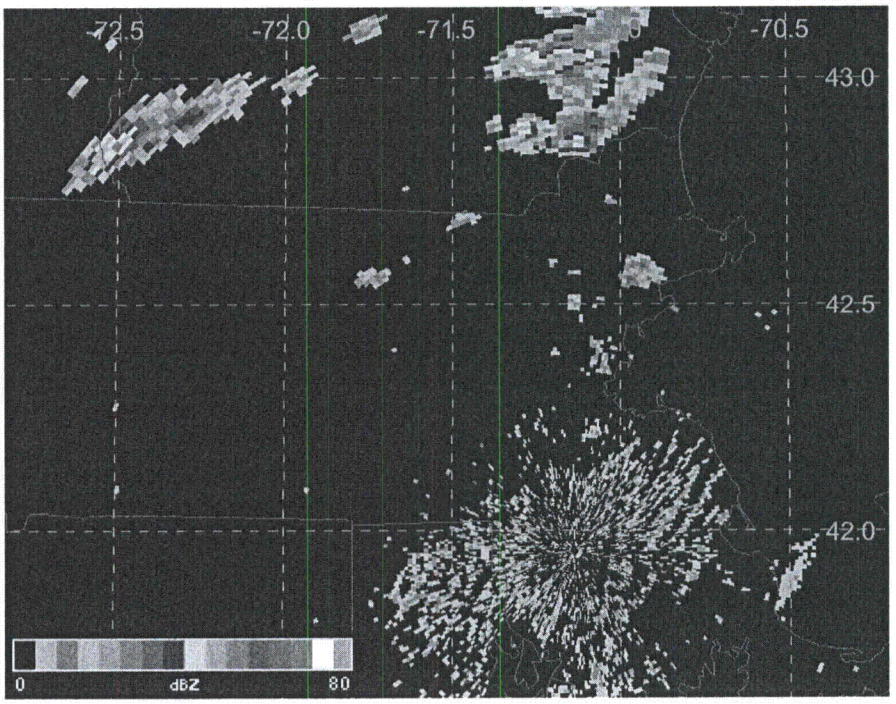

Figure 6.11: Same as Fig. 6.7 above except valid 1845 UTC.

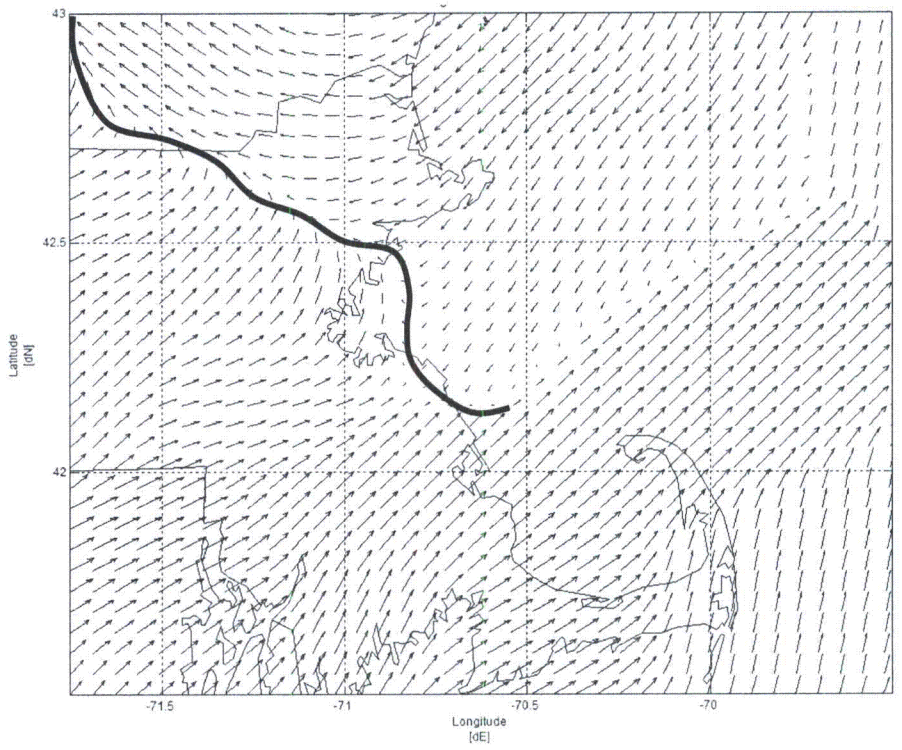

Figure 6.12: Wind vector plot for Aug. 29, 2004 at 1800 UTC. Solid black line indicates analyzed position of sea breeze front.

August 17, 2002 was a non-event and was categorized as a synoptic class 3 indicating a post-frontal cyclonic flow regime over Boston. The northwesterly flow is visible in the wind vector plots (Fig. 6.6 and 6.7). The event type was determined strictly from the KBOS METAR observations so although a sea breeze did not occur in Boston, it was still possible for one to develop somewhere along the coast.

August 29, 2004 was a fast event and was categorized as a synoptic class 4 indicating pre-frontal southwesterly surface flow which is visible in the wind vector plot (Fig. 6.12). The limited penetration of the sea breeze to the south of Boston matches the results of the inland penetration portion of this study in Chapter 4. The sea breeze is no longer in Boston at the time of the convection, but is still present inland, north of Boston.

b. No Sea Breeze, Convection Develops or is Enhanced

At 1900 UTC on July 10, 2006, a cell begins to develop at 41.90°N -71.30°E (Fig. 6.13). By 1912 UTC, the cell starts to strengthen and a tiny area of reflectivity equal to 40 dBZ develops (Fig. 6.14). The cell continues its progression northeast and intensifies slightly to 45 dBZ at 1918 UTC (Fig. 6.15). The cell reaches its maximum strength with a significant area of reflectivity around 45 dBZ at 1924 UTC (Fig. 6.16) and then weakens at 1941 UTC (Fig. 6.17). The wind vector plot for 1900 UTC shows this cell developed in an area of southwesterly winds with no visible convergence (Fig. 6.18).

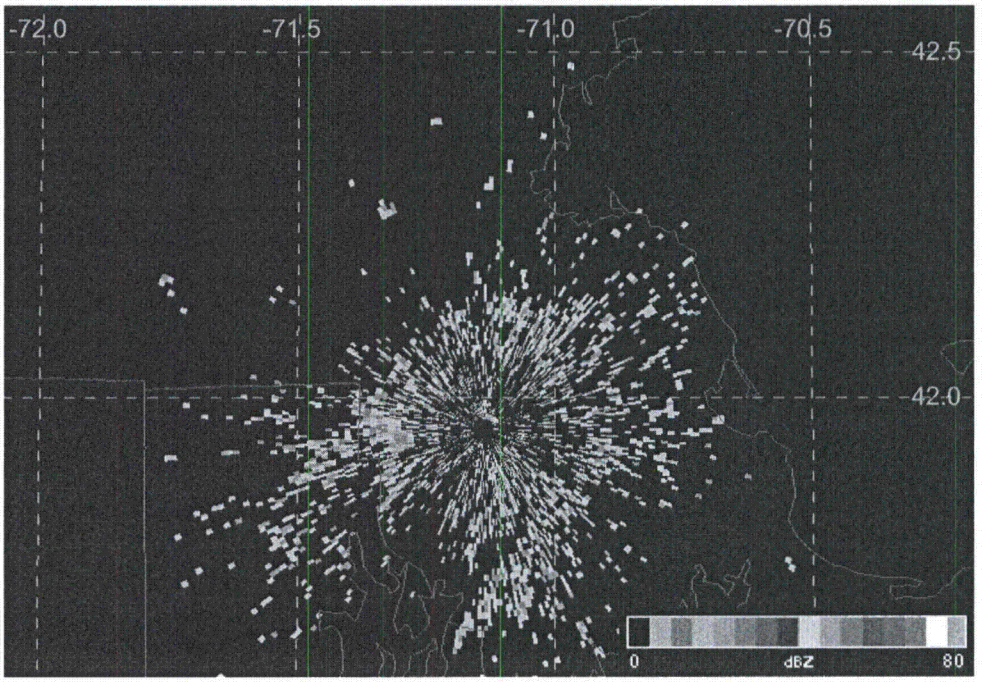

Figure 6.13: Base reflectivity at 1900 UTC from Taunton, MA (KBOX) radar on July 10, 2006. Magenta dashed lines represent latitude and longitude (labeled in degrees N and E). The blue lines are state borders. Refer to legend at bottom-right for reflectivity values.

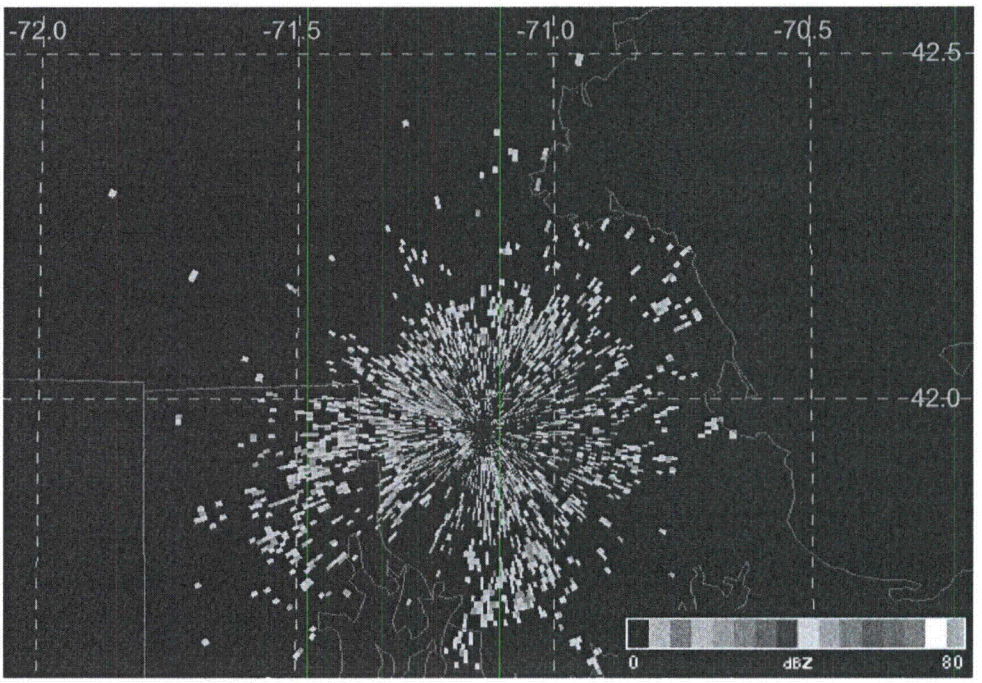

Figure 6.14: Same as Fig. 6.13 above except valid for 1912 UTC.

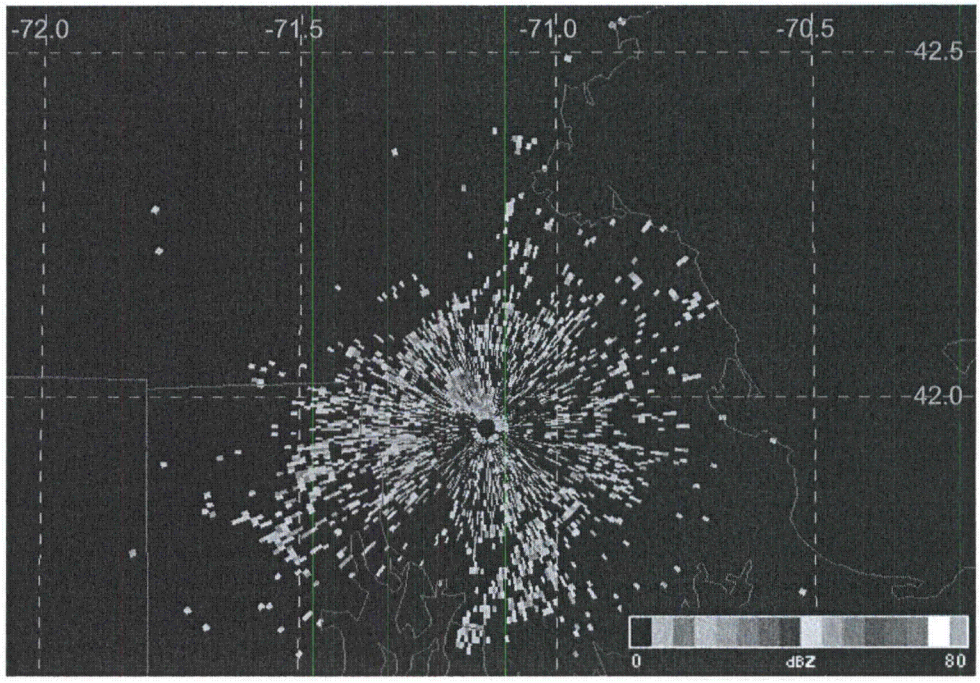

Figure 6.15: Same as Fig. 6.13 above except valid for 1918 UTC.

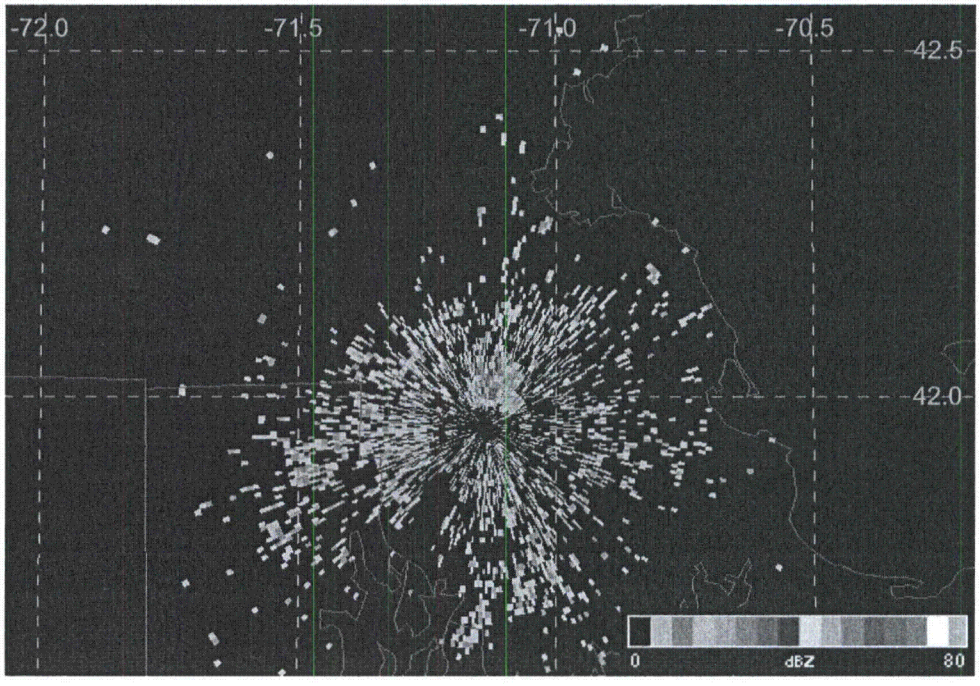

Figure 6.16: Same as Fig. 6.13 above except valid for 1924 UTC.

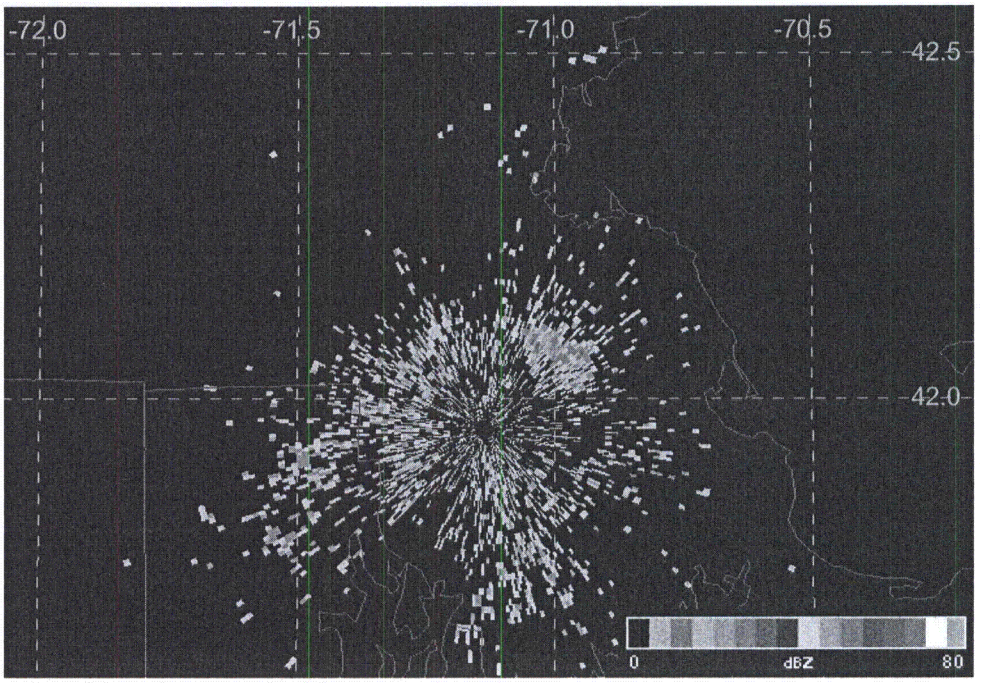

Figure 6.17: Same as Fig. 6.13 above except valid for 1941 UTC.

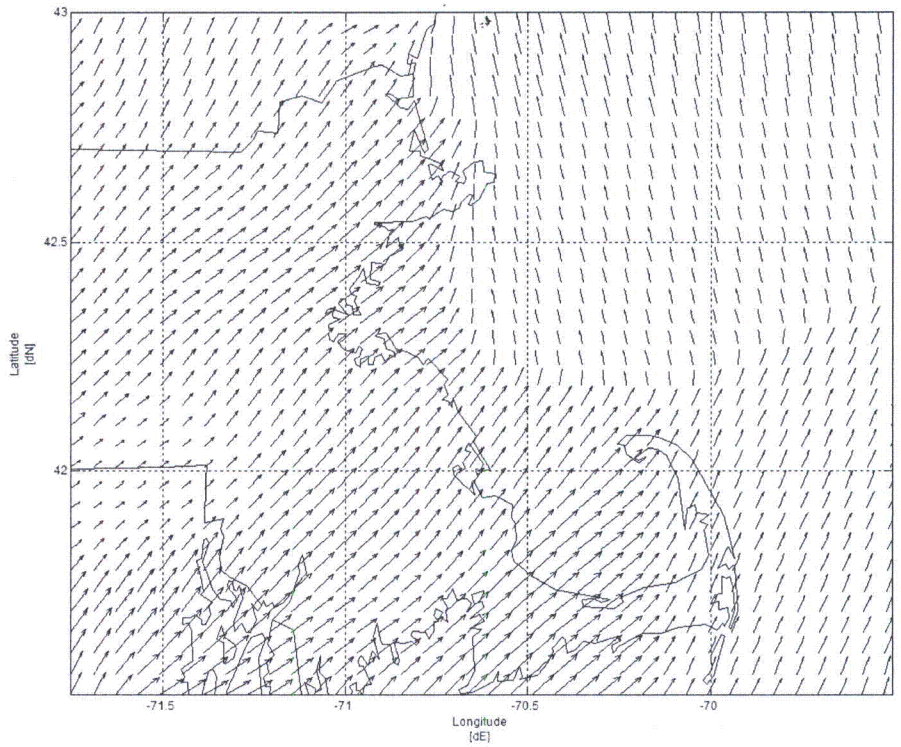

Figure 6.18: Wind vector plot for July 10, 2006 at 1900 UTC.

On September 9, 2006, a convective band of precipitation developed just west of Boston and intensified as it passed east of the city. The band begins development at 2306 UTC where three small cells can be seen at approximately 41.25°N -71.25°E (Fig. 6.19). The cells propagate east towards the coast (and Boston) becoming stronger and joining together (Fig. 6.20). Once the cells pass over Boston and out into the ocean (2334 UTC), they intensify to 45 dBZ (Fig. 6.21). The cells reach their maximum intensity (50 dBZ) and almost form a single cell at 2346 UTC (Fig. 6.22). At the 2357 UTC, the cells have begun to weaken (Fig. 6.23). The wind vector plots (Fig. 6.24 and 6.25) show some directional convergence as well as some weak speed convergence in this area which is causing the intensification of these cells. The large scale precipitation seen approaching the area in radar imagery is pre-frontal (Fig. 6.26).

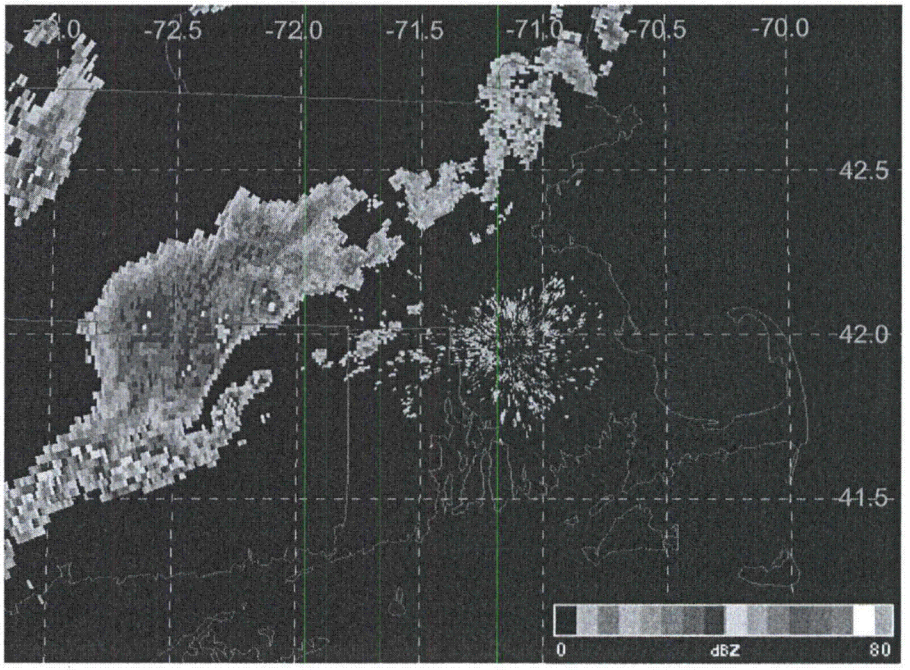

Figure 6.19: Base reflectivity at 2306 UTC from Taunton, MA (KBOX) radar on Sept. 9, 2006. Magenta dashed lines represent latitude and longitude (labeled in degrees N and E). The blue lines are state borders. Refer to legend at bottom-right for reflectivity values.

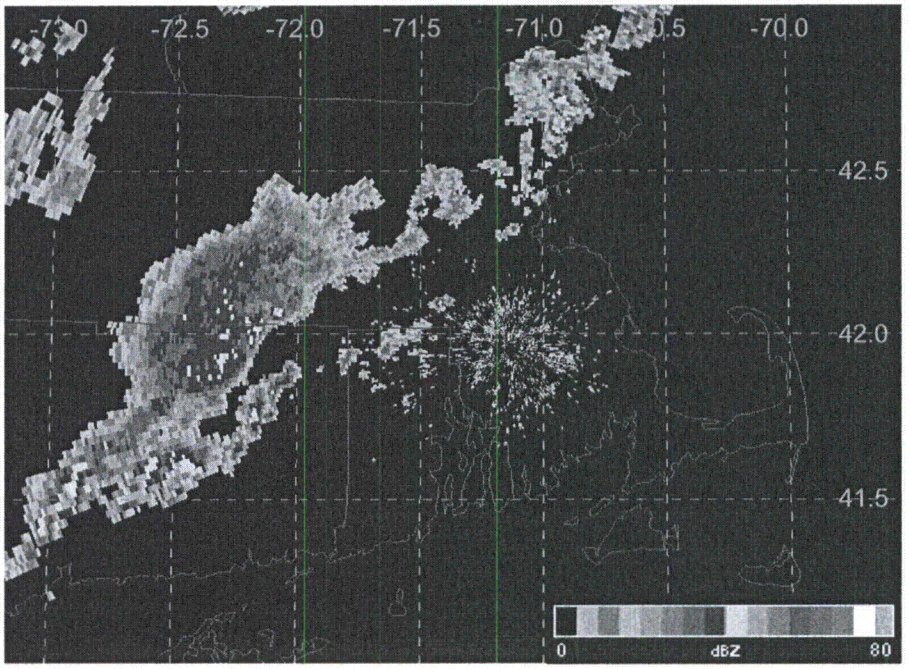

Figure 6.20: Same as Fig. 6.19 above except valid for 2317 UTC.

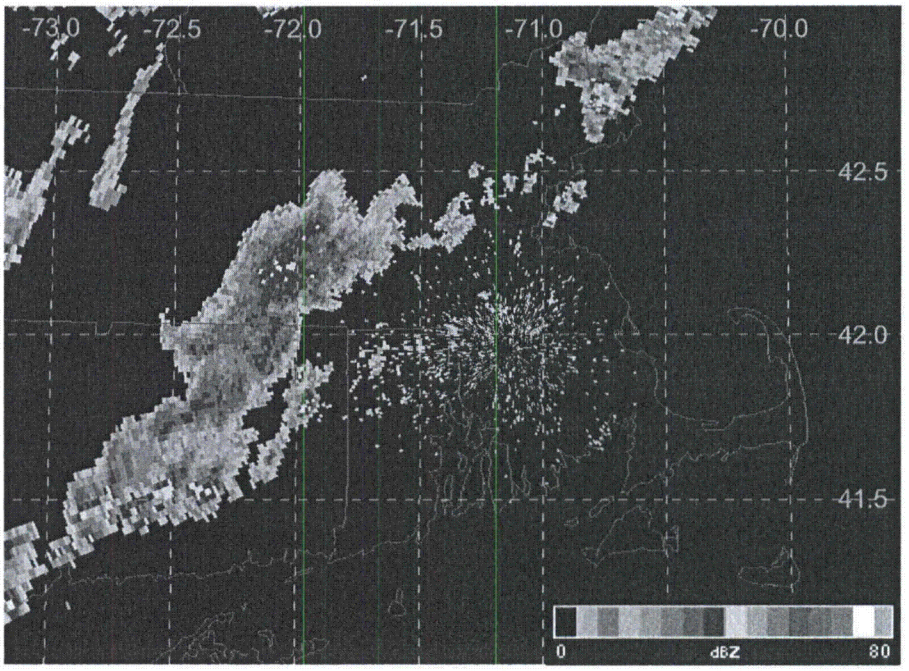

Figure 6.21: Same as Fig. 6.19 above except valid for 2334 UTC.

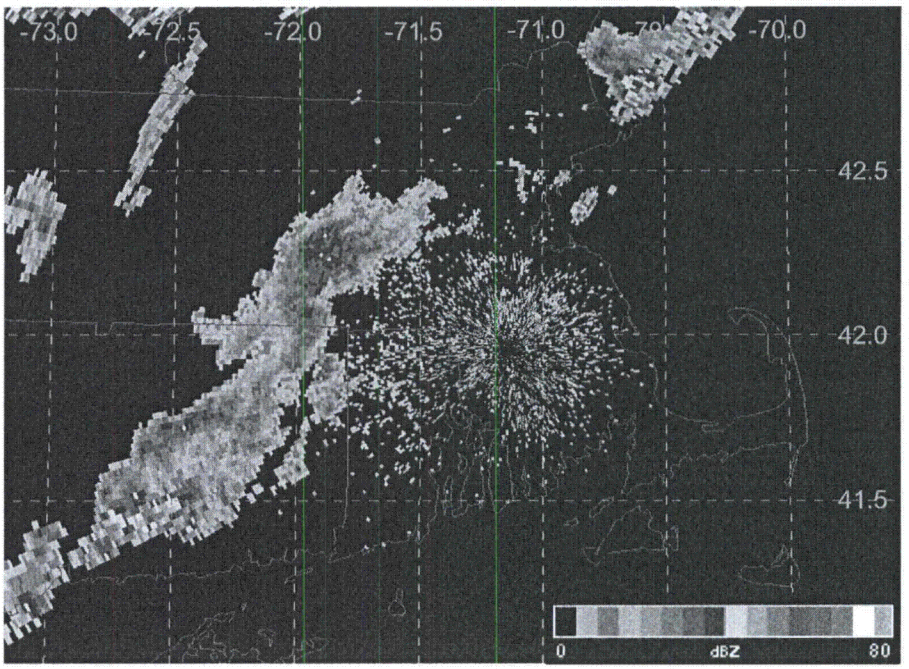

Figure 6.22: Same as Fig. 6.19 above except valid for 2346 UTC.

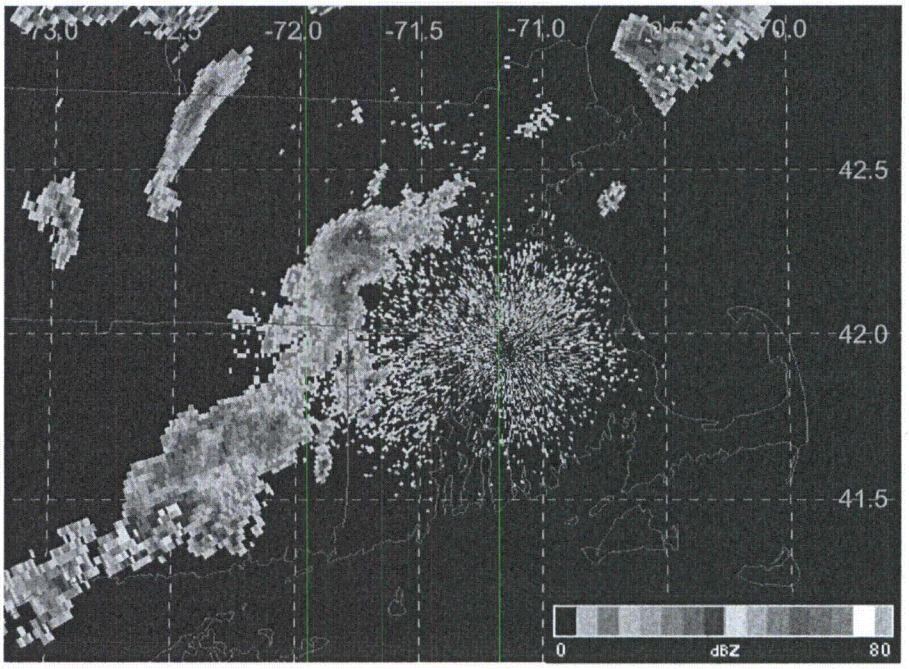

Figure 6.23: Same as Fig. 6.19 above except valid for 2357 UTC.

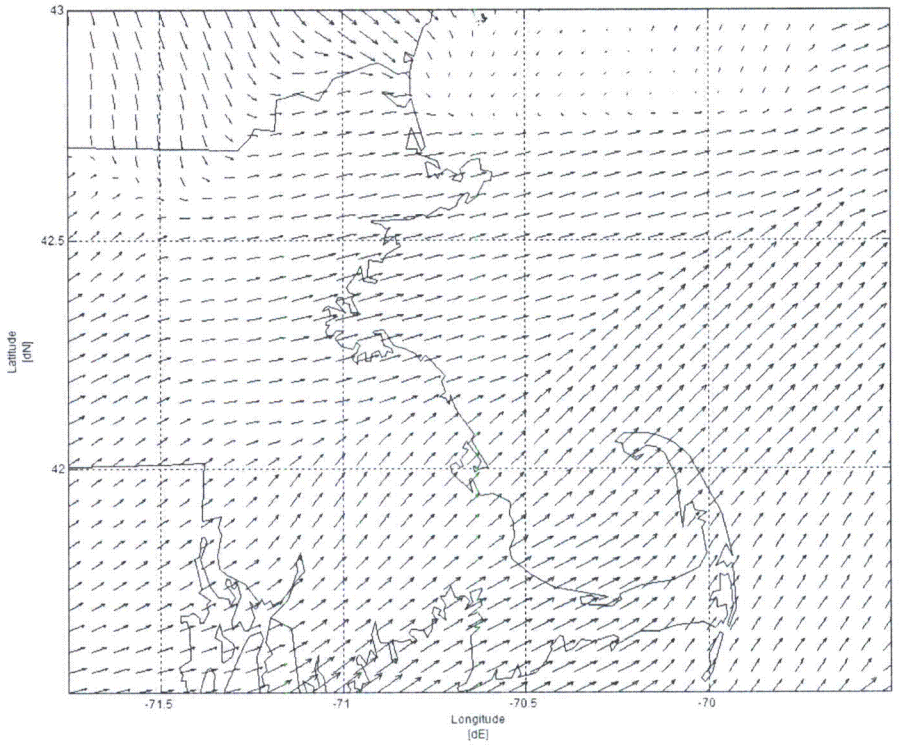

Figure 6.24: Wind vector plot for Sept. 9, 2006 at 2300 UTC.

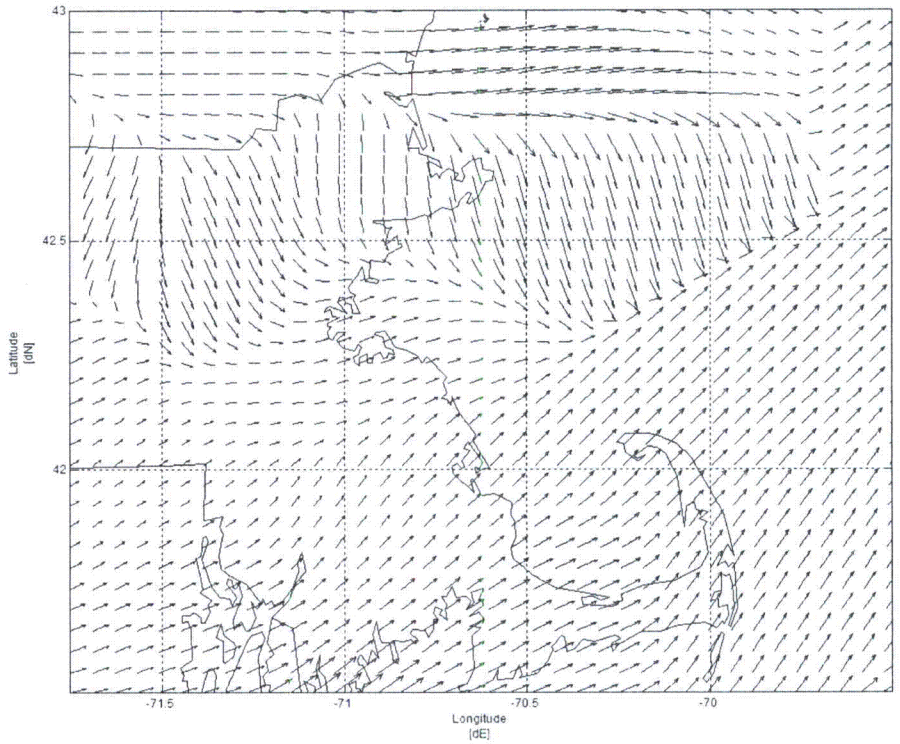

Figure 6.25: Wind vector plot for Sept. 10, 2006 at 0000 UTC.

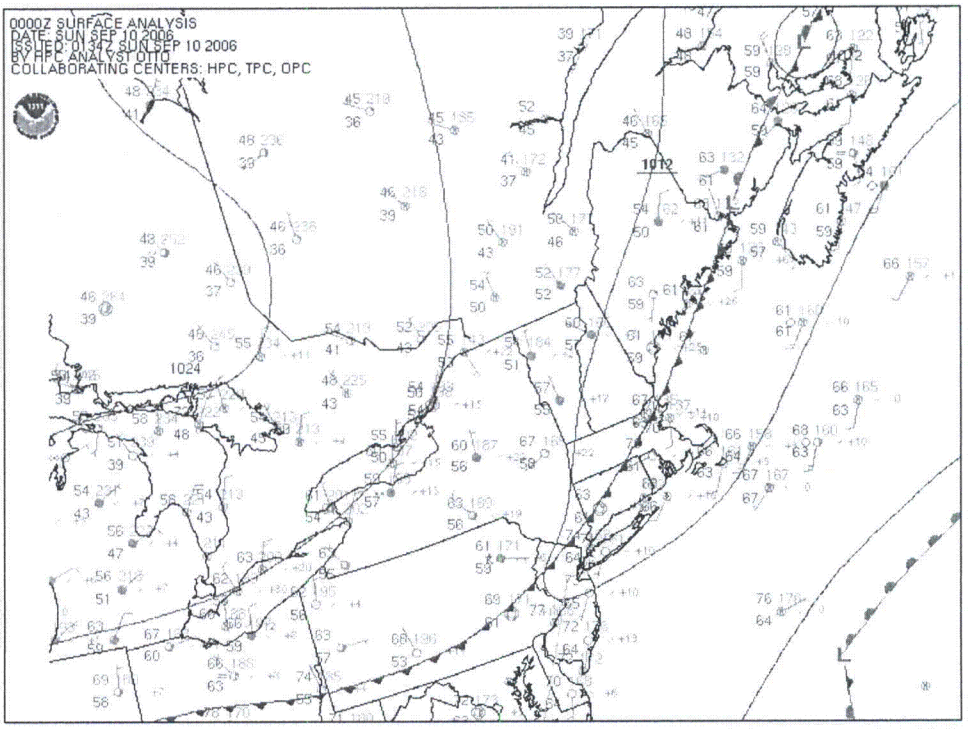

Figure 6.26: Surface analysis valid 0000 UTC Sept. 10, 2006. Obtained from NESDIS (2008).

Both events were non-sea breeze events and the sea breeze did not occur anywhere along the coast in these cases. July 10, 2006 was from synoptic class 4 and Sept. 9, 2006 was from synoptic class 7 (the miscellaneous class). The intensification of convection in September was due to convergence. Further research is needed to determine the cause of the convection in the July case.

c. No Sea Breeze, Convection Unchanged

On July 27, 2005, a line of pre-frontal precipitation passed through Massachusetts (and other New England states). At 2239 UTC, the line of storms has just begun to pass over the northern coast of Massachusetts (Fig. 6.27). The line contains many convective cells and is tracking northeast. By 2256 UTC, more of the storm has reached the coastline (Fig. 6.28). No intensification has occurred with these cells and at 2326 UTC more

convective storms have moved into the area (Fig. 6.29). By 2356 UTC, almost all of the convective precipitation has moved offshore and only stratiform precipitation remains (Fig. 6.30). Figures 6.31 and 6.32 show the absence of the SBF in the wind vectors.

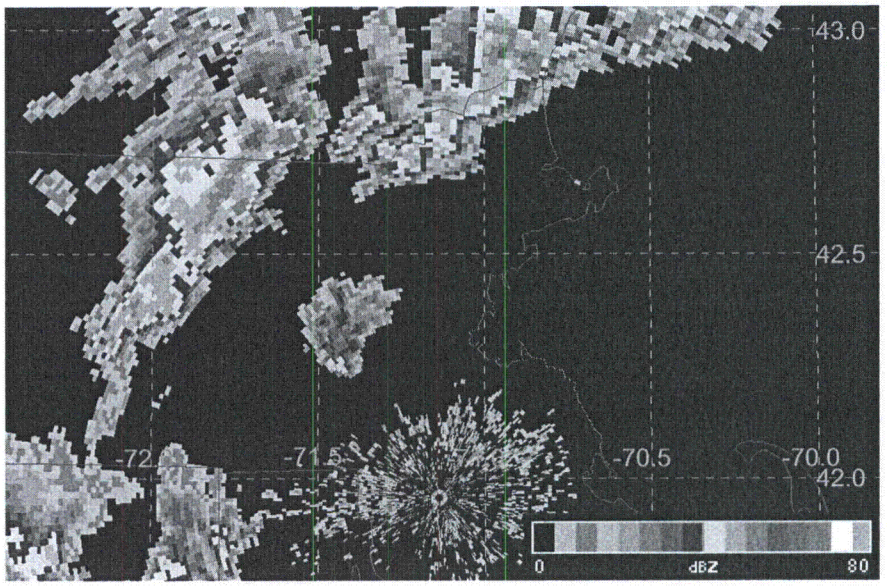

Figure 6.27: Base reflectivity at 2239 UTC from Taunton, MA (KBOX) radar on July 27, 2005. Magenta dashed lines represent latitude and longitude (labeled in degrees N and E). The blue lines are state borders. Refer to legend at bottom-right for reflectivity values.

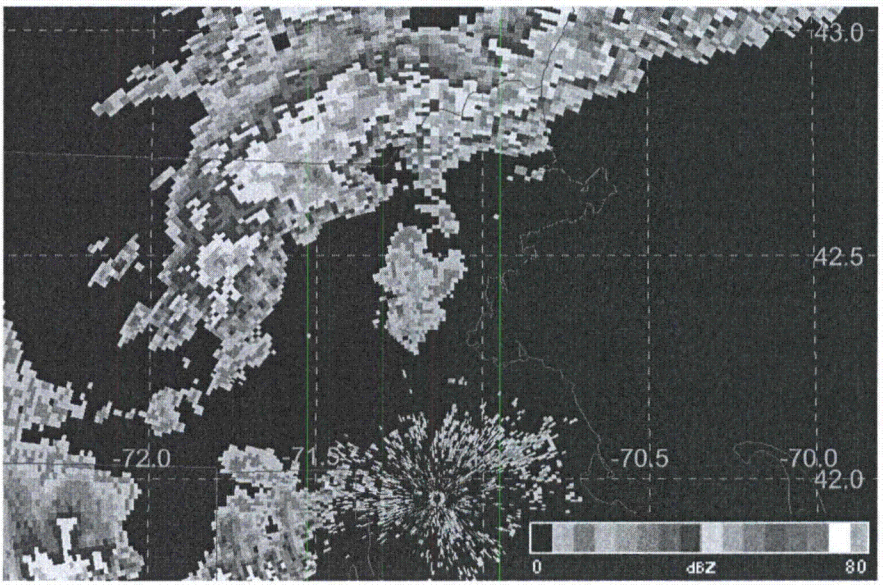

Figure 6.28: Same as Fig. 6.27 above except valid for 2256 UTC.

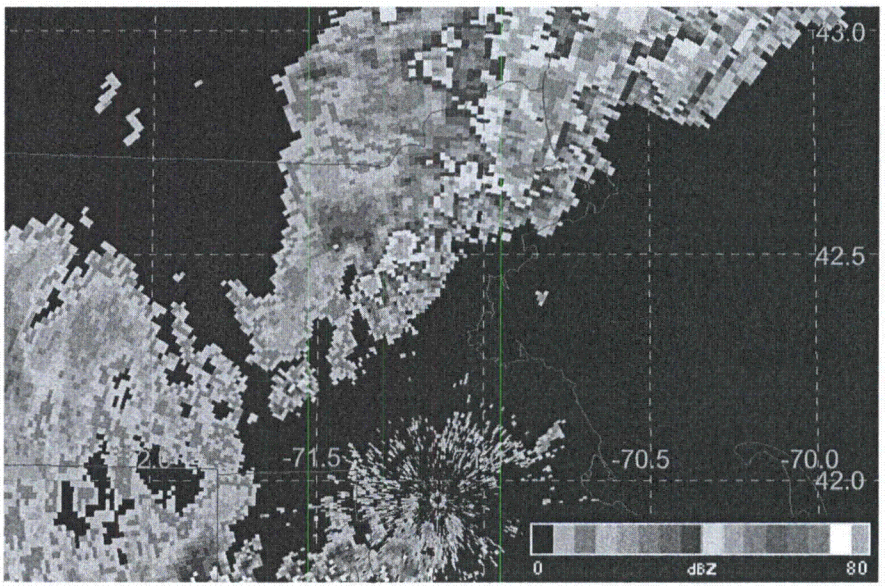

Figure 6.29: Same as Fig. 6.27 above except valid for 2326 UTC.

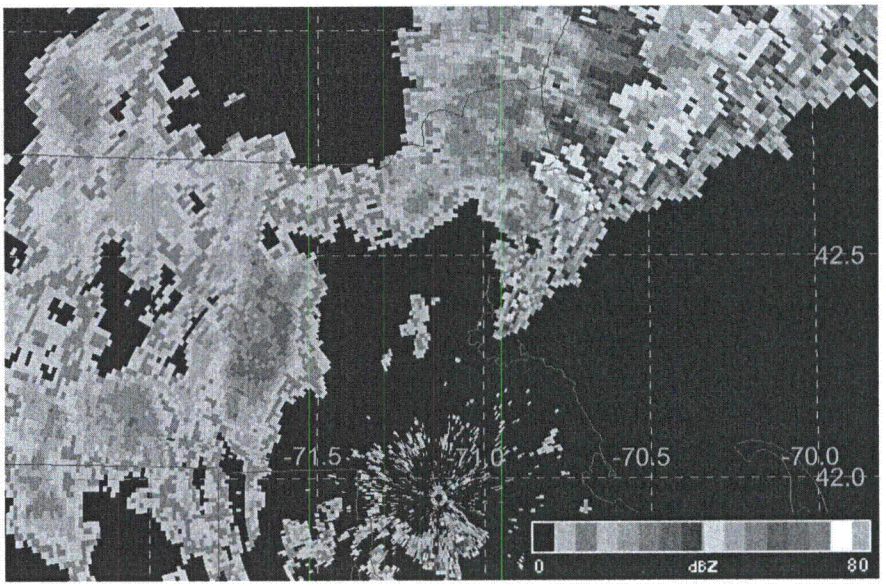

Figure 6.30: Same as Fig. 6.27 above except valid for 2356 UTC.

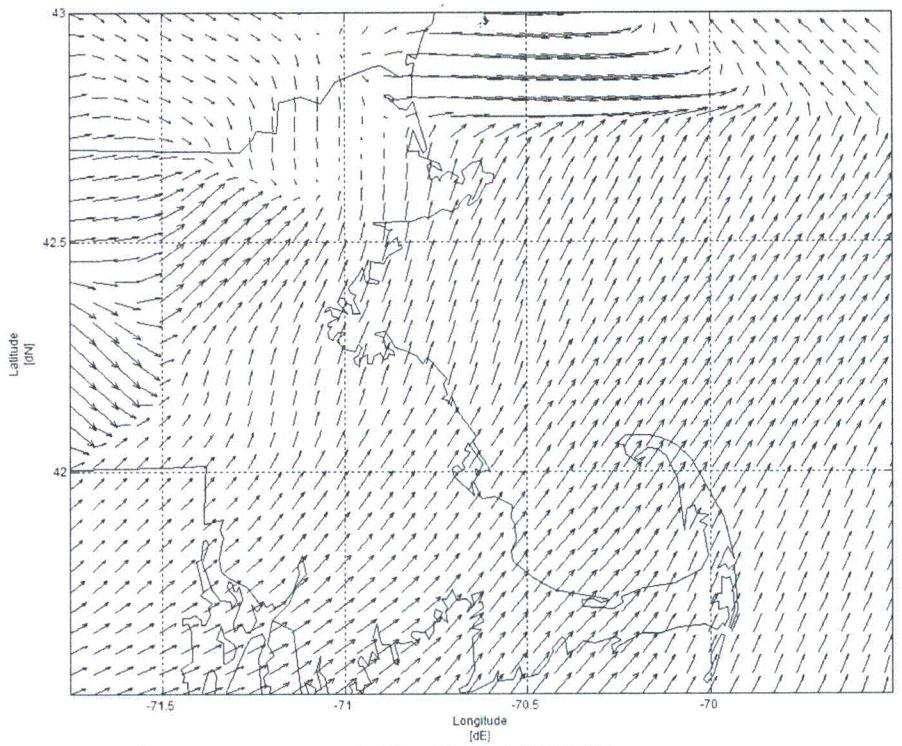

Figure 6.31: Wind vector plot for July 27, 2005 at 2300 UTC.

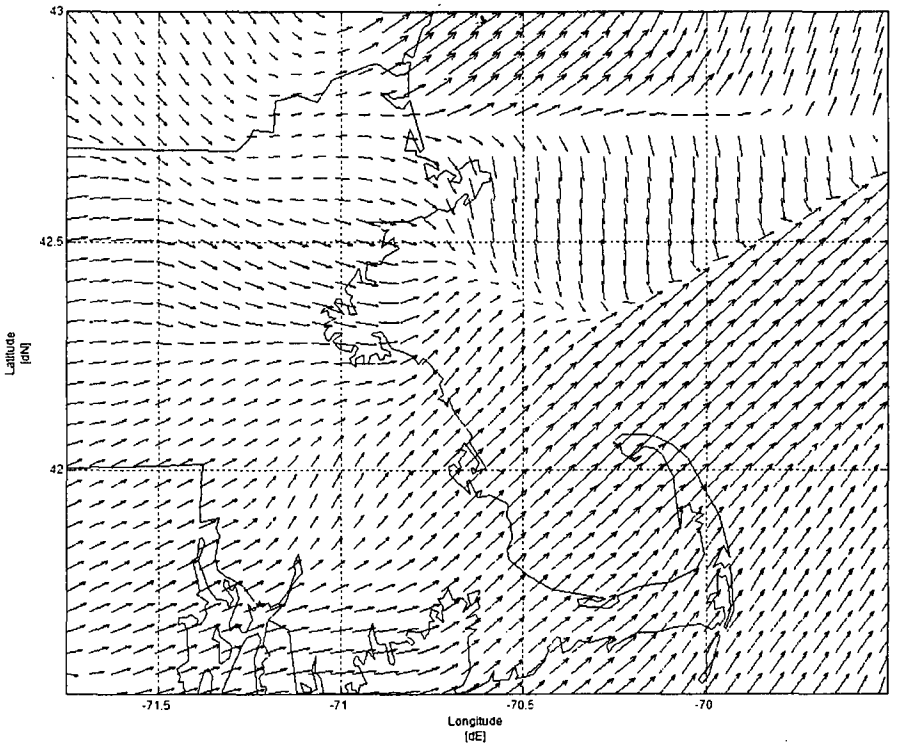

Figure 6.32: Wind vector plot for July 28, 2005 at 0000 UTC.

On August 2, 2006, a cluster of storms pushes its way through southern Massachusetts. At 2144 UTC, the storms can be seen along the southern border of Massachusetts (Fig. 6.33). These cells track southeasterly and by 2214 UTC, they have begun to enter northern Connecticut and Rhode Island (Fig. 6.34). The main cell cluster in Massachusetts passes directly over the radar (BOX) which distorts the reflectivity at 2231 UTC (Fig. 6.35). At 2243 UTC there is still no real intensification of convection (Fig. 6.36) and by 2334 UTC, the cells have begun to weaken (Fig. 6.37). The wind vector plots show no presence of a sea breeze at 2200 UTC or 2300 UTC (Fig. 6.38 and 6.39, respectively).

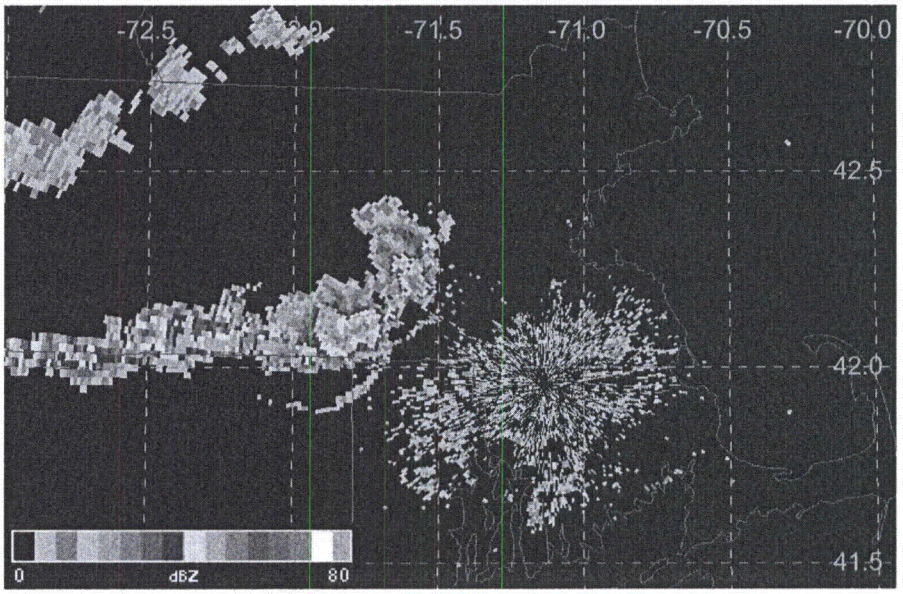

Figure 6.33: Base reflectivity at 2144 UTC from Taunton, MA (KBOX) radar on Aug. 2, 2006. Magenta dashed lines represent latitude and longitude (labeled in degrees N and E). The blue lines are state borders. Refer to legend at bottom-left for reflectivity values.

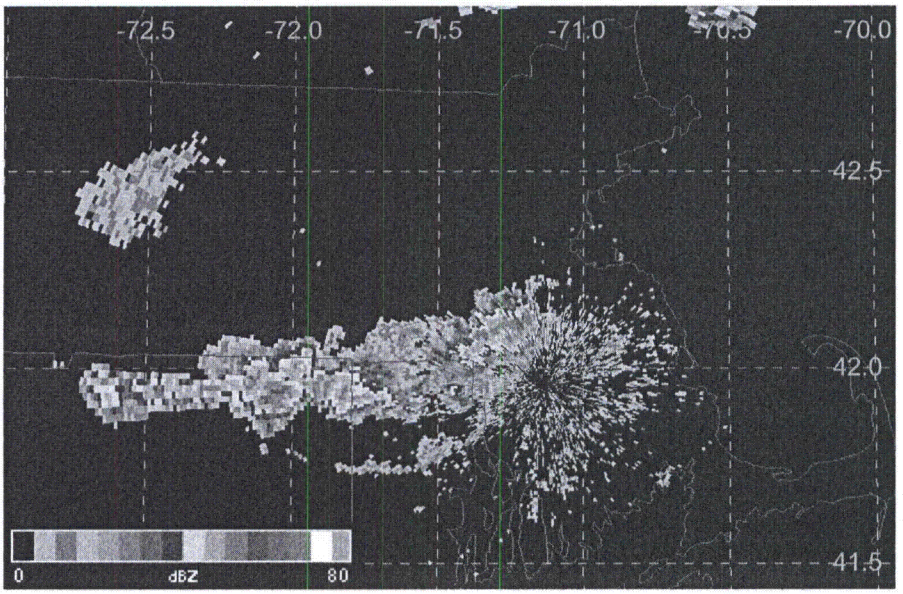

Figure 6.34: Same as Fig. 6.33 above except valid for 2214 UTC.

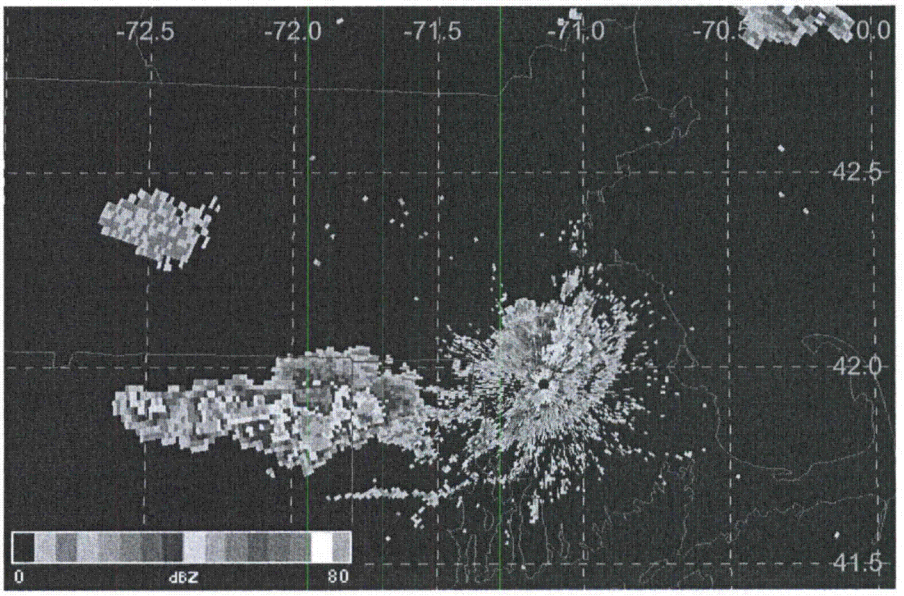

Figure 6.35: Same as Fig. 6.33 above except valid for 2231 UTC.

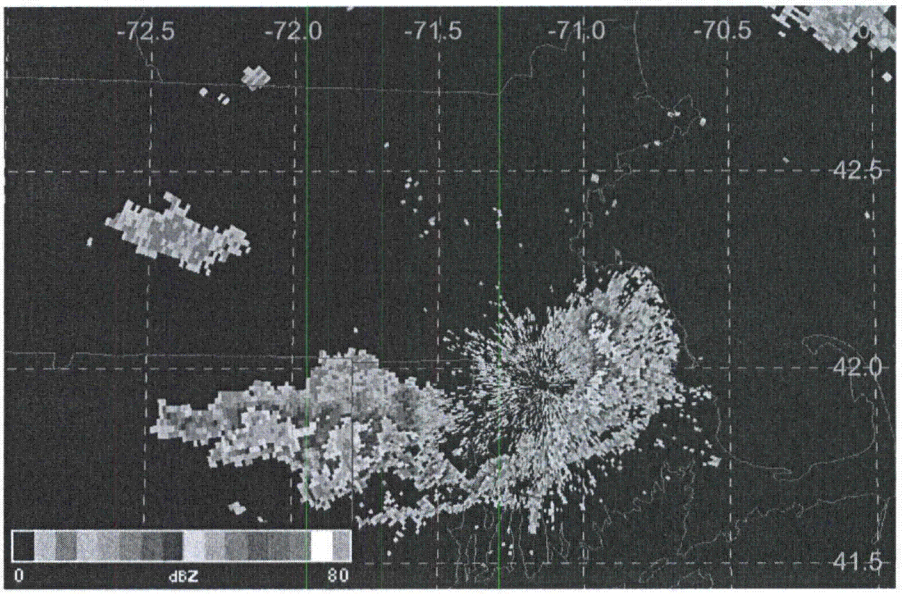

Figure 6.36: Same as Fig. 6.33 above except valid for 2243 UTC.

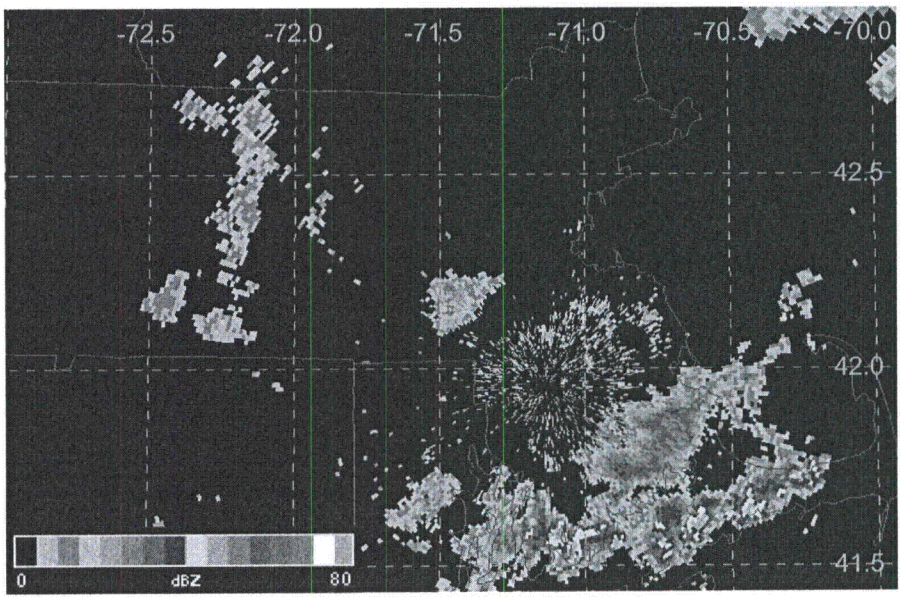

Figure 6.37: Same as Fig. 6.33 above except valid for 2334 UTC.

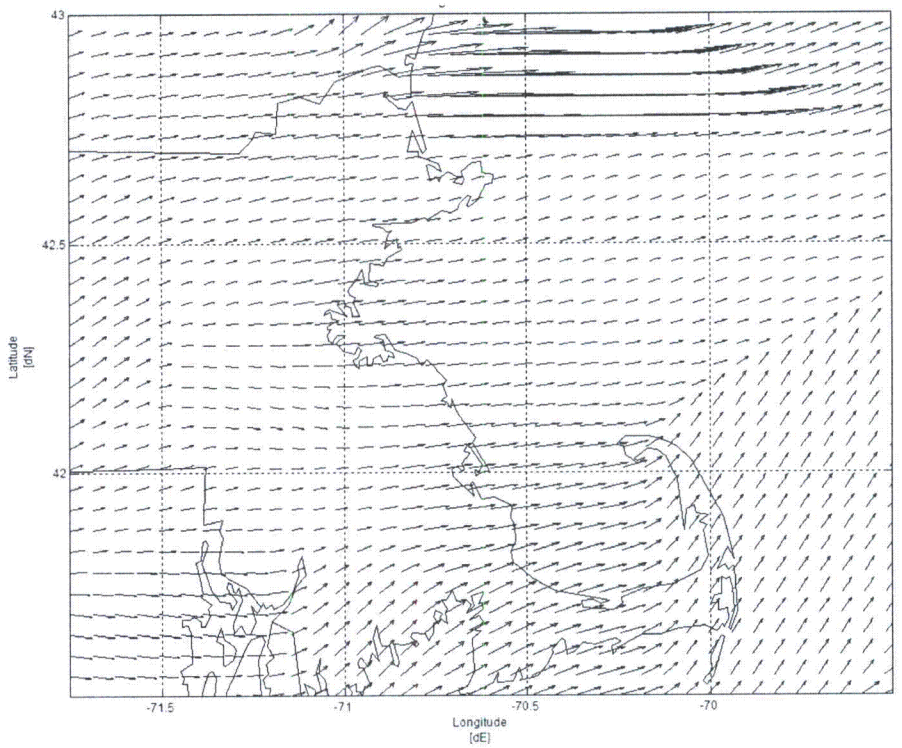

Figure 6.38: Wind vector plot for Aug. 2, 2006 at 2200 UTC.

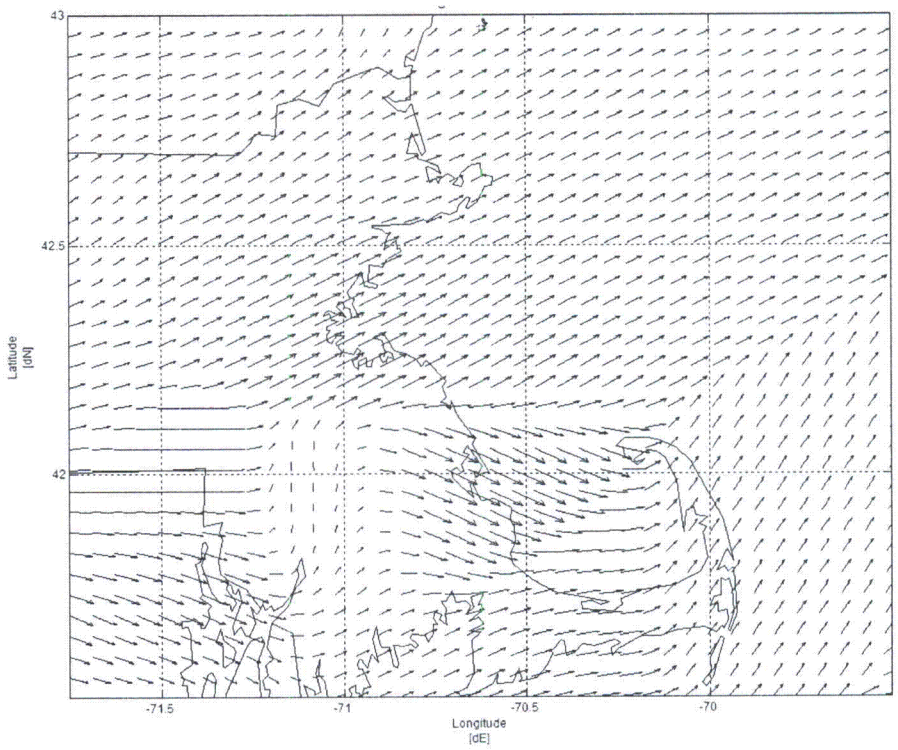

Figure 6.39: Same as Fig. 6.38 above except valid for 2300 UTC.

Both of these cases were non-sea breeze events. July 27, 2005 was identified as a synoptic class 5 event using the 1500 UTC surface analysis, which is characterized by post-frontal southwesterly flow (*See Appendix B*). By 2100 UTC, a secondary front has begun to move over Massachusetts causing pre-frontal precipitation in the area (Fig. 6.40). August 2, 2006 was classified as a synoptic class 7 and the precipitation was being caused by a trough passing through Massachusetts (Fig. 6.41).

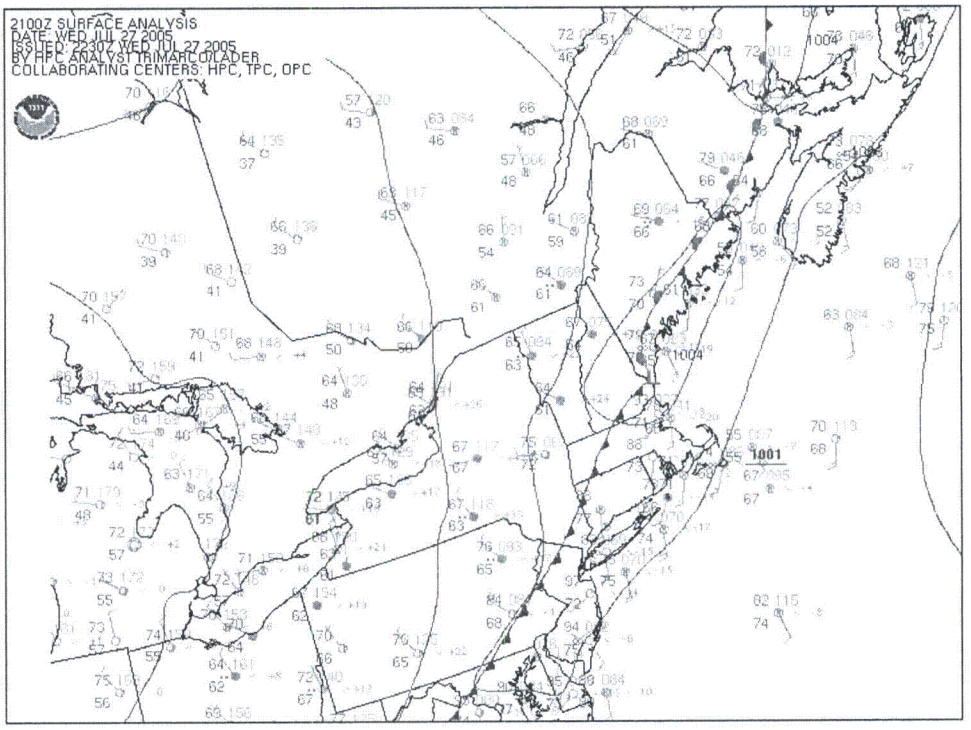

Figure 6.40: Surface analysis valid 2100 UTC July 27, 2005. Obtained from NESDIS (2008).

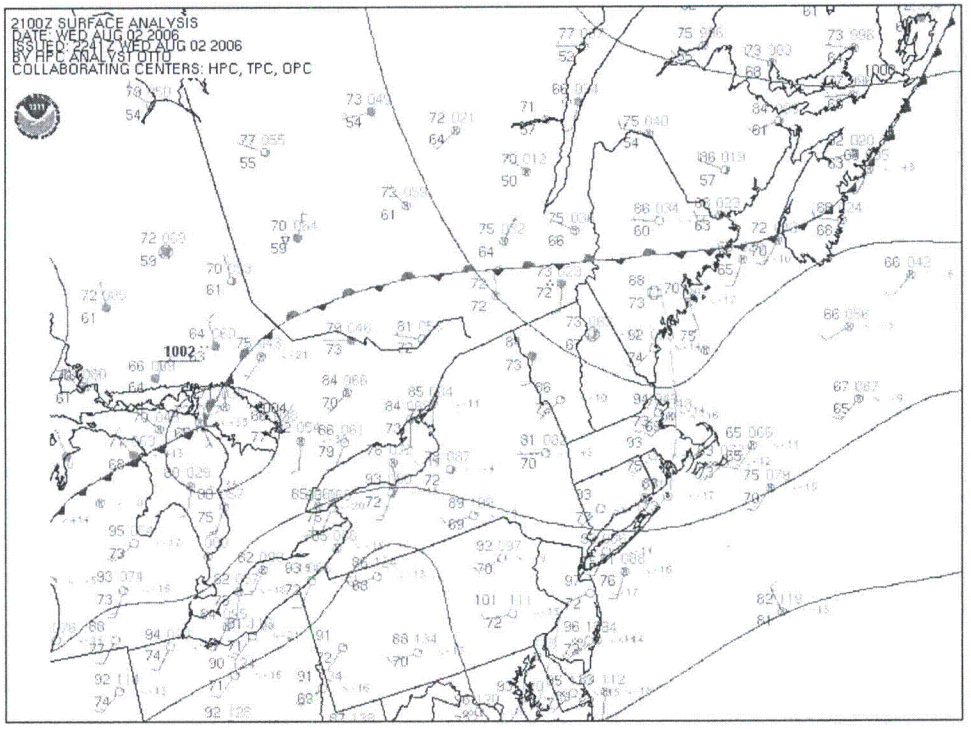

Figure 6.41: Surface analysis valid 2100 UTC Aug. 2, 2006. Obtained from NESDIS (2008).

Of a total of 562 events between 2002 and 2007, 24 events were selected for radar analysis. This analysis showed that the sea breeze was present for 14 of the 24 events. All of the 14 events showed an interaction between the sea breeze front and convection including some development. In the remaining 10 events the sea breeze was not present and convection developed or changed for 7 of these events; the other 3 events showed no changes in convection. The sample size of only 24 events is related to a bias created by the original methods used to define sea breeze events. The stipulations for cloud cover (no more than "broken" with a ceiling less than 18,000 ft) and precipitation (no precipitation within 6 hrs prior to or after the event) limited the number of thunderstorm days that could exist.

An important finding from this part of the study was that the sea breeze could occur at other locations along the coast even though in was a non-event day in Boston. More research is needed to determine what factors keep the sea breeze from penetrating into Boston on these non-event days.

CHAPTER 7

7. Summary & Conclusions

This study examined many different aspects of the Massachusetts sea breeze. A data set of events was created by determining if a sea breeze was possible and then categorizing the event as either a fast, slow, or marginal sea breeze event, or a non-sea breeze event. The data set was developed from nearly ten years (1998 to 2007) of METAR data from Logan Airport in Boston, Massachusetts (KBOS) and a total of 879 events were chosen. There were 171 fast sea breeze events, 60 slow sea breeze events, 78 marginal sea breeze events, and 570 non-sea breeze events.

The initial portion of study looked at basic characteristics such as time of onset and duration relative to Logan Airport in Boston, Massachusetts (KBOS). The data set was then classified using synoptic classes created by Miller and Keim (2003) and statistics were generated for these first three characteristics. The shape and depth of the inland penetration of the sea breeze air mass, relative to the entire Massachusetts coastline, was then analyzed as a function of synoptic class. Wind vector plots developed using surface observations and a Barnes analysis were used to create a mesoscale model of the sea breeze air mass and the sea breeze front was analyzed by windshift.

The mesoscale behavior of the sea breeze at KBOS was also investigated by using the cross-shore temperature gradient (dT/dx) and geostrophic wind component (u_G) at the surface. These two components were plotted to determine if there was a distinction between the balance of these two variables relative to sea breeze and non-sea breeze events. This was another method adapted from Miller and Keim (2003). A three

dimensional approach to this method was taken by incorporating a third variable, the 850 hPa geostrophic wind component, into the plot.

Lastly, the effect of the sea breeze on convection was examined using radar reflectivity data from the Taunton, Massachusetts radar (BOX). Events from 2002 to 2007 were studied using both the reflectivity data and wind vector plots to determine if a sea breeze was present during the event anywhere along the Massachusetts coastline and whether there was a change in convection.

a. Time of Onset and Event Duration

The time of onset showed variation not only by season, but by event type as well. The overall analysis of the time of onset stratified by event type revealed that slow sea breeze events begin the earliest and fast sea breeze events begin the latest. Marginal sea breeze events develop during a time between the fast and slow events. Seasonal variation showed that this scenario is not always true and in winter, marginal events occur a bit later than fast events; moreover, in spring marginal events occur slightly earlier than slow events. Winter and spring had the least number of marginal events of all the seasons so the sample size may be affecting the results. Events occurring in summer and fall followed the same time of onset pattern seen in the overall analysis. In regards to the time of onset itself, the latest time of onset of any sea breeze event was seen in winter when more time is needed for sufficient daytime heating to develop for the sea breeze to initiate.

The shortest duration of sea breeze events occurred during winter. This is attributed to the daytime heating issue discussed above with the time of onset. The longest duration for fast events occurred during spring, while that of slow and marginal

events occurred during summer. Slow events exhibited the longest duration overall which is related to the gradual transition of the wind direction into a strong sea breeze direction between 110° and 130°.

Future research for these aspects of the sea breeze could include breaking down the time of onset and event duration by synoptic class. This may lead to sample size issues which could be addressed by lengthening the data set. Increasing the sample size may also help with refining the time of onset for marginal events in winter and spring. Also, some of the variables that initiate the sea breeze could be investigated to determine the cause of the longest event duration for fast events occurring in spring versus that of the slow and marginal events occurring in fall.

b. Synoptic Classes

Synoptic classes were used to examine the effect of large scale flow on the occurrence or non-occurrence of the sea breeze. The classes were originally created by Miller and Keim (2003) for use in research of the sea breeze at Portsmouth, New Hampshire. This study improved upon these classes by creating composite analyses based on the synoptic classes. This provided unique classes for each event type. The composite analyses were used to examine the strength of the pressure gradient force over the study area and how much resistance there was to the initiation of the sea breeze. Non-events had the strongest pressure gradient for all of the synoptic classes, which is expected as this would stop the sea breeze from penetrating inland.

Statistics were generated to determine any seasonal patterns that might exist for the events based on the synoptic scale patterns. Plots were created to show the seasonal variation of each event type with a synoptic class. Synoptic classes 1, 2, and 3,

anticyclonic, neutral, and cyclonic northwesterly flow, respectively, behaved as if they were along one single spectrum of class. The minima and maxima of seasonal occurrence were most exaggerated with class 1, becoming less pronounced with synoptic class 2. Synoptic class 3 showed very little seasonal variation in occurrence. Non-events mirrored fast events with synoptic class 4, showing a non-event maximum when fast events were at a minimum and vice versa. Slow and marginal events reacted in the same way. With synoptic class 6, each event type showed its peak occurrence in a different season with slow and marginal events peaking in both summer and fall. The sample size of synoptic class 6 events for summer is only 8 events and for fall the sample size is 20 events. The summer peaks is not statistically significant. In fall, 50% of the synoptic class 6 events are slow transition sea breezes. Non-events peaked in the winter, which is expected due to a lack of sufficient daytime heating. The fast events peaked in the spring when a strong temperature difference between the land and ocean develops because the ocean is still rather cool from the winter.

c. Inland Penetration

Wind vector plots were created using a Barnes analysis and surface observations. The sea breeze front was analyzed based on changes in wind direction at the leading edge of the marine air mass. The mid-event average positions of the sea breeze front for each synoptic class were compared. Results showed that penetration was limited by the opposing synoptic scale flow. Of the northwesterly flow classes (1, 2, and 3), synoptic class 1 showed the deepest inland penetration towards the opposing northwest flow, which is related to the weaker anticyclonic winds associated with the class. Synoptic classes 2 and 3 did not penetrate as far inland. Synoptic class 4, southwesterly flow,

showed very limited inland penetration along the coastline south of Boston. The plot for synoptic class 6 (northeasterly flow) showed comparable penetration all along the coastline.

Further research can be done with this portion of the study. Only a limited number of events were used to create these plots. Increasing the sample size might improve the results. Also, only fast events were used in this analysis. A comparison of the effect of event type on inland penetration may produce interesting results.

d. Mesoscale Calculations

Mesoscale calculations were used to distinguish between the occurrence of a sea breeze event versus a non-sea breeze event. The cross-shore temperature gradient (dT/dx) and surface geostrophic wind component (u_G) were calculated and then plotted. Lines were analyzed between sea breeze and non-sea breeze events to identify the critical limits between the event types. The plot was then broken down by synoptic class to determine if a smaller transition area (area containing both sea breeze and non-sea breeze events) could be created. Classes 1, 2, and 3 again reacted as though they were along a single spectrum of class as they did with the statistics in the synoptic scale analysis. This break down proved successful in reducing the transition area size. A three dimensional plot was also created using the 850 hPa u_G component. There was a large transition area as with the two dimensional plot.

The three dimensional plot could be broken down by synoptic class just as with the two dimensional plot which may help reduce the size of the transition area. Also, changing the level of the third variable from 850 hPa to 925 hPa may show better results as it may be slightly deeper into the sea breeze circulation. Doppler VAD wind profile

(VWP) data could be used for low level wind data instead of the RAOB data from KCHH. Unfortunately, archived data only goes back to March 2009, so a new data set would need to be developed in order to employ it.

e. Radar Analysis of Convection

A radar analysis was done to determine if the sea breeze front along the Massachusetts coastline affected or caused convection. Events between 2002 and 2007 were examined for the occurrence of convection along the coastline in an area favorable for the sea breeze front. Out of the 562 events (both sea breeze and non-sea breeze events), convection only entered the favorable region 4% of the time (24 events). Of the 24 events, 14 events had convection affected or caused by the sea breeze front. During the remaining 10 events, the sea breeze did not occur in the area of convection. A total of 7 of these 10 events showed intensification or development of convection.

The methodology used to develop the overall data set has strict stipulations against precipitation and cloud cover. It is likely that convection reaches the coastline with the presence of a sea breeze front more often than this study shows. In order to avoid this bias, a future study could determine thunderstorm days first and then examine METAR data to determine if a sea breeze wind shift occurred, ignoring cloud cover and precipitation in the observations.

Future research could expand the dataset used to the length of the full data set (1998 to 2007) to create a larger sample size. This part of the study has shown that even though the sea breeze may not be occurring in Boston, it still can be occurring in other locations along the coastline. More research is needed to determine why the sea breeze does not occur evenly along the coastline in the case of the non-events with sea breezes.

Overall this study has uncovered many interesting details regarding the sea breeze both in Boston and along the Massachusetts coastline. There is ample room for further research on many of the different aspects discussed.

APPENDIX A

Convective Analysis in Maine

An investigation into thunderstorm interaction along the sea breeze front for the northern New England Coast yields interesting results. Nine sea breeze events, six contaminated sea breeze events, and nine non-sea breeze events were used in this study. A contaminated event is an event where all the criteria for a sea breeze event are met except for the cloud cover and precipitation stipulations. METAR data from the region as well as WSR-88D level II reflectivity data from Gray, Maine (KGYX) were used. The results showed four sea breeze events where thunderstorms developed or were enhanced along the sea breeze front. There were two contaminated events where enhancement was present. One contaminated event showed convection being weakened by the marine airmass. The overall conclusion from this study was that enhancement, development, and weakening of thunderstorms does occur along the northern New England coast. Further investigation needs to be done to identify the controlling factor for development versus enhancement. (Thorp, 2008)

APPENDIX B

Miller and Keim, (2003): Synoptic Classes

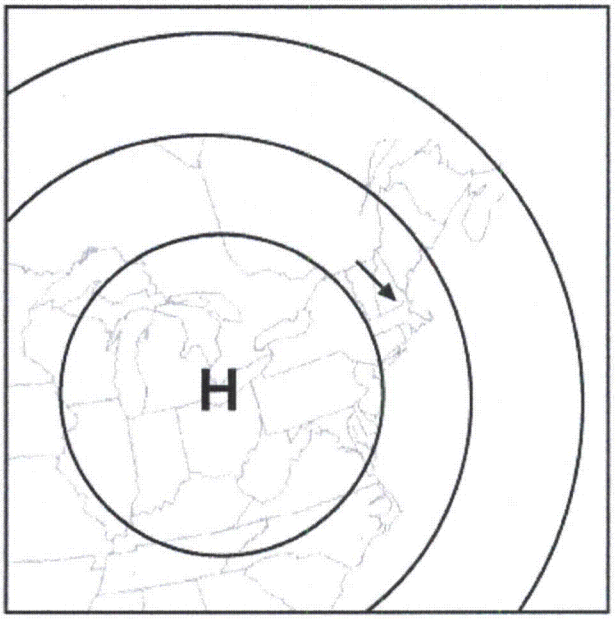

Figure A 1: Synoptic class 1, anticyclonic northwesterly boundary layer flow. Figure from Miller and Keim (2003).

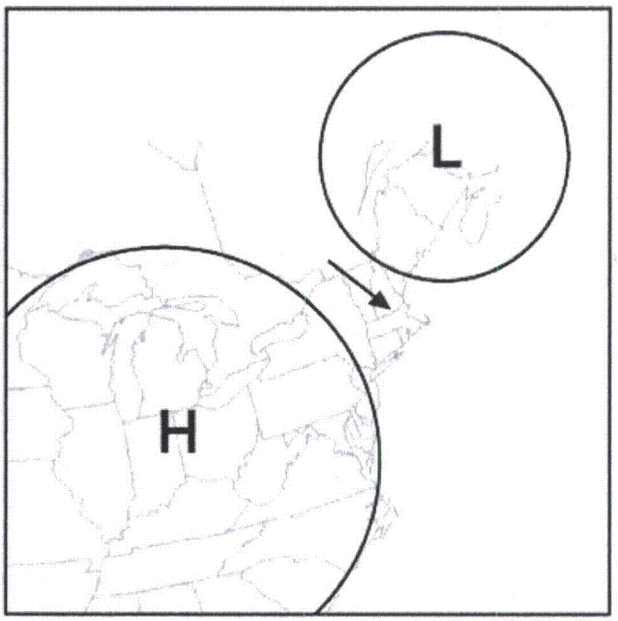

Figure A 2: Synoptic class 2, neutral northwesterly boundary layer flow. Figure from Miller and Keim (2003).

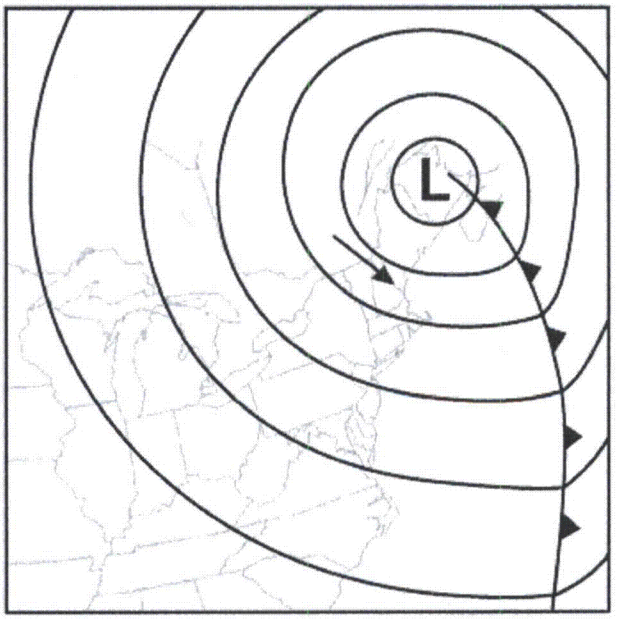

Figure A 3: Synoptic class 3, cyclonic northwesterly boundary layer flow. Figure from Miller and Keim (2003).

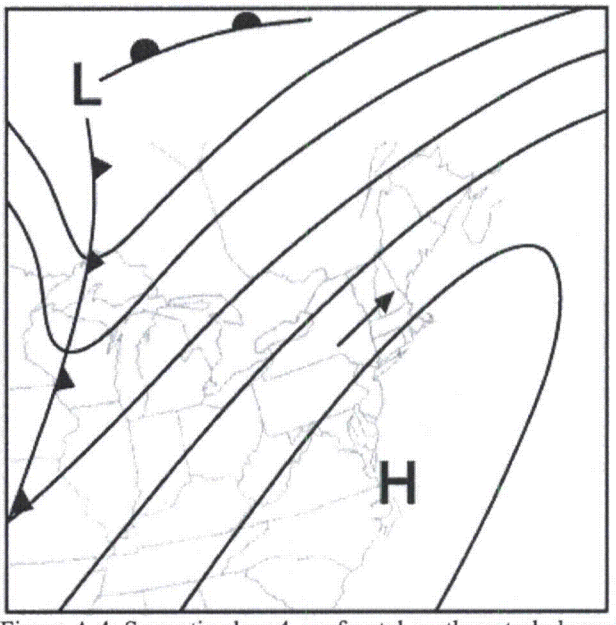

Figure A 4: Synoptic class 4, prefrontal southwesterly boundary layer flow. Figure from Miller and Keim (2003).

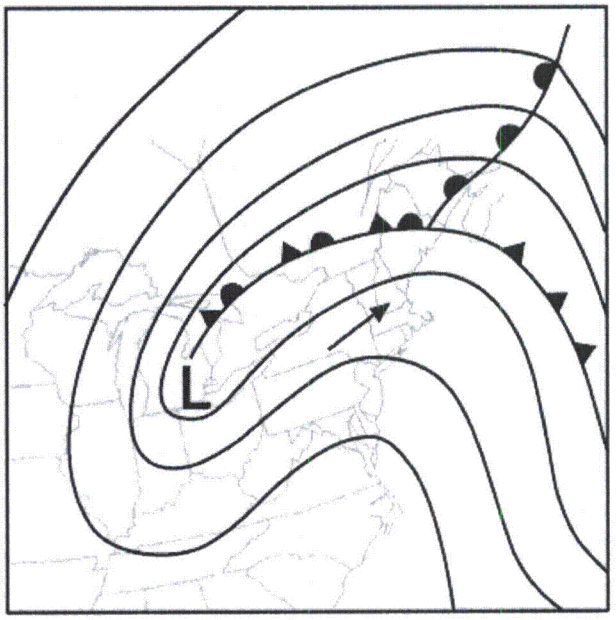

Figure A 5: Synoptic class 5, postfrontal southwesterly boundary layer flow. Figure from Miller and Keim (2003).

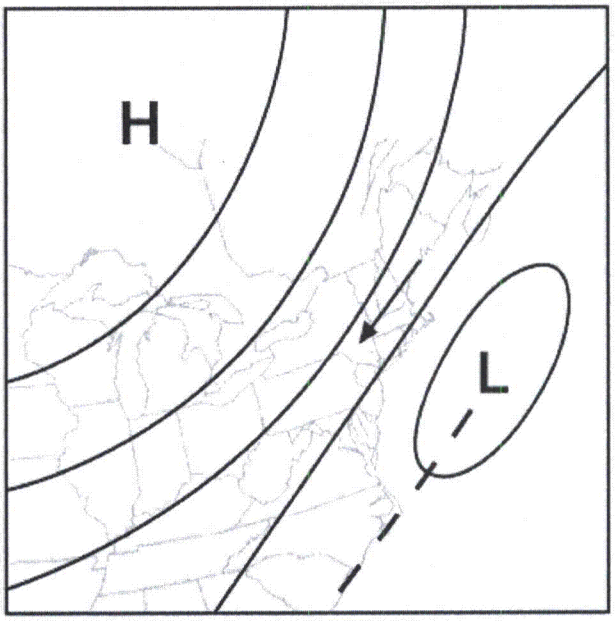

Figure A 6: Synoptic class 6, northeasterly boundary layer flow. Figure from Miller and Keim (2003).

Synoptic class 7 was reserved for boundary layer flow regimes that did not fall into classes 1 through 6.

APPENDIX C

Barnes Analysis (Barnes, 1964)

$$\widehat{wt}_n = \exp\left(-\frac{r^2}{a^2}\right)$$

$\widehat{wt}_n$ = unnormalized weight for observation point

r = distance (km) between observation and grid point

a = radius of influence (km). The radius of influence used for this study was 15 km.

$$wt_n = \sum_{i=0}^{n} \widehat{wt}_n$$

wt_n = normalized weight for observation point

$$x_{gridpoint} = \sum_{i=0}^{n} (x_n)(wt_n)$$

$x_{gridpoint}$ = interpolated value of gridpoint

x_n = observation value

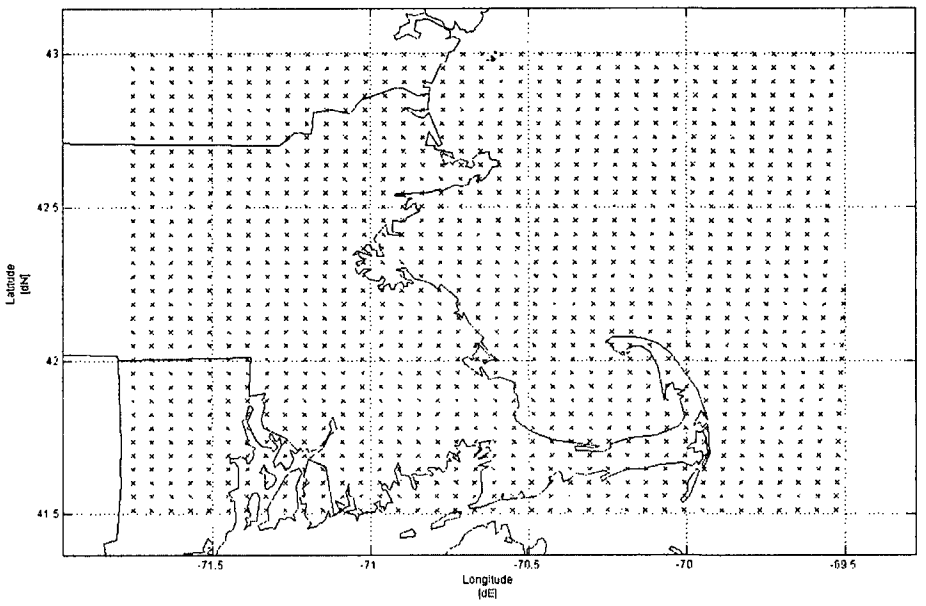

Figure B 1: Grid used for Barnes analysis.

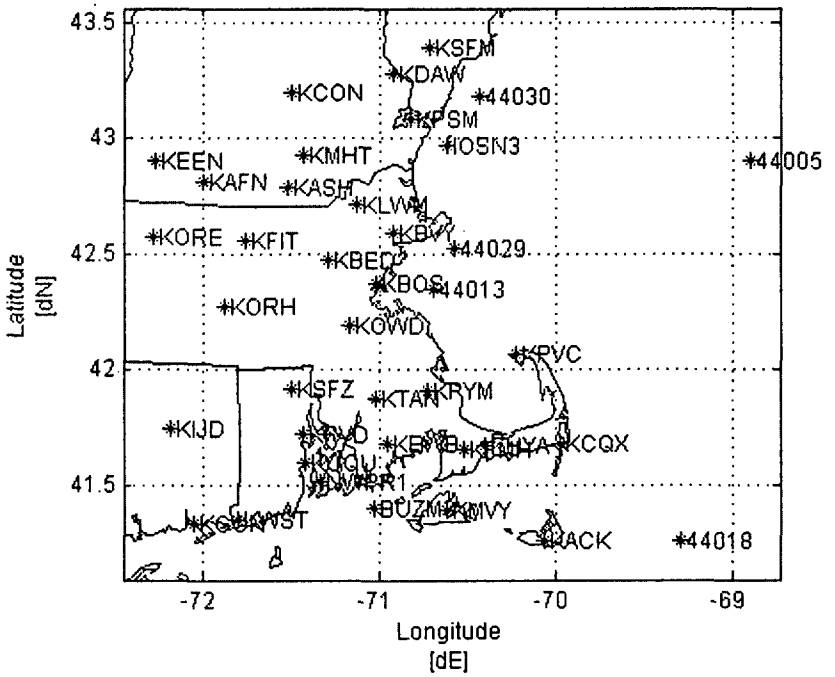

Figure B 2: Diagram of the weather stations used for Barnes analysis.

Table B 1: List of stations used in Barnes analysis.

Station Identity	Latitude (°N)	Longitude (°E)	Elevation (m above MSL)
KSFM	43.40	-70.72	74
KDAW	43.28	-70.92	100
44030	43.18	-70.43	0
KPSM	43.08	-70.82	31
KCON	43.20	-71.50	103
IOSN3	42.97	-70.62	0
KMHT	42.93	-71.44	81
KEEN	42.90	-72.27	149
KAFN	42.81	-72.00	313
KASH	42.78	-71.52	61
KLWM	42.71	-71.13	45
KBVY	42.58	-70.92	33
44029	42.52	-70.57	0
KORE	42.57	-72.28	169
KFIT	42.55	-71.76	106
KBED	42.47	-71.29	40
KBOS	42.37	-71.02	6
44013	42.35	-70.69	0
KORH	42.27	-71.87	307
KOWD	42.19	-71.17	15
KPYM	41.91	-70.73	45
KPVC	42.07	-70.22	2
KSFZ	41.92	-71.50	134
KIJD	41.74	-72.18	75
KPVD	41.72	-71.43	16
KOQU	41.60	-71.42	6
NWPR1	41.51	-71.33	4.5
KTAN	41.88	-71.02	13
KEWB	41.68	-70.96	24
KHYA	41.67	-70.40	15
KFMH	41.65	-70.52	40
KCQX	41.68	-69.98	20
KMVY	41.39	-70.62	20
KACK	41.25	-70.06	14
KWST	41.35	-71.80	24
KGON	41.33	-72.05	6
44018	41.26	-69.29	0
BUZM3	41.40	-71.03	0
44005	42.90	-68.90	0

APPENDIX D

Equations used in Mesoscale Calculations

Miller and Keim (2003) used cross shore components to examine the relationship between the forcing mechanism of the sea breeze and the flow resisting the inland penetration of the sea breeze. The cross shore potential temperature gradient represents the forcing mechanism that begins the sea breeze event and the cross shore surface geostrophic wind component represents the resistance to the inland penetration of the sea breeze. There was a lot missing pressure data for buoy 44013, so the cross shore temperature gradient was used instead the cross shore potential temperature gradient. The following equations were used in the mesoscale calculations.

Surface u_G equation

$$u_G = -\frac{1}{f\rho}\frac{dP}{dy} \qquad \text{(C1)}$$

$$\frac{dP}{dy} = \frac{(P_{KLWM} - P_{KTAN})}{dy} \qquad \text{(C2)}$$

u_G = surface geostrophic wind u-component (m s^{-1})

f = coriolis force (s^{-1})

ρ = density of air (approx. 1.25 kg m^{-3})

P_{KLWM} = Sea level pressure (Pa) at Lawrence, MA (KLWM)

P_{KTAN} = Sea level pressure (Pa) at Taunton, MA (KTAN)

dy = distance (m) between KLWM and KTAN

Surface dT/dx equation

$$\frac{dT}{dx} = \frac{(T_{44013} - T_{KORH})}{dx} \quad \text{(C3)}$$

T_{44013} = Temperature (°C) at buoy 44013

T_{KORH} = Temperature (°C) at Worcester, MA (KORH)

dx = distance (m) between 44013 and KORH

850 hPa u-component equation

$$u_{onset} = \left[\frac{(u_{00} - u_{12})}{12} \times t_{onset}\right] + u_{12} \quad \text{(C4)}$$

u_{onset} = 850 hPa interpolated wind u-component (m s^{-1}) for time of onset

u_{00} = 850 hPa wind u-component (m s^{-1}) at 00 UTC

u_{12} = 850 hPa wind u-component (m s^{-1}) at 12 UTC

t_{onset} = time of onset (UTC) of event

APPENDIX E

Miller and Keim, (2003): Mesoscale Calculations

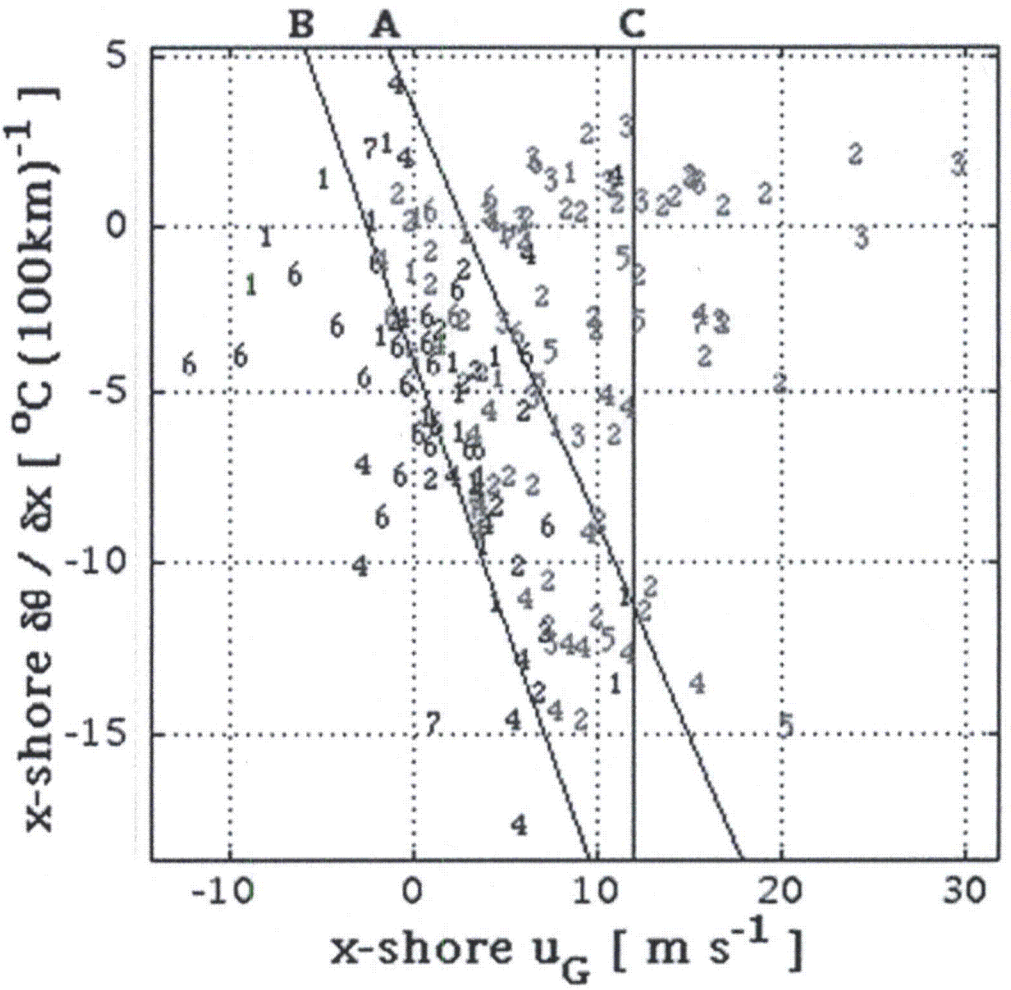

Figure D 1: All sea-breeze, marginal, and non-sea breeze events as a function of their associated cross-shore regional-scale temperature gradients and geostrophic wind components. The numbers represent the synoptic class of the event. Sea breezes are blue (•), marginal sea breezes are black (•), and non-sea breezes are red (•). Figure from Miller and Keim (2003).

REFERENCES

Barbato, J.P., 1978: Areal Parameters of the Sea Breeze and Its Vertical Structure in the Boston Basin. *Bull. Amer. Meteor. Soc.*, **59**, 1420–1431

Barnes, S.L., 1964: A Technique for Maximizing Details in Numerical Weather Map Analysis. *J. Appl. Meteor.*, **3**, 396–409.

Bedka, K. M., and J. M. Mecikalski, 2004: Nowcasting convective initiation and thunderstorm characteristics through the use of real-time geostationary satellite information. Preprints, *2004 EUMETSAT Met. Satellite Conf.,* Prague, Czech Republic, Czech Hydromet. Instit., P.41.

Colby, F.P., 2004: Simulation of the New England Sea Breeze: The Effect of Grid Spacing. *Wea. Forecasting*, **19**, 277–285.

ESRL PSD, 2008: 6-hourly NCEP/NCAR reanalysis data composites. Retrieved from http://www.cdc.noaa.gov/Composites/Hour/.

Estoque, M., 1961: A theoretical investigation of the sea breeze. *Quart. J. Roy. Meteor. Soc.*, **87**, 136-146.

Estoque, M., 1962: The sea breeze as a function of the prevailing synoptic situation. *J. Atmos. Sci.*, **19**, 244–250.

McPherson, R.D., 1970: A numerical study of the effect of a coastal irregularity on the sea breeze. *J. Appl. Meteor.*, **9**, 767–777.

Medlin, J.M., and P.J. Croft, 1998: A Preliminary Investigation and Diagnosis of Weak Shear Summertime Convective Initiation for Extreme Southwest Alabama. *Wea. Forecasting*, **13**, 717–728.

Miller, S.T.K., and B.D. Keim, 2003: Synoptic-Scale Controls on the Sea Breeze of the Central New England Coast. *Wea. Forecasting*, **18**, 236–248.

Miller, S.T.K., B.D. Keim, R.W. Talbot, and H. Mao, 2003: Sea breeze: Structure, forecasting, and impacts, Rev. Geophys., **41(3)**, 1011, doi:10.1029/2003RG000124.

NCDC, 2008: Radar data. Retrieved from http://www.ncdc.noaa.gov/oa/ncdc.html.

NESDIS, 2008: SRRS analysis and forecast charts. Retrieved from http://nomads.ncdc.noaa.gov/ncep/NCEP.

PSU Weather Center, 2008: METAR data. Retrieved from http://vortex.plymouth.edu.

Thorp, J., 2007: Improved sea breeze forecasting for Boston's General Edward Lawrence Logan International Airport. COMET Outreach Program. Retrieved from http://www.comet.ucar.edu/outreach/abstract_final/0658394_plymouth.pdf.

Thorp, J., 2008: Interaction of Thunderstorms and the Sea Breeze Front along the Northern New England Coast.

Suresh, R., 2007: Observation of Sea Breeze Front and its Induced Convection over Chennai in Southern Peninsular India Using Doppler Weather Radar. *Pure Appl. Geophys,* **164**, 1511-1525.